

**WET ADHESION OF POLYVINYLAMINE-
PHENYLBORONIC ACID TO CELLULOSE
HYDROGEL**

**WET ADHESION OF POLYVINYLAMINE-
PHENYLBORONIC ACID TO CELLULOSE
HYDROGEL**

By

WEI CHEN, B. ENG., M. ENG.

A Thesis

Submitted to the School of Graduate Studies

In Partial Fulfillment of the Requirements

For the Degree

Doctor of Philosophy

McMaster University

© Copyright by Wei Chen, November 2008

DOCTOR OF PHILOSOPHY (2008)

McMaster

University

(Chemical Engineering)

Hamilton, Ontario

**TITLE: Wet Adhesion of Polyvinylamine-phenylboronic Acid to
Cellulose Hydrogel**

AUTHOR: Wei Chen

B. Eng. (Tianjin University)

M. Eng. (Tianjin University)

SUPERVISOR: Professor Robert H. Pelton

NUMBER OF PAGES: xiv, 141

Abstract

The ability of a never-dried paper web on a paper machine to resist breakage is commonly referred to as paper wet-web strength. Low wet-web strength can lead to frequent breaks which interrupt production and lower paper machine efficiency. Currently, no commercial products provide the function of enhancing wet-web strength. Boronic acid derivatized polyvinylamine (PVAm-PBA) showed high instantaneous wet adhesion to regenerated cellulose membranes. The objective of the research summarized in this thesis was to determine the factors and mechanisms dictating PVAm-PBA adhesion to wet cellulose. In addition, narrowly distributed PVAm microgel was prepared and the wet adhesion of boronate-microgels to cellulose is reported.

The phase behavior and surface tension of PVAm-PBA were measured as functions of pH and the degree of PBA substitution. The pH ranges over which phase separation occurred increased with PBA substitution. 150 kDa PVAm-PBA with 4% derivatization phased separated at pH 8.5 to 9.5. The copolymer based on 51% substitution was insoluble over most of the pH range. The hydrophobicity of copolymers was reflected in the significant lowering of surface tension particularly at high pH. Additionally, fructose, which binds to borate, influenced the titration curves but did not influence surface tension.

Pairs of wet, regenerated cellulose films were laminated with PVAm-PBA and the forces required to delaminate the never-dried laminates, were measured as functions of adhesive structure and application conditions. The greatest wet adhesion was obtained with 150 kDa PVAm with 16% of the amines bearing phenylboronic moieties. The pH at which the PVAm-PBA was adsorbed onto the cellulose was the dominant process parameter. The specific role of the phenyl boronic groups was illustrated in two ways: a) replacing the $B(OH)_2$ with OH (*i.e.* phenol) gave much lower adhesion; and, b) wet adhesion was greatly reduced by the presence of sorbitol which effectively competes with cellulose for boronate binding sites.

The interaction of boronate and cellulose was studied. Owing to poor solubility of cellulose, two model polymers: dextran and hydroxyethyl cellulose (HEC) and two saccharides: glucose and cellobiose were measured by boron NMR measurement, tensile extension, fluorescence spectra, viscometer and peeling test methods. In conclusion, carbon-1, 2 diols at one end of cellulose chain can react with boronic acid. By contrast, carbon-2, 3 diols, which are abundant on cellulose chains, cannot react with boronic acid and the other diols, such as carbon-3, 4 diols and carbon-4, 6 diols cannot react with boronic acid. The high adhesion of boronate containing polymers to cellulose membranes was

attributed to boronate ester formation with the cellulose end groups on the membrane surfaces.

Finally, a simple and effective methodology was demonstrated for the preparation of polyvinylamine microgel with a narrow distribution. Boronate derivatives of PVAm microgels displayed very high wet adhesion to cellulose over a broad pH range.

Acknowledgement

Firstly, deepest thanks are expressed to my supervisor, Professor Robert Pelton. He led me into the magic world of colloidal and interface science. I also wish to thank him for crucial advice in my research, freedom of academic work, opportunities to attend international conferences and discuss with experts in the field, and precious advice for my career plan. I also wish to thank my Supervisor Committee members, Professor Harald Stöver and Professor John Vlachopoulos for their priceless advice and kindly help in my research work.

I would also like to take this opportunity to extend my appreciation to Dr. Marc Leduc for his important academic advice and experimental assistance.

Drs. Bob Berno and Donald Hughes are acknowledged for their invaluable advice and excellent skills in NMR measurements. Special thanks are due to Ms. Rena Cornelius and Ms. Marcia West for the labelling radio probe and the assistance with TEM. In addition, I am indebted to Doug Keller, Paul Gatt and Francis Lima for their assistance with my research projects.

Thanks to all group members at the McMaster Interfacial Technologies Group for academic and day-to-day life support. I am deeply thankful to Dr. Chen Lu for his important academic help, Dr. Boxin Zhao for his help with advice on academia and career direction, Dr. Sheng Dai for sharing his extensive knowledge in physical chemistry, Dr. Chengming Li for his comprehensive help in polymer chemistry, Dr. Todd Hoare for many discussions about particle characterization, Drs. Yaling Xu, Xiaonong Chen and Zhinan Feng for their help starting my research work, Professor Hiroo Tanaka for cooperating with boronate quantifications and Dr. Xianhua Feng for help with mathematical modeling and polymer knowledge.

I also indebted to two brilliant undergraduate students, Mrs. Vincent Leung and Darryl Sivakumaran, for their excellent experiments in the completion of this thesis. Particularly, Mr. Vincent Leung is also thanked for his outstanding academic discussions and assistance with my English writing.

I am also grateful to BASF Canada and the Natural Sciences and Engineering Research Council of Canada for financial support of this thesis work.

Finally, I would like to thank my parents for their infinite love and support throughout my life. I would also like to express my gratitude to my wife, Wenli Jia, for her priceless love, advice and devotion to our family and my career adventure.

TABLE OF CONTENTS

| | |
|--|-----------|
| Abstract..... | iii |
| Acknowledgments..... | v |
| Chapter 1 Introduction and Literature Review..... | 1 |
| 1.1 Literature review and theoretical analysis of wet-web strength | 2 |
| 1.1.1 Papermaking process and wet-web strength..... | 2 |
| 1.1.2 The theoretical analysis of wet-web strength..... | 3 |
| 1.2 An introduction of PVAm and boronic acid..... | 7 |
| 1.2.1 PVAm and its application in papermaking | 7 |
| 1.2.2 Boronic acid and its complexation with diols..... | 8 |
| 1.3 Microgels as wet-web-strength enhancing agent..... | 10 |
| 1.4 Objective..... | 11 |
| 1.5 Thesis Outline..... | 12 |
| Chapter 2 Solution Properties of Polyvinylamine Derivatized with Phenylboronic Acid..... | 16 |
| 2.1 Introduction..... | 16 |
| 2.2 Experimental section..... | 16 |
| 2.2.1 Materials | 16 |
| 2.2.2 Surface tension measurement | 18 |
| 2.2.3 Interaction force measurement..... | 18 |
| 2.3 Results..... | 18 |
| 2.3.1 PVAm-PBA phase behaviour | 18 |
| 2.3.2 Charge-pH behaviour of PVAm-PBA | 19 |
| 2.3.3 Surface activity of PVAm-PBA..... | 20 |
| 2.3.4 Interaction force of cellulose and PVAm-PBA coated colloidal probe..... | 21 |
| 2.4 Discussion..... | 21 |
| 2.5 Conclusions..... | 22 |
| 2.6 Tables and Figures | 23 |
| 2.7 Appendix..... | 38 |
| 2.7.1 Comparison of the surface tension of PVAm-PBA-1, PVAm- PBA-4 and PVAm (Mw= 15 kDa) as functions of pendant drop age..... | 38 |
| 2.7.2 Modeling the ionization behavior of PVAm-PBA..... | 39 |
| 2.7.3 Modeling the isoelectric points of PVAm-PBAs..... | 45 |
| Chapter 3 PVAm-Boronate: A New Wet Adhesive to Cellulose Hydrogel ... | 46 |
| 3.1 Introduction..... | 46 |
| 3.2 Experimental section..... | 47 |
| 3.2.1 Materials | 47 |
| 3.2.2 Methods | 47 |
| 3.3 Results..... | 49 |

| | |
|--|------------|
| 3.4 Discussion..... | 54 |
| 3.5 Conclusions..... | 56 |
| 3.6 Tables and Figures | 58 |
| 3.7 Appendices..... | 71 |
| 3.7.1 Adsorption Application..... | 71 |
| 3.7.2 Direct Application..... | 72 |
| 3.7.3 An illustration of ninety degree peeling test..... | 73 |
| 3.7.4 The influence of water content on wet adhesion of applied polymers | 74 |
| 3.7.5 Modeling wet adhesion of PVAm-PBA in the presence of sugars..... | 75 |
| | |
| Chapter 4 A Detailed Investigation of the Interaction between Cellulose and Boronate..... | 82 |
| 4.1 Introduction..... | 82 |
| 4.2 Experiment section..... | 83 |
| 4.2.1 Materials | 83 |
| 4.2.2 Methods | 84 |
| 4.3 Results..... | 85 |
| 4.4 Discussion..... | 88 |
| 4.5 Conclusions..... | 93 |
| 4.6 Table and Figures..... | 94 |
| 4.7 Appendix..... | 102 |
| | |
| Chapter 5 Preparation and characterization of polyvinylamine microgels . | 105 |
| 5.1 Introduction..... | 105 |
| 5.2 Experiments | 106 |
| 5.2.1 Materials | 106 |
| 5.2.2 Preparation of completely hydrolyzed PVAm..... | 106 |
| 5.2.3 Preparation of PVAm microgels..... | 106 |
| 5.2.4 Characterization of PVAm microgels..... | 106 |
| 5.3 Results..... | 107 |
| 5.3.1 The influence factors of forming PVAm microgels | 107 |
| 5.3.1.1 The salt concentration of PVAm..... | 107 |
| 5.3.1.2 The pH of PVAm | 107 |
| 5.3.1.3 The pH of TPP | 108 |
| 5.3.1.4 The Mw of PVAm | 108 |
| 5.3.1.5 The volume of TPP | 108 |
| 5.3.1.6 The concentration of TPP | 108 |
| 5.3.1.7 The storage time..... | 108 |
| 5.3.1.8 The dropping speed..... | 109 |
| 5.3.1.9 The stirring speed..... | 109 |
| 5.3.2 Electrophoretic mobility result | 109 |
| 5.3.3 The size by dynamic light scattering | 109 |
| 5.3.4 The morphology and size by TEM | 109 |
| 5.3.5 The size distribution by Mastersizer..... | 109 |

| | |
|--|------------|
| 5.4 Discussion..... | 110 |
| 5.5 Summary..... | 111 |
| 5.6 Tables and Figures..... | 113 |
| Chapter 6 Boronate Microgels Adhesion to Wet Cellulose..... | 130 |
| 6.1 Introduction..... | 130 |
| 6.2 Experiments..... | 131 |
| 6.2.1 Materials..... | 131 |
| 6.2.2 Preparation of Boronate-modified microgels..... | 131 |
| 6.2.3 Wet adhesion measurement..... | 132 |
| 6.3 Results..... | 132 |
| 6.4 Discussion..... | 133 |
| 6.5 Conclusions..... | 134 |
| 6.6 Tables and figures..... | 135 |
| Chapter 7 Concluding Remark..... | 140 |

LIST OF FIGURES

| | | |
|-------------------|--|----|
| Figure 1.1 | The influence of moisture content w on the wet-web tensile strength of three fiber pulps..... | 3 |
| Figure 1.2 | The effect of surfactant on wet-web strength. 1-groundwood pulp, 2-groundwood pulp with the addition of 0.1% of surfactant | 4 |
| Figure 1.3 | The wet-web strength of glass fibers with different diameters..... | 5 |
| Figure 1.4 | The influence of different adhesive agents on wet-web strength. 1-original pulp, 2-glass fibers without bonding agents, 3-glass fibers with the addition of hydrofluoric acid and gelatin, 4-glass fibers with the addition of sodium silicate, 5-glass fibers with the addition of hydrofluoric acid and gelatin..... | 5 |
| Figure 1.5 | The influence of adding cationic polyacrylamide on wet-web strength of unbeaten Kraft fibers..... | 6 |
| Figure 1.6 | Fluorescence intensity of ARS at 10^{-4} M in pH=7.4 (A): ARS (B): ARS+ Phenylboronic acid (C): ARS+ Phenylboronic acid + Fructose..... | 10 |
| Figure 1.7 | The viscosity change of boronic acid containing system with time. The upper curve of rectangular boxes represents the viscosity of the blank solution without any glucose. The other curves represent the viscosities of the solutions with the addition of different concentrations of glucose..... | 10 |
| Figure 2.1 | 1H NMR spectra of PVAm-PBA-4 150 kDa..... | 26 |
| Figure 2.2 | Phase boundaries of PVAm-PBA as functions of pH and degree of substitution. All the measurements were made in 5 mM NaCl and at 25 °C..... | 27 |
| Figure 2.3 | The intrinsic viscosity of PVAm, PVAm-PBA-4 and PVAm-PBA-4 plus fructose in 0.3 M NaCl at 25 °C (Molar ratio of boronic acid to fructose was 1:10.)..... | 29 |
| Figure 2.4 | Degree of neutralization ($1-\beta$) versus pH for three PVAm-PBA copolymers and the parent PVAm homopolymer. All measurements were performed in 5 mM NaCl at 25 °C..... | 30 |
| Figure 2.5 | The influence of 0.017 M fructose on the ionization behavior of PVAm-PBA-3..... | 31 |
| Figure 2.6 | Electrophoretic mobility as functions of pH for 0.1 g/L PVAm-PBA adsorbed onto 0.01g/L 200nm diameter anionic polystyrene latex. All measurements were made in 5 mM NaCl aqueous solution at 25 °C. For the experiments with fructose the molar ratio of boronic acid to fructose was 1:10..... | 32 |
| Figure 2.7 | Surface tension versus drop age for 0.5 % (wt) PVAm-PBA-1 in 5 mM NaCl as functions of pendant drop age at 22 °C..... | 33 |
| Figure 2.8 | Equilibrium surface tension of PVAm-PBA-1 as functions of pH. Molar ratio of boronic acid to fructose was 1:10..... | 34 |

| | | |
|-------------------|--|-----------|
| Figure 2.9 | Force-distance curves between cellulose surfaces with adsorbed PVAm-PBA as a function of pH. Crosses are pH 3.8, filled circles are pH 5, open diamonds are pH 7 and closed squares are pH 10. The data for pH 3.8, 5 and 7 may be fit to DLVO theory within the limits of constant charge and potential with ψ_0 of +39 mV, +32 mV and +30 mV respectively..... | 35 |
| Figure 3.1 | Comparison of delamination force versus displacement curves for PVAm-PBA-5, PVAm-Ph-2 and PVAm (Mw=150 kDa). The adsorption application was employed..... | 61 |
| Figure 3.2 | The influence of degree of substitution on the delaminating peel force of two cellulose films. Plot A: Direct Application, the applied PVAm-PBA and PVAm-Ph were 0.1 wt%, 0.03 M NaCl aqueous solution, 25 °C. Plot B: Adsorption Application, the applied PVAm-PBA and PVAm-Ph were 0.01 wt%, 0.03 M NaCl aqueous solution, 25 °C. The error bars are the standard derivations of the mean based on four measurements..... | 62 |
| Figure 3.3 | Electrophoresis mobility of PVAm-PBA-5 as a function of pH, 1000 ppm polymer in 0.03 M NaCl aqueous solution, 25 °C. The error bars are the standard deviations of the mean based on five measurements..... | 63 |
| Figure 3.4 | The delaminating peeling strength and maximum adsorbed amount of PVAm-PBA-5 onto cellulose membranes as functions of adsorption pH. The applied PVAm-PBA-5 was 0.01 wt%, 0.03 M NaCl aqueous solution, 25 °C. The error bars are the standard derivations of the mean based on four measurements. Plot A shows both curves of peeling strength and adsorption content against adsorption pH, wherein a final pH 5 for the former and a final pH 5.9 for the latter. Plot B replotted A to a curve of peeling strength as a function of corresponding adsorption content..... | 64 |
| Figure 3.5 | The delaminating peeling strength as a function of final pH. PVAm-PBA-5 applied was 0.01 wt%, 0.03 M NaCl aqueous solution, 25 °C. Plot A is the wet adhesion curves at different adsorption pH as functions of final pH. The error bars are the standard derivations of the mean based on four measurements. Plot B is the contour plot of delamination force against adsorption and final pH..... | 65 |
| Figure 3.6 | The influence of the addition of 5g/L sorbitol on the wet adhesion strength of PVAm-PBA-5 to cellulose. The applied PVAm-PBA-5 was 0.01 wt%, 0.03 M NaCl aqueous solution, 25 °C. The error bars are the standard derivations of the mean based on four measurements..... | 66 |
| Figure 3.7 | The influence of the addition of sorbitol on the wet adhesion strength of PVAm-PBA-5 to cellulose. The red line is experimental | |

| | | |
|--------------------|--|-----|
| | data and the blue line is the simulation curve. The applied PVAm-PBA-5 was 0.01 wt%, 0.03 M NaCl aqueous solution, 25 °C..... | 67 |
| Figure 3.8 | The effect of molecular weight of PVAm-PBA on the adhesion strength. PVAm-PBA applied was 0.5 wt%, 0.03 M NaCl aqueous solution, 25 °C. The error bars are the standard derivations of the mean based on four measurements..... | 68 |
| Figure 3.9 | The change of delaminating peel force of cellulose films against ionic concentration for PVAm-PBA-5 that was applied in 0.1 wt% aqueous solution, 25 °C. The error bars are the standard derivations of the mean based on four measurements..... | 69 |
| Figure 3.10 | Comparison of pH- and polymer- dependent adhesion. The top graph was from peeling test whereas the bottom one was from CPM measurement. In the bottom graph, open circles, filled triangles and open squares represented PVAm, PVAm-Ph and PVAm-PBA, respectively..... | 70 |
| Figure 4.1 | ¹¹ B NMR of PVAm-PBA-3 (polymer concentration 10g/L) and saccharides. The molar ratio of boronate to saccharides or polysaccharides was 1:1..... | 97 |
| Figure 4.2 | The reduced viscosity of mixed solution of HEC and PVAm-PBA-3 at pH 3.9 and 9.5. Each viscosity value in the figure represents the average of three measurements..... | 98 |
| Figure 4.3 | Fluorescence emission intensity for different saccharides with ARS and boric acid. The molar ratio of ARS, boric acid and saccharides/polysaccharides was 1:50:500. Emission wavelength is 480 nm. ARS concentration and pH were set to 0.2 mM and 9.0, respectively..... | 99 |
| Figure 4.4 | The influence of the conversion from hemiacetal to acetal on the delamination force of regenerated cellulose membranes. PVAm-PBA-5 applied was 0.1 wt%, 0.03 M NaCl aqueous solution, 25 °C. The error bars are the standard derivations of the mean based on four measurements..... | 100 |
| Figure 4.5 | The delamination force of cellulose ester. PVAm-PBA-5 applied was 0.1 wt%, 0.03 M NaCl aqueous solution, 25 °C. The error bars are the standard derivations of the mean based on four measurements..... | 101 |
| Figure 5.1 | Two steps in the production of uniform-sized PVAm microgels. Step 1 is the production of uniform-sized microgels. Step 2 is the chemically crosslinked process to obtain stable microgels..... | 114 |
| Figure 5.2 | The influence of salt concentration on the size and distribution of PVAm microgels. The unit of salt concentration is mol/L. PVAm (Mw=150 kDa) 0.1 g/L (50mL) pH=10, TPP 1g/L (20 mL) pH=3, stirring speed level 8, dropping speed 0.333 mL/s, storage for 10 minutes..... | 115 |

| | | |
|--------------------|---|------------|
| Figure 5.3 | The influence of PVAm pH on the size and distribution of PVAm microgels. PVAm (Mw=150 kDa) 0.1 g/L (50 mL), [NaCl] =5 mM, TPP 1g/L (20 mL) pH=3, stirring speed level 8, dropping speed 0.333 mL/s, storage for 10 minutes..... | 116 |
| Figure 5.4 | The influence of TPP pH on the size and distribution of PVAm microgels. PVAm (Mw=150 kDa) 0.1 g/L (50 mL) pH=10, [NaCl] =5 mM, TPP 1g/L (20 mL) pH=3, stirring speed level 8, dropping speed 0.333 mL/s, storage for 10 minutes..... | 117 |
| Figure 5.5 | The influence of PVAm Mw on the size and distribution of PVAm microgels. PVAm (Mw as shown in figure and unit is kDa) 1 g/L (50 mL) pH=10, [NaCl] =5 mM, TPP 1g/L (20 mL) pH=3, stirring speed level 8, dropping speed 0.333 mL/s, storage for 10 minutes..... | 118 |
| Figure 5.6 | The influence of TPP volume on the size and distribution of PVAm microgels. PVAm (Mw=150 kDa) 0.1 g/L (50 mL) pH=10, [NaCl] =5 mM, TPP 1g/L (20 mL) pH=3, stirring speed level 8, dropping speed 0.333 mL/s, storage for 10 minutes..... | 119 |
| Figure 5.7 | The influence of TPP concentration on the size and distribution of PVAm microgels. PVAm (Mw=150 kDa) 0.1 g/L (50 mL) pH=10, [NaCl] =5 mM, TPP 1g/L (20 mL) pH=3, stirring speed level 8, dropping speed 0.333 mL/s, storage for 10 minutes..... | 120 |
| Figure 5.8 | The influence of Storage time on the size and distribution of PVAm microgels. PVAm (Mw=150 kDa) 0.1 g/L (50 mL) pH=10, [NaCl] =5 mM, TPP 1g/L (20 mL) pH=3, stirring speed level 8, dropping speed 0.333 mL/s..... | 121 |
| Figure 5.9 | The influence of dropping speed on the size and distribution of PVAm microgels. PVAm (Mw=150 kDa) 0.1 g/L (50 mL) pH=10, [NaCl] =5 mM, TPP 1g/L (20 mL) pH=3, stirring speed level 8, storage for 10 minutes..... | 122 |
| Figure 5.10 | The influence of stirring speed on the size and distribution of PVAm microgels. PVAm (Mw=150 kDa) 0.1 g/L (50 mL) pH=10, [NaCl] =5 mM, TPP 1g/L (20 mL) pH=3, dropping speed 0.333 mL/s, storage for 10 minutes..... | 123 |
| Figure 5.11 | pH effect on the electrophoretic mobility of 500 ppm microgel in 5 mM NaCl aqueous solution, 25 °C. The preparation condition: PVAm (Mw=150 kDa) 1 g/L (50 mL) pH=10, [NaCl] =5 mM, TPP 1g/L (20 mL) pH=3, stirring speed level 8, dropping speed 0.333 mL/s, storage for 10 minutes. The error bars are the standard deviations from the mean based on five measurements. 0.1 M HCl and NaOH were used to adjust pH..... | 124 |
| Figure 5.12 | The hydrodynamic diameter of PVAm microgel-1 as a function of pH. The preparation condition: PVAm (Mw=150 kDa) 1 g/L (50 mL) pH=10, [NaCl] =5 mM, TPP 1g/L (20 mL) pH=3, stirring speed level 8, dropping speed 0.333 mL/s, storage for 10 minutes. | |

| | | |
|--------------------|---|------------|
| | The error bars are the standard deviations from the mean based on six measurements. 0.1 M HCl and NaOH were used to adjust pH. 50 ppm microgel in 5 mM NaCl aqueous solution, 25 °C..... | 125 |
| Figure 5.13 | TEM images of PVAm microgel. The scale bars are 500 and 200 nm, respectively. The preparation condition: PVAm (Mw=150 kDa) 1 g/L (50 mL) pH=10, [NaCl] =5 mM, TPP 1g/L (20 mL) pH=3, stirring speed level 8, dropping speed 0.333 mL/s, storage for 10 minutes..... | 126 |
| Figure 5.14 | Size distribution of PVAm microgel. Experiments were measured at pH 10.2, I=5 mM. The preparation condition: PVAm (Mw=150 kDa) 1 g/L (50 mL) pH=10, [NaCl] =5 mM, TPP 1g/L (20 mL) pH=3, stirring speed level 8, dropping speed 0.333 mL/s, storage for 10 minutes..... | 127 |
| Figure 6.1 | The delamination force of PVAm microgel and boronate modified PVAm microgel as functions of final pH. The adsorption pH was 3.3, 0.03 M NaCl aqueous solution, 25 °C..... | 135 |
| Figure 6.2 | The delamination force of PolyNIPAM microgel and boronate modified PolyNIPAM microgel as functions of final pH. The adsorption pH was 3.2, 0.03 M NaCl aqueous solution, 25 °C... | 136 |
| Figure 6.3 | The delamination force of PVAm microgel and boronate modified PVAm microgel as functions of adsorption pH. The final pH was 11.15, 0.03 M NaCl aqueous solution, 25 °C..... | 137 |
| Figure 6.4 | The delamination force of boronate PVAm microgel and linear PVAm-boronate (DS 15%, 150 kDa) as functions of final pH. The adsorption pH was 3.3 for microgel and 3.8 for linear PVAm-boronate, in 0.03 M NaCl aqueous solution at 25 °C..... | 138 |

LIST OF TABLES

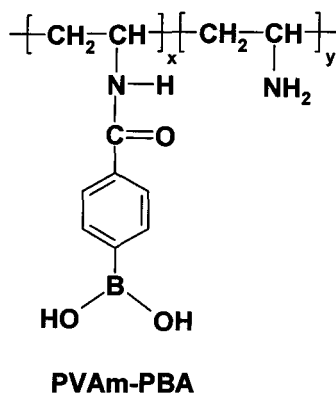
| | | |
|--------------------|--|------------|
| Table 2.1 | Polymer compositions and molecular weight. The degree of substitution is the number of substituted function groups per nitrogen atom, and the maximum possible value is 200% corresponding to tertiary amines..... | 23 |
| Table 3.1 | Polymer compositions and molecular weight. The degree of substitution is the number of substituted function group per nitrogen and the maximum possible value is 2 corresponding to tertiary amines..... | 58 |
| Table 4.1 | Polymer compositions and molecular weight. The degree of substitution is the number of substituted function groups per nitrogen atom, and the maximum possible value is 200% corresponding to tertiary amines..... | 94 |
| Table 4.2 | Tensile strength of film made of HEC and PVAm-PBA-3. The concentration of HEC and PVAm-PBA-3 are 2.5 g/L..... | 95 |
| Table 4.3 | Literature summary of association constants between boronate and saccharides (log K). R5, R6 represent five and six member ring of the complex of boronate and diols, respectively..... | 96 |
| Table 4.7.1 | Viscosity of mixed solution of boric acid + HP-Guar or boric acid + HEC. The concentration of HEC, HP-Guar and boric acid are 2g/L, 1g/L and 0.62 g/L, respectively..... | 102 |

Chapter 1

Introduction and Literature Review

Introduction

This thesis summarizes research aimed at understanding why a new synthetic polymer, polyvinylamine-phenylboronate (PVAm-PBA), strongly adheres to wet cellulose. In addition to being a scientific challenge, this work points to potential applications in papermaking technology, biomaterials and other application requiring adhesion to wet, hydrophilic carbohydrates. This project was inspired by the possibility that PVAm-PBA could be the first wet-web strength enhancing polymer.



Scheme 1.1 Chemical structure of PVAm-PBA

Wet-web strength is a “never-dried strength”, which means the ability of a wet paper sheet to resist breakage during the papermaking process. Wet-web strength is of importance in the papermaking industry. Low wet-web strength can lead to frequent breaks which interrupt production and lower paper machine efficiency.¹

Dr. Chen Lu firstly found that the complex of guar and polyvinylamine derivatized with boronate group (PVAm-PBA) could provide a high wet adhesion compared only with the guar or polyvinylamine system.² In addition, PVAm-PBA showed a pH-dependent property that substantially increased wet adhesion at high pH values. It is proposed that boronate groups could react with hydroxyl groups in cellulose. Therefore, the bonding strength between fibers could be enhanced by the addition of boronate containing polymers in fibers.

The overall objective of this thesis is to investigate the mechanism of wet adhesion of PVAm-PBA to cellulose and application in papermaking technology. This chapter presents reviews of the literature and the theoretical analysis of wet-web strength, an introduction to polyvinylamine and boronic acid, the study of the wet adhesion of microgels, and an outline of the thesis. The following section reviews the relevant background of science and technology.

1.1 Literature review and theoretical analysis of wet-web strength

1.1.1 Papermaking process and wet-web strength

A simple description of the papermaking process is as follows:

(a)Pulping section: Material pulps were dispersed and bleached according to requirements. Water-soluble polymers or other additives are added to this fiber slurry.

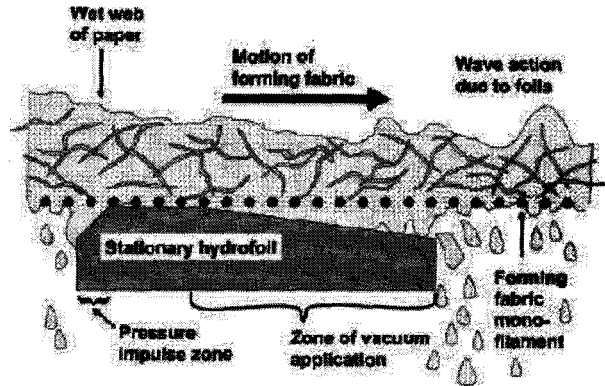
(b)Wire section: The slurry from (a) is sent onto a wire web to dewater so that a fairly uniform sheet can be made.

(c)Press section: The fiber web from (b) is further dried by pressure to remove excess water and achieve a sufficiently high bonding strength in order to ensure that the web is transferred to the drying section without any breakage.

(d)Drying and packaging section: By the use of pressure and evaporation, the fiber web from (c) is fully dried and paper is produced.

Wet paper webs are multilayer wet fiber on the support fabric. In modern papermaking, to meet the needs of continuous ongoing production, the supporters under paper webs consist of a series of rolls (as shown in scheme 1.2). Consequently, the ability to resist breakage of wet-web is critically important for paper production. Lower wet-web strength will make the wet paper web fragile and therefore lower production efficiency and increase production costs. Thus, wet-web strength is an important issue in the papermaking industry. However, there is no commercial wet-web strength agent to solve this problem. In addition, the speed of newsprint machines has increased from 1966s' speed of 900 m/min to 2000s' speed of 2000 m/min, which means the breakage of wet-web is becoming increasingly more important.

The fiber content in a wire section is 8-20 %. In comparison, the fiber content in a press section is 20-65 %, depending on different paper grades. The easiest breakage sites of a paper web are located between press (b) and the dry section (c), or at the beginning of the drying section, where the fiber content is less than 65 %.³



Scheme 1.2 A wet-web passing over a hydrofoil (Adapted from Rojas *et al.* 2004)³

1.1.2 The theoretical analysis of wet-web strength

The solid content of fibers plays an important role in influencing fiber surfaces and wet-web strength. The wet-web tensile strengths of different solid contents were measured and shown in Fig 1.1. In general, the wet-web strength increased with the solid content, that is, the wet-web strength decreased with the moisture content.

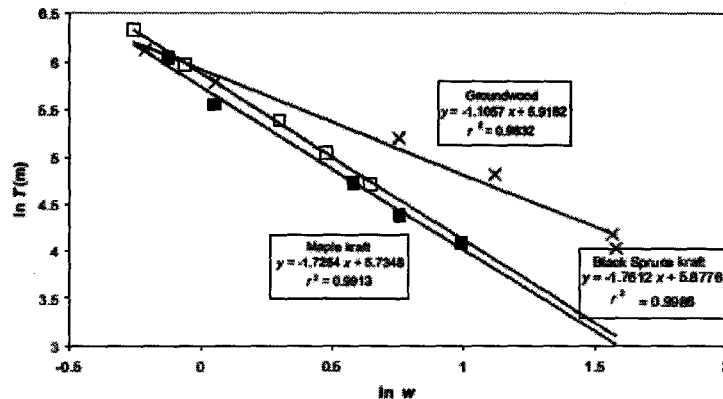


Figure 1.1 The influence of moisture content w on the wet-web tensile strength of three fiber pulps (Adapted from Shallhorn 2002)⁴

However, two mechanisms were put forward for low and high solid content by Lyne *et al.*⁵ In the low solid content, the surface tension plays the main

role in the increase of wet-web strength. To prove this, surfactants were added and low strength was observed. (As shown in Fig 1.2)

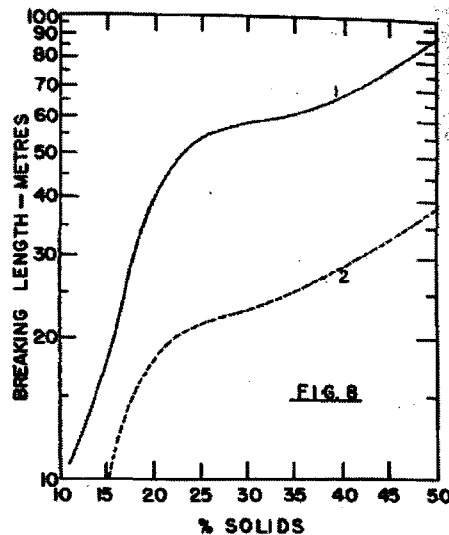


Figure 1.2 The effect of surfactant on wet-web strength. 1-groundwood pulp, 2-groundwood pulp with the addition of 0.1% of surfactant (Adapted from Lyne *et al.*1954) ⁵

For high solid content, the fiber-fiber bonding (entanglement or hydrogen bonding) was proposed as the main control factor. Fig 1.3 shows the wet-web strength curves of glass fibers with different diameters. The glass fibers were used because of their very weak interaction. All curves show a maximum value in the solid content of approximately 25% and then decrease rapidly with the increase of dry content. This data shows the importance of inter-fiber interactions. To verify this control factor, the adhesive agents were added to increase inter-fiber interaction of glass fibers and the results are shown in Fig 1.4. When bonding agents were added, the curves showed two striking inflections, which were compatible with the explanation of the two mechanisms provided before. In other words, when solid content was lower than 25%, the surface tension mainly contributed to the bonding strength. However, if dried content was higher than 25%, the interfiber or adhesive bonding played a main role in the wet-web strength.

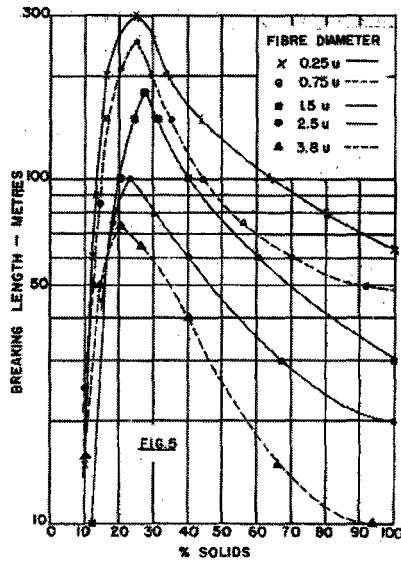


Figure 1.3 The wet-web strength of glass fibers with different diameters (Adapted from Lyne *et al.*1954)⁵

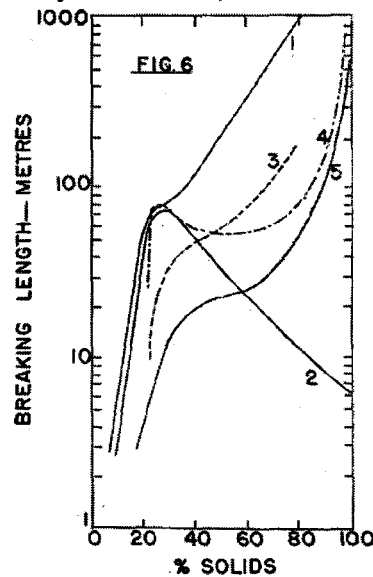


Figure 1.4 The influence of different adhesive agents on wet-web strength. 1-original pulp, 2-glass fibers without bonding agents, 3-glass fibers with the addition of hydrofluoric acid and gelatin, 4-glass fibers with the addition of sodium silicate, 5-glass fibers with the addition of hydrofluoric acid and gelatin (Adapted from Lyne *et al.*1954)⁵

For the transition region between low and high solids contents, the mechanism of wet-web strength is unclear.

van de Ven *et al.* studied the influence of polyelectrolyte on the wet-web strength. It is plausible that the addition of polyelectrolyte will increase wet-web strength through enhancing interfiber bonding. However, the experiment results showed that cationic polyacrylamide was detrimental to the wet-web strength (shown in Figure 1.5). The explanation was that the introduction of the polyelectrolyte resulted in a stronger steric and electrosteric repulsion, which reduced the friction force and made fibers easier to slide.⁶

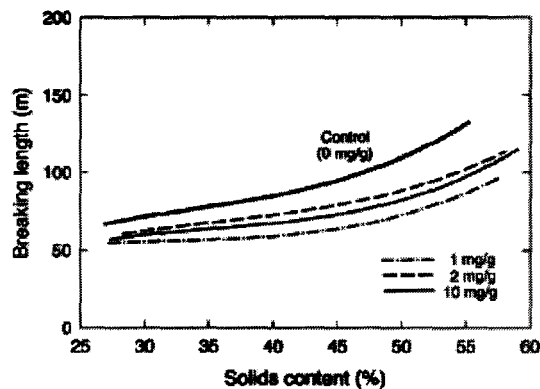


Figure 1.5 The influence of adding cationic polyacrylamide on wet-web strength of unbeaten Kraft fibers (Adapted from Alinec *et al.* 2006)⁶

The current methods to increase the wet-web strength in industry are to decrease the water content, increase fiber length or beat the cellulose to increase the fibers' ratio surface area. However, any method mentioned above increases cost. Furthermore, the change of conditions can cause negative effects. For example, the temperature was increased to decrease water content but, at the same time, the wet-web strength dropped 1% per °C of the increase of temperature.⁷ Therefore, an effective and inexpensive wet-web strength agent is urgently needed to address the wet-web strength problem in modern papermaking.

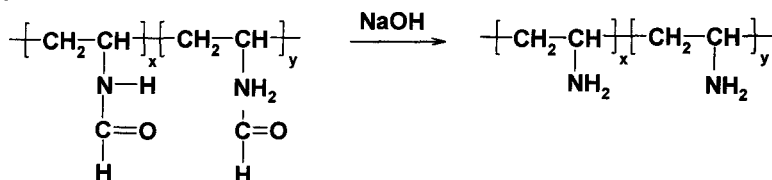
Based on the analysis above, wet-web strength can be enhanced in two ways. One is surface tension, the other is interfiber bonding. Surface tension is controlled by the property and temperature of the solution, which are hard to control. Thus, the only remaining opportunity to acquire a high wet-web strength lies in the enhancement of interfiber bonding. The surface of cellulose is a hydrogel-like layer.⁸ The abundance of water produces a strong contest with

bonding agents and, thus, results in a strong hydrolysis effect on the potential bonding of wet adhesion additives. From the angle of forces in natural environments, there exist three types of interaction. They are 1) basic interaction force 2) specific interaction and 3) covalent bonds. Basic interaction force includes van der Waals, electrostatic, hydrogen bonding, hydrophobic and steric interaction. Those forces are also called non-specific forces. In contrast, specific interactions consist of a combination of several of the above forces and show a much stronger interaction. Specific force needs a strict conformation and distance limitation and is consequently also named a “lock-and-key” or “ligand-receptor” interaction.¹⁰ Last but not least, covalent bonds provide the strongest strength in most cases (typical dissociation energy is 437 kJ/mol¹¹). However, in some cases, the electrostatic (typical dissociation energy is 412 kJ/mol⁶) or other non-specific interaction can show a very strong interaction which is decided by distance, shape or other factors. It is well known that electrostatic, van der Waals and hydrogen bonding can be destroyed or made very weak in aqueous environments. For specific interaction, there need to be a very complicated and intricate spatial structure. It is difficult to design one specific interaction for cellulose. Cellulose binding domain is a good example, however, the high cost limits its application in papermaking.⁹ Thus, the only option for good wet-web strength is to form covalent bonds. Therefore, a) water stable b) instantaneously reactive in an aqueous environment (needed for the papermaking process) and c) strong bonding in an alkaline condition (for modern papermaking needs) are the three basic requirements for a good wet-web strength agent. It is often difficult to form a strong adhesive joint with a wet surface, particularly when the substrate is a swollen hydrogel, such as cellulose. Dr. Chen Lu proposed that the covalent bonding of polyvinylamine-boronate to cellulose could be used to provide high wet-web strength in papermaking process.¹²

1.2 An introduction of PVAm and boronic acid

1.2.1 PVAm and its application in papermaking

Polyvinylamine (PVAm) was invented 50 years ago. However, it has not been realized in industry until the 1990s by BASF, Mitsubishi and Air Products. In the BASF product, PVAm is hydrolyzed from polyvinylformamide (PNVF), which is polymerized from N-vinylformamide. The synthetic process is shown in Scheme 1.3.



Scheme 1.3 The synthetic process of PVAm

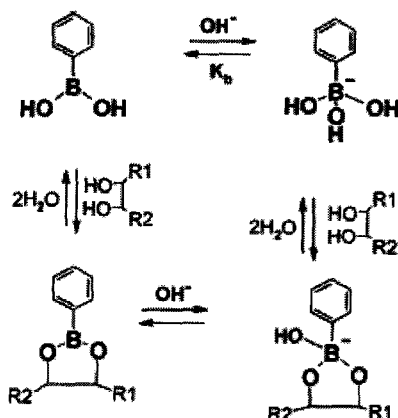
Weisgerber first reported that PVAm worked as a conventional paper strength agent.¹³ Hong *et al.* studied the adhesion behaviors of PNVF and PVAm by using newsprint paper as a model.¹⁴ Their results can be summarized as follows: PNVF shows good dry strength but weak wet strength (wet strength is a “rewet strength”, that is, the ability of a dry paper web to resist breakage after soaking in water). And PNVF-PVAm copolymer shows good wet strength when the hydrolysis degree is up to 56%. In comparison, PVAm awards good wet and dry strength. However, along with polyetheneimine (PEI), the mechanism of PVAm is still an issue to be addressed.

DiFlavio *et al.* studied the mechanism of PVAm wet strength and showed that drying at 23 °C and 50% humidity is sufficient to demonstrate a good wet strength. It is proposed that both electrostatic and covalent bondings contribute to the high adhesion.⁸ Oxidation of cellulose to introduce aldehyde groups is very important to get a high adhesion. Another interesting point which needs to be emphasized is that the adhesion force eventually increased and finally remained constant with the increase of the PVAm amounts applied between cellulose membranes.¹⁵ With the increase of PVAm thickness, the possible fracture mechanism changed from adhesion only to the combination of adhesion and cohesion. The above results indicated that PVAm applied between regenerated cellulose membranes showed high cohesion strength. However, it is known that PVAm itself has an excellent solubility in aqueous solutions, that is, low cohesion strength was expected in PVAm adhesion. The mechanism for this result is still unknown. Entanglement of polymer chains and penetration into cellulose membranes are possible reasons.

The wet adhesion experiment results showed that pure PVAm systems could enhance wet-web strength no more than 5%. Therefore, the introduction of boronic acid is important to prepare a high wet-web strength in papermaking industry.

1.2.2 Boronic acid and its complexation with diols

Boronic acid is an important chemical in inorganic chemistry. Boronic acid is a Lewis acid. A property of boric acid is that it can react with polyol containing substances in alkaline condition (as shown in scheme 1.4). The weak strength and reversible bonding are other special properties of this bond. For example, the equilibrium constant of boronic acid for bonding to glucose is 26 L/mol which corresponds to a free energy of -1.9 kcal/mol which is less than a hydrogen bond.¹⁶



Scheme 1.4 The interaction of phenylboronic acid and diols-containing substances (Adapted from Keita *et al.* 1995)¹⁷

The first report of the complexation of boronic acid with polyol was published in 1842¹⁸ and the interaction of boronic acid saccharide was first reported in 1954.¹⁹ These works have since attracted huge attention. Today, there are dozens of papers published that make use of the covalent bonds between boronic acids and diols.^{20,21} Among these works, two fields are most interesting. One is boronic acid based fluorescent probes. For example, Shinkai *et al.* made a saccharide responsive fluorescence substance, which made use of the neighboring amine group to influence fluorescence.²² The other is the glucose sensitive systems which contain boronic acid as responsible sites. For example, Hoare *et al.* prepared a series of boronic containing microgels, which showed good responsive properties to the change of glucose in the environment.²³

The most common methods to study the complexation of boronic acid and diols are NMR and fluorescence.^{24,16} For example, Wang *et al.* used Alizarin Red S (ARS) as a fluorescent probe to monitor the interaction of boronic acids and diols.(as shown in Fig 1.6)

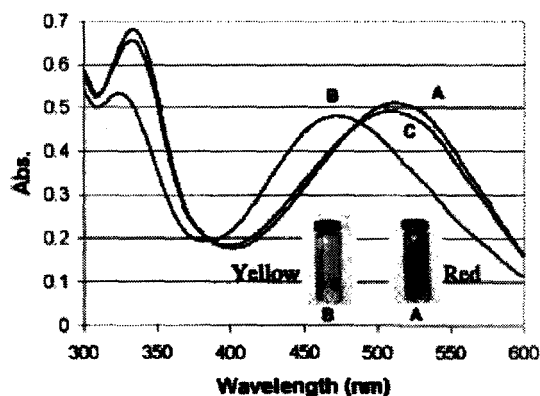


Figure 1.6 Fluorescence intensity of ARS at 10^{-4} M in pH=7.4. (A): ARS, (B): ARS+ Phenylboronic acid, (C): ARS+ Phenylboronic acid + Fructose. (Adapted from Springsteen *et al.* 2002)¹⁶

The reaction speed of boronic acids and diols is very quick. They began to react instantaneously as long as they were mixed together. The kinetic curves of interaction between boronic acid and glucose are shown in Fig 1.7.

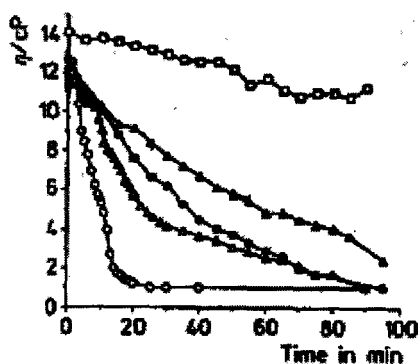


Figure 1.7 The viscosity change of boronic acid containing system with time. The upper curve of rectangular boxes represents the viscosity of the blank solution without any glucose. The other curves represent the viscosities of the solutions with the addition of different concentrations of glucose. (Adapted from Kitano *et al.* 1991)²⁵

1.3 Microgels as wet-web-strength enhancing agent

Microgels are polymers cross-linked by physical or chemical cross-linkers. The typically average sizes of microgels are between 50 nm to 5 μ m. The

most interesting property of microgels is that their volume can swell or shrink according to environmental conditions. In essence, they are three dimensional polymer networks.

Paper wet-web strength experiments show that the breakage occurs among fiber-fiber contact areas instead of within the fiber itself. Thus, it is necessary to enhance the bonding of the inter fiber to acquire high wet adhesion of the paper web. Because of the coarse property of fibers, there are many gaps among the paper web. This contributes to the low wet strength of paper. But this also provides a location for the work of some adhesive fillings. Theoretically, the monolayer adsorption of linear polymers limits their maximum adsorption amounts and, therefore, the filling effect to the web gaps. Only at a very close distance can interactions work, no matter which type they are. The furthest distance is van der Waals' interaction; its functional range is shorter than 10\AA . Although several polysilicate based microgels were applied in papermaking,²⁶ there are few reports about microgels used for enhancing wet strength.

Miao *et al.* prepared a series of PVAm microgels with different average sizes and cross-linking degrees and studied their application in papermaking. The wet strength of linear PVAm and microgels was compared in three application conditions. (1) With impregnated filter paper, linear PVAm showed a higher wet strength. (2) In the handsheet experiments, microgels displayed a higher wet strength. (3) In the peeling test of cellulose membranes, both linear polymers and microgels had the same strength. The results indicated that microgels can adsorb more on fibers than on linear polymers, but their big dimension limited the penetration of microgels into fibers. By contrast, linear PVAm had a smaller adsorption amount on fibers, but was easier to impregnate into the gaps between fibers.^{27, 28} In addition, the results from delaminating regenerated cellulose membranes showed that the highest wet strength was not observed for the large and highly cross-linked microgels.²⁷

1.4 Objective

The objectives of this thesis are to study the solution property of PVAm-PBA, investigate the reason that PVAm-PBA shows a high wet adhesion to cellulose, which groups on cellulose can react with boronic acid, probe the affecting of pH, degree of substitution, molecular weight, salt concentration and adding sugars on the wet adhesion of PVAm-PBA to cellulose, discuss the potential application of PVAm-PBA in papermaking industry, preparation and characterization of narrowly distributed PVAm microgels and the comparison of wet adhesion of linear boronate containing polymers to boronate containing microgels to cellulose.

1.5 Thesis Outline

Chapter 1: Introduction and Literature Review. This chapter presents the background and literature reviews of this work, the objectives and outlines of this thesis.

Chapter 2: Solution Properties of Polyvinylamine boronate. This chapter studies the solution properties of PVAm-PBA in terms of surface mobility, phase diagrams, solution viscosity and surface tension. A model based on the dissociation of PVAm and phenylboronic acid is presented in this chapter to predict the ionization of PVAm-PBA. The work in this chapter was submitted in October, 2008.

Chapter 3: Wet Adhesion of Polyvinylamine boronate to cellulose. In this chapter, all influential factors, including adsorption pH, final pH, molecular weight of PVAm-PBA, salt concentration, the addition of sugars and degree of substitution, are systematically studied. A contour plot of adhesion force based on adsorption pH and final pH is developed. A model predicting the influence of sugars addition on adhesion is set up and agrees well with experimental results. A paper has been published based on part work in this chapter.¹²

Chapter 4: An Investigation of the interaction between cellulose and Polyvinylamine boronate. In this chapter, the interaction mechanism of boronic acid and cellulose is investigated. A theoretical analysis of cellulose-boronic acid interaction, which is based on the interaction of boronic acid and small molecular sugars, is processed and a hypothesis of the mechanism is proposed. The interaction of boronic acid and two model polymers, dextran and hydroxyethylcellulose, are investigated to provide experimental evidences to prove the hypothesis.

Chapter 5: Preparation and Characterization of Narrowly Distributed Polyvinylamine Microgel. This chapter proposed a simple methodology to make PVAm microgels. For the first time, narrowly distributed PVAm microgels are prepared. The influential factors, *e.g.* solution pH, salt concentration, stirring speed, storage time *etc.*, are investigated based on the size and distribution of microgels. The obtained PVAm microgels are characterized by using light scattering, electrophoresis and transmission electron microscope facilities.

Chapter 6: Boronate Microgels Adhesion to Wet Cellulose. Presented in this chapter are the preliminary results of boronate microgel adhesion to wet cellulose. Two microgels, polyNIPAM and PVAm, are employed as the materials. Both microgels show substantially higher wet adhesion to cellulose after modified with boronate. In addition, boronate PVAm microgels show a high adhesion which is never obtained from linear PVAm-PBA.

Chapter 7: Concluding Remark. This chapter summarizes the major contribution of this thesis.

Reference

1. Gurnagul, N.; Seth, R. S., Wet-web strength of hardwood kraft pulps. *Pulp & Paper Canada* **1997**, *98*, (9), 44-48.
2. Pelton, R.; Lu, C., POLYMERIC BORONIC ACID DERIVATIVES AND THEIR USE FOR PAPERMAKING. In WO Patent WO/2006/010,268: **2006**.
3. Rojas, O. J.; Hubbe, M. A., The dispersion science of papermaking. *Journal of Dispersion Science and Technology* **2004**, *25*, (6), 713-732.
4. Shallhorn, P. M., Effect of moisture content on wet-web tensile properties. *Journal of Pulp and Paper Science* **2002**, *28*, (11), 384-387.
5. Lyne, L. M.; Gallay, W., Measurement of wet-web strength *Tappi Journal* **1954**, *37*, 694-698.
6. Alince, B.; Vanerek, A.; de Oliveira, M. H.; van de Ven, T. G. M., The effect of polyelectrolytes on the wet-web strength of paper. *Nordic Pulp & Paper Research Journal* **2006**, *21*, (5), 653-658.
7. Back, E. L.; Andersson, L. I., The Effect of Temperature on Wet Web Strength Properties. *Tappi Journal* **1993**, *76*, (5), 164-172.
8. Pelton, R., On the design of polymers for increased paper dry strength - A review. *Appita Journal* **2004**, *57*, (3), 181-190.
9. Levy, I.; Shani, Z.; Shoseyov, O., Modification of polysaccharides and plant cell wall by endo-1,4-beta-glucanase and cellulose-binding domains. *Biomolecular Engineering* **2002**, *19*, (1), 17-30.
10. Leckband, D.; Israelachvili, J., Intermolecular forces in biology. *Quarterly Reviews of Biophysics* **2001**, *34*, (2), 105-267.
11. Neimo, L., *Papermaking Chemistry: 4 (Papermaking science and technology)* TAPPI: **1999**; p 329.
12. Chen, W.; Lu, C.; Pelton, R., Polyvinylamine boronate adhesion to cellulose hydrogel. *Biomacromolecules* **2006**, *7*, (3), 701-702.
13. Weisgerber, C. A. Wet-strength paper Oct 18, 1955, 1955.
14. Hong, J.; Pelton, R., The surface tension of aqueous polyvinylamine and copolymers with N-vinylformamide. *Colloid and Polymer Science* **2002**, *280*, (2), 203-205.
15. DiFlavio, J. L.; Bertoia, R.; Pelton, R.; Leduc, M. In *The Mechanism of Polyvinylamine Wet-Strengthening*, 13th Fundamental Research Symposium, Cambridge, UK, 2005; FRC: Cambridge, UK, **2005**; pp 1293-1316.
16. Springsteen, G.; Wang, B., A detailed examination of boronic acid-diol complexation. *Tetrahedron* **2002**, *58*, (26), 5291-5300.
17. Keita, G.; Ricard, A.; Audebert, R.; Pezron, E.; Leibler, L., The Poly(Vinyl Alcohol) Borate System - Influence of Polyelectrolyte Effects on Phase-Diagrams. *Polymer* **1995**, *36*, (1), 49-54.
18. Deutsch, A.; Osoling, S., Conductometric and potentiometric studies of the stoichiometry and equilibria of the boric acid-mannitol complexes. *Journal of the American Chemical Society* **1949**, *71*, 1637-40.

19. Kuivila, H. G.; Keough, A. H.; Soboczinski, E. J., Areneboronates from diols and polyols. *Journal of Organic Chemistry* **1954**, *19*, 780-3.
20. De Geest, B. G.; Jonas, A. M.; Demeester, J.; De Smedt, S. C., Glucose-responsive polyelectrolyte capsules. *Langmuir* **2006**, *22*, (11), 5070-5074.
21. Islam, T. M. B.; Yoshino, K.; Sasane, A., B-11 NMR study of p-carboxybenzeneboronic acid ions for complex formation with some monosaccharides. *Analytical Sciences* **2003**, *19*, (3), 455-460.
22. Kawanishi, T.; Romey, M. A.; Zhu, P. C.; Holody, M. Z.; Shinkai, S., A study of boronic acid based fluorescent glucose sensors. *J Fluoresc FIELD Full Journal Title: Journal of fluorescence* **2004**, *14*, (5), 499-512.
23. Hoare, T.; Pelton, R., Charge-switching, amphoteric glucose-responsive microgels with physiological swelling activity. *Biomacromolecules* **2008**, *9*, (2), 733-740.
24. Norrild, J. C.; Eggert, H., Evidence for Mono- and Bidentate Boronate Complexes of Glucose in the Furanose Form. Application of $^1\text{J}_{\text{C-C}}$ Coupling Constants as a Structural Probe. *Journal of the American Chemical Society* **1995**, *117*, (5), 1479-84.
25. Kitano, S.; Hisamitsu, I.; Koyama, Y.; Kataoka, K.; Okano, T.; Sakurai, Y., Effect of the incorporation of amino groups in a glucose-responsive polymer complex having phenylboronic acid moieties. *Polymers for Advanced Technologies* **1991**, *2*, (5), 261-4.
26. Moffett, R. H., On-Site Production of a Silica-Based Microparticulate Retention and Drainage Aid. *Tappi Journal* **1994**, *77*, (12), 133-138.
27. Miao, C. W.; Pelton, R.; Chen, X. N.; Leduc, M., Microgels versus linear polymers for paper wet strength - size does matter. *Appita Journal* **2007**, *60*, (6), 465-468.
28. Miao, C. W.; Chen, X. N.; Pelton, R., Adhesion of poly (vinylamine) microgels to wet cellulose. *Industrial & Engineering Chemistry Research* **2007**, *46*, (20), 6486-6493.

Chapter 2

Solution Properties of Polyvinylamine Derivatized with Phenylboronic Acid

2.1 Introduction

The borate ion, $B(OH)_4^-$, and alkyl substituted borates (*i.e.* boronates) are known to condense with carbohydrates¹ to give usually 5 or 6 member rings. The condensation occurs in water under mild alkaline conditions and is characterized by low binding constants that are specific to the carbohydrate.² Reversible, selective borate-carbohydrate binding has stimulated much literature describing the development of affinity columns^{3,4} based on immobilized borate ions and a number of glucose detection strategies based on fluorescent boronates⁵⁻⁷ and boronate hydrogels⁸⁻¹¹. Furthermore, many of these publications described the preparation of synthetic, water-borne polymers bearing boronate groups. More specifically, the boronate moieties are usually a derivative of phenylboronic acid (PBA). The PBA-containing polymers can be prepared either by free radical copolymerization with a vinyl-PBA monomer⁵, or by covalent coupling of activated PBA derivatives to a polymer.¹²⁻¹⁵

Our interest in PBA-containing polymers arose from the discovery that PBA derivatives of polyvinylamine (PVAm) displayed remarkable instantaneous adhesion to wet cellulose.¹⁶ In working with polyvinylamine-boronate (PVAm-PBA, see Scheme 2.1) polymers, we observed a strong tendency of the copolymers to phase separate depending upon pH and the degree of boronate substitution. In spite of the large number of publications involving water-borne boronate polymers, we found little information about the strong influence of PBA on solubility and surface tension of PBA-containing polymers. It seems that the phenylboronic acid group is hydrophobic. Herein we present the solution properties of PVAm-PBA as functions of pH, ionic strength, the level of boronate substitution, and the molecular weight. Although we present results for only one type of boronate, the PVAm derivatives, we believe that our results have implications for the wide range of linear polymers and gels that have been of interest in many applications.

2.2 Experimental section

2.2.1 Materials

Polyvinylamine samples with molecular weights of 15 kDa and 150 kDa were obtained from BASF. To ensure complete hydrolysis from poly (N-vinyl formamide), the polymers were treated further under nitrogen purge with 5%

NaOH at 70°C for 48 hours to remove residual formamide groups. The polymers were dialyzed against water for ten days using regenerated cellulose dialysis tubing (Spectra/Por® 4 product No: 132684 12kDa molecular weight and PVAm Spectra/Por® 4 product No: 132724 3500 Da molecular weight cut-off, Spectrum Laboratories, Inc.) and were subsequently freeze-dried. 4-carboxyphenylboronic acid, N-(3-dimethylaminopropyl)-N'-ethylcarbodiimide hydrochloride (EDC), 2-(N-morpholino) ethanesulfonic acid (MES) and fructose were purchased from Sigma-Aldrich and used as received. All experiments were performed with water from a Millipore Milli-Q system.

A series of PVAm pendant phenylboronic acid groups (PVAm-PBA) were synthesized using the method described in our previous publication – see Scheme 2.1.¹⁶ In a typical experiment, 0.2 g of PVAm was dissolved in 10 mL 0.1M MES buffer at pH 6.1 and 90 mL of 3 g/L 4-carboxyphenylboronic acid in the same buffer; 8 g EDC were added and the mixture was stirred for 120 min at 25 °C. The product was dialyzed against water for two weeks. Proton NMR was used to characterize the degree of substitution (DS) and the properties of the PVAm-PBA copolymers are summarized in Table 2.1. ¹H NMR experiments were performed at an AVANCE200 NMR instrument (Bruker) with 200 MHz at room temperature. A small amount of DCl in D₂O was used to dissolve the PVAm-PBA samples with high DS.

The charge-pH properties of PVAm-PBA copolymers were probed by electrophoresis measurements. To facilitate the measurements, the copolymers were adsorbed onto 200 nm anionic polystyrene latex (Bangs Laboratories, Inc.) and electrophoretic mobility measurements were made at 25 °C using a ZetaPlus from Brookhaven Instruments Corporation using PALS (phase analysis light scattering) Software Version 2.5. The reported values were based on 5 measurements with 25 cycles for each.

The phase behaviours of the polymer solutions were determined by optical transmittance using a Beckman DU800 UV-vis. Spectrophotometer. The solutions were considered single phase if the transmittance at 600 nm was higher than 99%. The colloiddally dispersed regions corresponded to transmittance values between 90% and 99% whereas more turbid solutions contained macroscopic precipitates which settled quickly.

Potentiometric and conductometric titrations were performed simultaneously with a PC-Titration Plus (ManTech Associates) at 25 °C. In a typical experiment, 50 mL 0.01 % PVAm-PBA was prepared in a 5 mM KCl solution and the pH was adjusted to 3.0. The solution obtained was titrated by 0.1 M NaOH to pH 11. The addition rate was 1 drop per 30 seconds, using increments between 0.0001 and 0.04 mL. The conductometric titration was used to determine the total content of titratable acid. The degree of neutralization at

intermediate pH values was calculated as the difference in the difference between the base consumed in a blank titration and the polymer titration divided by the total titratable acid.

Intrinsic viscosity measurements were made to identify changes in PVAm-PBA configuration with pH change. Polymers were dissolved into a 0.3 M salt solution and the pH was adjusted to required values using 1 M NaOH and HCl. An Ubbelohde capillary viscometer (size 75, Cannon Instrument Company) was used to measure the viscosity of PVAm-PBA solutions at 25 °C.

2.2.2 Surface tension measurement

Surface tension was measured by the pendant drop method using a Kruss V1.80 Drop Shape Analyzer. The temperature and humidity were kept at 22 °C and 100%. In a typical experiment, 0.5 wt% PVAm-PBA was dissolved in a 5 mM NaCl solution, and the pH values were adjusted by 0.1 M HCl, or NaOH. Drops were formed using a 1 mL syringe with a 1.43 mm flat needle and the volumes of drop were between 14-22 μL . Surface tension values were recorded as functions of drop lifetime.

2.2.3 Interaction force measurement

The interaction force between spin-coated celluloses and polymers-adsorbed colloidal probes were measured by Dr. Shannon Notley at Department of Applied Mathematics, Research School of Physical Sciences and Engineering, Australian National University. Cellulose spheres in the size range of 10 – 14 μm in radius were used. The cellulose spheres were attached to triangular shaped atomic force microscopy cantilevers (Veeco Inc, USA) with a small amount of epoxy. The spring constant of the cantilevers was measured to be 0.35 N/m using the thermal noise method. A multi-mode scanning probe microscope (Veeco Inc, USA) was used for the measurement of the apparent surface forces between the cellulose surfaces in the absence and presence of the polymeric additives.

2.3 Results

Two PVAm homopolymers, 15 kDa and 150 kDa, were derivatized with 4-carboxyphenylboronic acids to give the seven copolymers summarized in Table 2.1. The structures and proton NMR spectra for PVAm-PBA-4 is shown in Figure 2.1. The PBA content of the copolymers were expressed in Table 2.1 as a degree of substitution we defined as the number of PBA moieties per PVAm nitrogen. These values were determined from the relative areas of the aliphatic and aromatic peaks in the proton NMR spectra.

2.3.1 PVAm-PBA phase behaviour

Substitution of PVAm with phenylboronic acid lowered the water solubility of the polymer. Figure 2.2 shows the phase boundary diagrams for the higher molecular weight (150 kDa) copolymers in Table 2.1. All the 150 kDa copolymers showed both colloidal phase and macroscopic precipitate separation regions. In colloidal phase separation domains, the copolymers were present as a slightly turbid (90 to 99% transmittance at 600 nm) suspension whereas the polymer formed macroscopic precipitates in the macro-phase domain. The most striking observation from the results in Figure 2.2 is that the pH range over which PVAm-PBA was insoluble, increased with the degree of PBA substitution. The 4% copolymer displayed a narrow range, ~ 1.5 pH units whereas the 51% copolymer was insoluble virtually over the whole pH range.

The phase separation domains for the PVAm-PBA copolymers are centered around pH 9 which approximately corresponds to the pH giving zero electrophoretic mobility – see below. We propose that the colloidally stable, phase separated copolymers were electrostatically stabilized. Thus colloidal stability was lost when the pH approached pH 9.

The phase behavior was dependent upon PVAm molecular weight. The PVAm-PBA (DS=4%) based on 15 kDa did not phase separate between pH 1 to 12 in 5 mM NaCl.

PBA substitution also caused soluble copolymer chains to contract slightly compared to the parent PVAm. Figure 2.3 compares the intrinsic viscosity of PVAm-PBA-4 with the parent PVAm at three pH values. For all pH values, PBA substitution lowered the intrinsic viscosity suggesting a more compact configuration in solution. Fructose addition had no effect on intrinsic viscosity.

2.3.2 Charge-pH behaviour of PVAm-PBA

The charge-pH behaviors of the PVAm-PBA copolymers were probed by potentiometric titration and by microelectrophoresis. Figure 2.4 shows the potentiometric titration behavior the three 15 kDa copolymers and the parent PVAm – the data points are experimental whereas the solids lines were calculated with a model described below. The results are displayed as $(1-\beta)$ where β is the degree of neutralization defined as the titrated acid divided by the total titratable acid. Note that for PVAm homopolymer, $(1-\beta)$ is the degree of ionization.

The PVAm curve in Figure 2.4 is approximately linear over the whole pH range reflecting an extreme polyelectrolyte effect, first reported by Katchalsky many years ago¹⁷. The extent of deviation from the PVAm curve displayed by the PVAm-PBA copolymers increased with PVAm substitution. The main

consequence of adding phenylboronate groups was to retard the removal of protons.

In an effort to understand the shapes of the titration curves in Figure 2.4 we modeled the copolymer titrations based on two assumptions: 1) the ionization behavior of the vinyl amine moieties were given by Katchalsky's model¹⁷ as implemented by Feng¹⁸; and, 2) the ionization behavior of the PBA moieties was described by an equilibrium constant which we assigned to equal 5.01×10^{-9} M, the value for 4-carboxyphenylboronic acid⁴. Thus, we ignored interactions between the phenylboronic groups and neighboring primary amines or ammonium groups. The calculated curves, shown as solid lines, show the same general trends as the experimental data. However, the difference between the model and the data was greatest for the polymer with the highest boronate substitution. Therefore, in analogy with small molecule behavior summarized in Scheme 2.2, we propose that electrostatic interactions between the alkyl boronic groups and the ammonium groups inhibit deprotonation at low pH.

We also used the model to estimate the isoelectric points (IEP) for the three PVAm-PBA and the results are also displayed in Figure 2.5. The calculated values are compared to experimental estimates – see below.

Figure 2.5 illustrates the influence of fructose on the potentiometric titration of PVAm-PBA-3. The presence of fructose facilitated the release of protons from the copolymer at low pH.

Microelectrophoresis was also used to probe the charge versus pH behavior of the copolymers. Figure 2.6 shows the electrophoretic mobility of two PVAm-PBA copolymers as functions of pH with and without fructose. The copolymers were adsorbed onto cationic polystyrene latex to facilitate measurements. At low and neutral pH the copolymers were positively charged whereas at high pH the copolymers were negatively charged, reflecting the presence of the charged phenyl borate moieties. The point of zero electrophoretic mobility of PVAm-PBA-1 was 10.3 (model 9.7) whereas PVAm-PBA-2 was at pH 9.8 (model 8.9) reflecting the higher PBA content. The model values were calculated from the ionization model, described above. The model predictions were systematically lower than the electrophoresis results. Finally, the presence of fructose shifted the mobility-pH curves towards lower pH values due to the formation of fructose boronate esters. Similar effects have been reported for small molecule boronates.¹⁹

2.3.3 Surface activity of PVAm-PBA

PVAm is not surface active at low pH, where it is highly charged, whereas it is slightly surface active at high pH (56 mN/m at pH >9) where the degree of

ionization is low.²⁰ Chen et al. showed that benzylic or aliphatic substituents on PVAm greatly increased surface activity particularly at higher pH.²¹ Figure 2.7 shows pendant drop surface tension data as functions of drop age and pH for PVAm-PBA-1, a 15 kDa copolymer. Preliminary experimentation with 150 kDa copolymers gave surface tension curves which continually drifted, never reaching a steady state – Chen et al observed similar behaviors with the hydrophobically modified higher MW PVAm derivatives.²¹

Figure 2.8 shows the equilibrium surface tension values, from Figure 2.7, as functions of pH and the extent of neutralization, β . Also shown, are the corresponding data measured in the presence of 1 M fructose. Fructose bonding to PVAm-PBA-1 did not influence the surface activity of the copolymer as a function of pH. Interestingly, there is no discontinuity in the surface tension versus pH curve at pH 10.3 corresponding to the isoelectric point of PVAm-PBA-1. Thus the polymeric surfactant can be switched from being a negatively charged surfactant to a positive one simply by increasing pH.

2.3.4 Interaction force of cellulose and PVAm-PBA coated colloidal probe

Figure 2.9 shows the interaction force between cellulose and PVAm-PBA coated colloidal probe as a function of pH. With the increase of pH, the charge density of PVAm-PBA decreased. From pH 3.8 to 7, the surface forces may be fit within the limits of constant charge and constant potential with progressively lower surface potentials. At pH 3.8, a surface potential of +39 mV is measured while at pH 7, the surface potential has dropped to +30 mV. At pH 10, however, the data can no longer be fit using DLVO theory and a steric repulsive interaction is observed. The results showed the influence of pH on the conformation of PVAm-PBA.

2.4 Discussion

PVAm-PBA chains have a very high concentration of weakly basic primary amine groups decorated with boronic groups behave as Lewis acids. This combination gives complex pH dependent behaviors which can be partially understood by considering the properties of analogous small molecules. A number of publications have reported the properties of phenylboronic acid derivatives bearing amine groups. A very convincing recent paper from Anslyn's group proposes the structures shown in Scheme 2.2.¹⁹ Structure **1** exists at low pH; the amine is protonated and boron is not charged. Adding base gives structures **2** and **3**. Structure **2**, which contains a B-N dative bond, has been proposed by a number of authors.²² With our PVAm-PBA, dative B-N bond formation should give crosslinking converting the copolymers to hydrogels. However, Anslyn argues that in polar solvents **3** is far more prevalent than **2**. Since we did not observe hydrogel formation, we do not believe that B-N bond

formation is significant in our polymers. Finally, at high pH the model small molecule aminoboronate, **4** in Scheme 2.2, has negatively charged boron and a neutral amine.

For the small molecules in Scheme 2.2, pK_{a1} is approximately 6.5 and pK_{a2} is in the range 9-10.¹⁹ Thus, when titrating an acid solution, the two base-consuming steps in Scheme 2.2 will occur nearly sequentially. By contrast, PVAm displays the archetypical polyelectrolyte effect meaning the effective pK_{a2} value is a strong function of pH.²³ Thus, some of the most acidic primary amines may release protons before the boron becomes negatively charged.

The PBA moieties seem to dominate the phase behavior. The phenyl boronic groups display two influences on the phase behavior. The hydrophobic benzene rings tend to drive phase separation in water whereas the ionized form of boron is hydrophilic. For example, PVAm-PBA-5 becomes soluble when the pH is raised above 10. Under these conditions the amines are mainly not ionized whereas the borates are. However, the copolymers with high PBA contents, PVAm-PBA-6 and PVAm-PBA-7, are phase separated over most of the pH range. In these cases the hydrophobic benzene rings dominate the influence of hydrophilic ionized borate groups.

2.5 Conclusions

The major conclusions of this work are as follows:

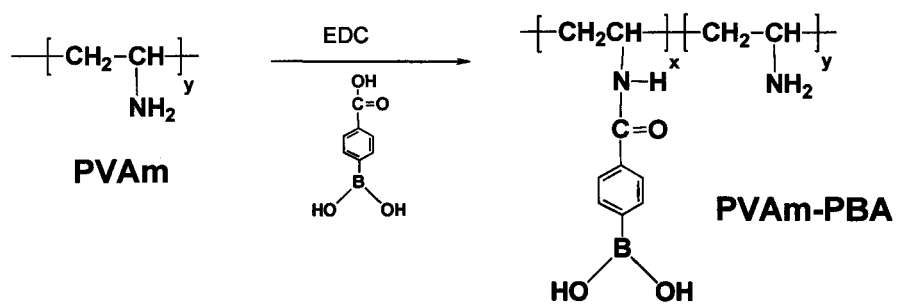
1. PBA derivatization lowers the water solubility of PVAm. For example, PVAm-PBA-7 with 51% substitution is phase separated over most of the pH range whereas PVAm-PBA-4 with 4% substitution is only insoluble at pH 8 to 10.
2. The presence of phenylboronic moieties retards the deprotonation of PVAm at low pH suggesting an acid-base interaction borate and primary amines.
3. Polyvinylamine is slightly surface active at high pH (56 mN/m¹⁵), whereas, surface activity is substantially increased at high pH by adding as little as 4% PBA.
4. Fructose-boronate ester formation increased the PBA ionization at neutral pH values as evidence by potentiometric titration and the electrophoretic mobility of PVAm-PBA adsorbed onto polystyrene latex.
5. The force-distance curve of CPM reflected the steric effect of PVAm-PBA and PVAm-Ph at high pH.

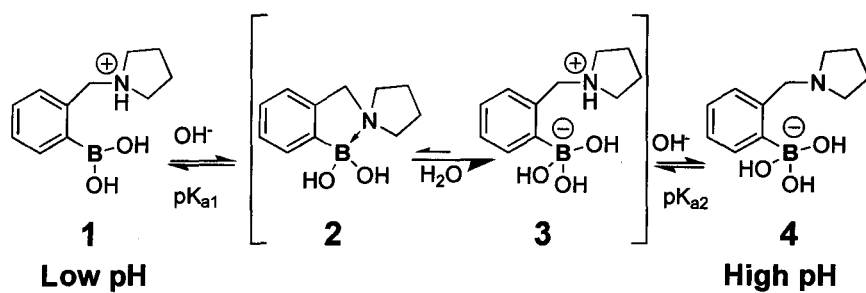
2.6 Tables and Figures

Table 2.1 Polymer compositions and molecular weight. The degree of substitution is the number of substituted function groups per nitrogen atom, and the maximum possible value is 200% corresponding to tertiary amines.

| Sample Name | Degree of Substitution | Molecular Weight (kDa) |
|-------------|------------------------|------------------------|
| PVAm-PBA-1 | 4% | 15 |
| PVAm-PBA-2 | 19% | 15 |
| PVAm-PBA-3 | 30% | 15 |
| PVAm-PBA-4 | 4% | 150 |
| PVAm-PBA-5 | 16% | 150 |
| PVAm-PBA-6 | 29% | 150 |
| PVAm-PBA-7 | 51% | 150 |

Scheme 2.1 Derivatization of PVAm



Scheme 2.2 Anslyn's analysis of amino borate species equilibria ¹⁹

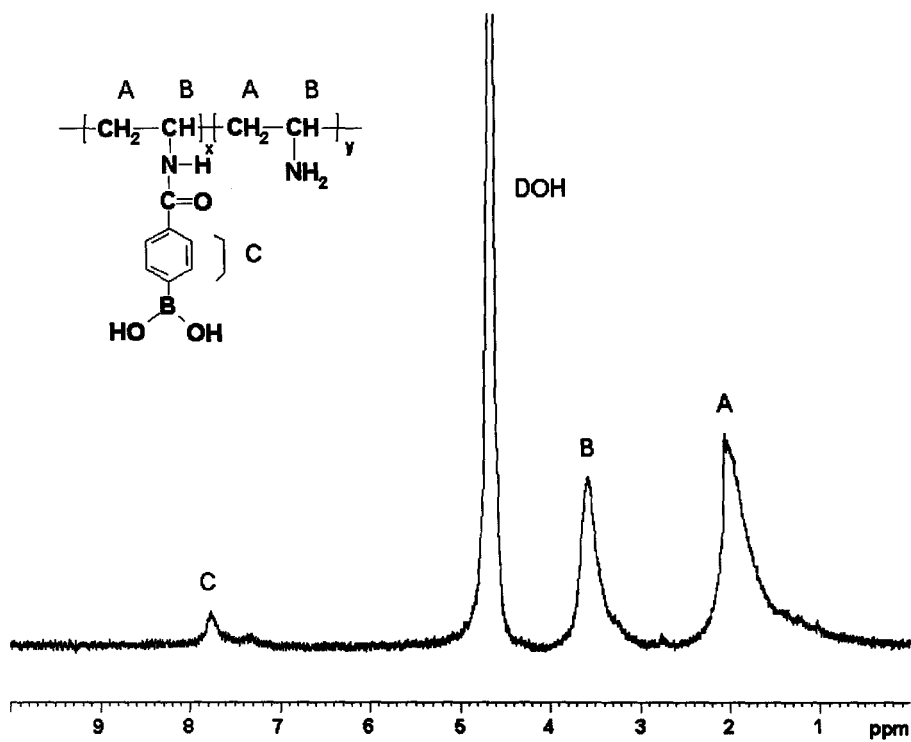
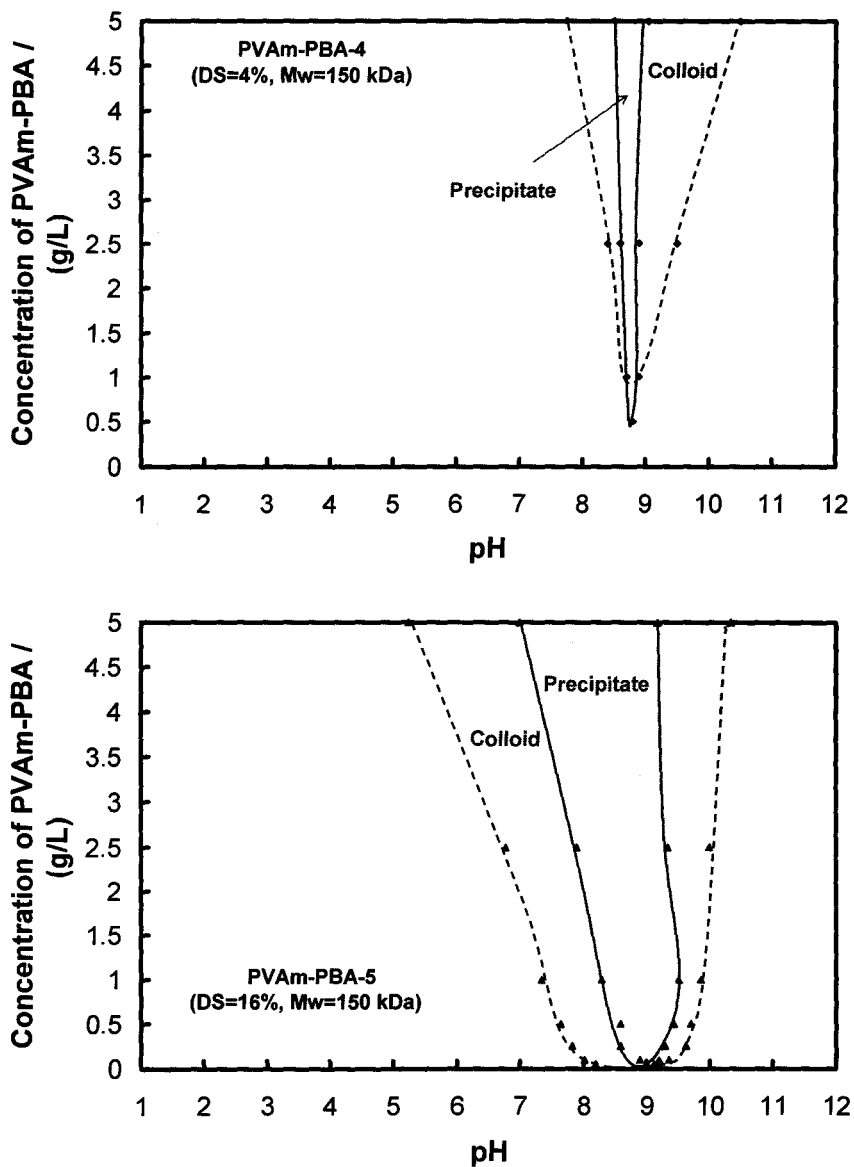
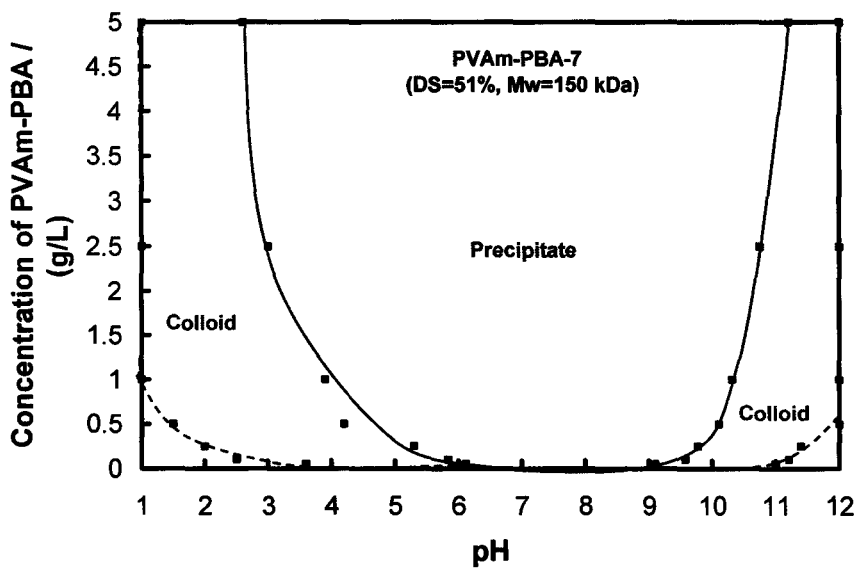
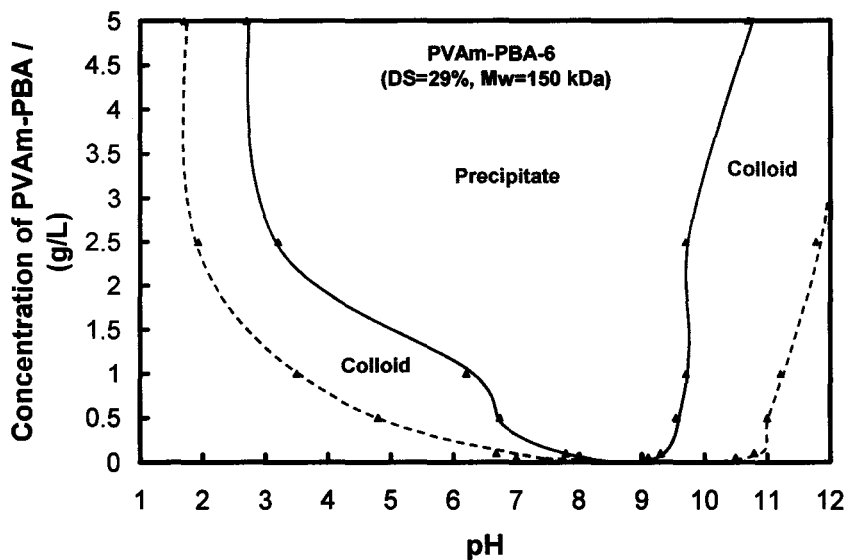


Figure 2.1 ^1H NMR spectra of PVAm-PBA-4 150 kDa

Figure 2.2 Phase boundaries of PVAm-PBA as functions of pH and degree of substitution. All measurements were made in 5 mM NaCl at 25 °C





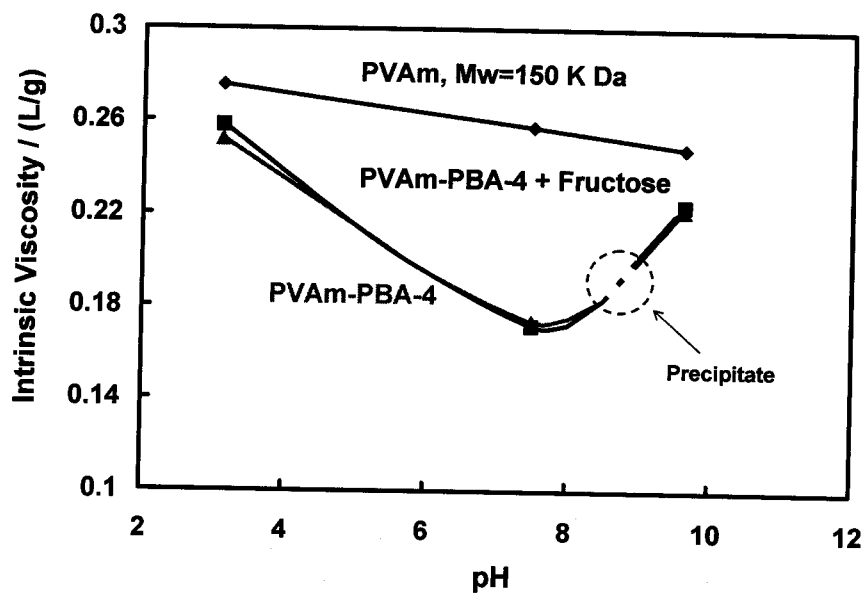


Figure 2.3 The intrinsic viscosity of PVAm, PVAm-PBA-4 and PVAm-PBA-4 plus fructose in 0.3 M NaCl at 25 °C. (Molar ratio of boronic acid to fructose was 1:10.)

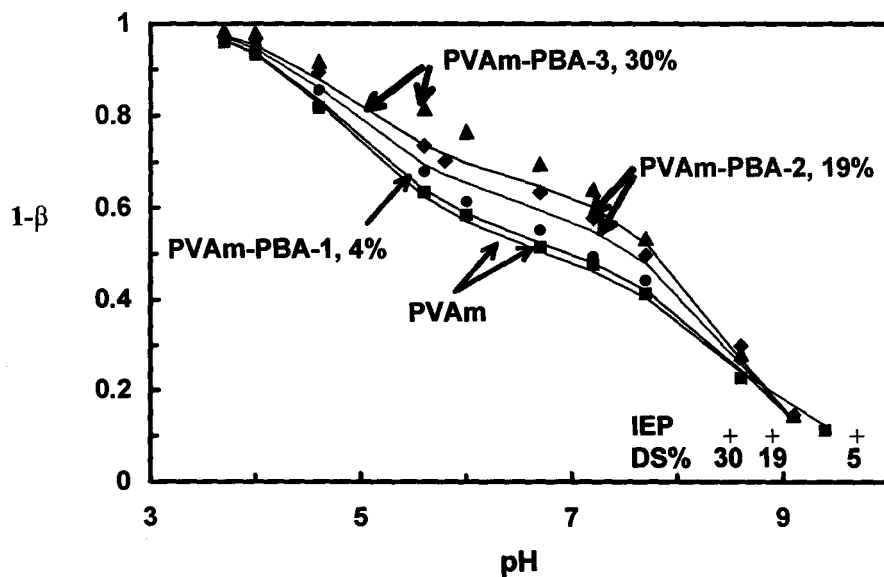


Figure 2.4 Degree of neutralization ($1-\beta$) versus pH for three PVAm-PBA copolymers and the parent PVAm homopolymer. All measurements were performed in 5 mM NaCl at 25 °C. The solid lines were the theoretical curves calculated from the model.

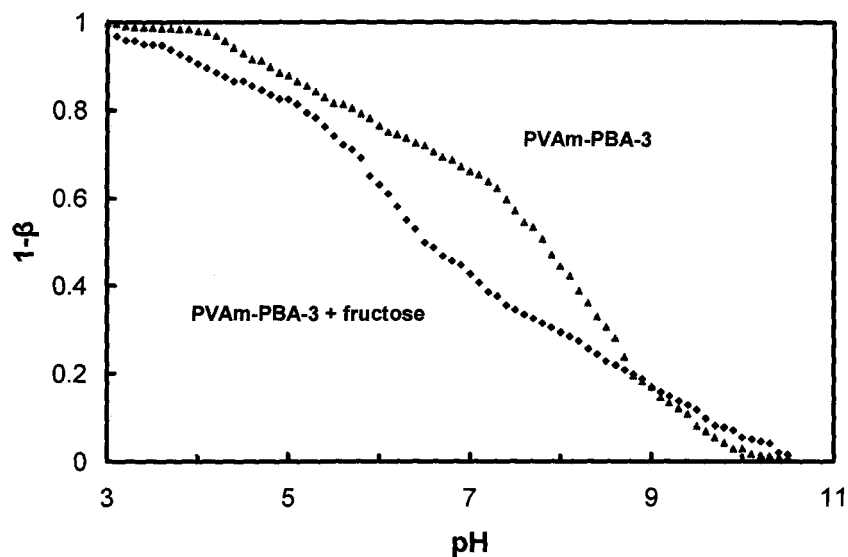


Figure 2.5 The influence of 0.017 M fructose on the ionization behavior of PVAm-PBA-3 (the molar ratio of boronic acid to fructose was 1:10).

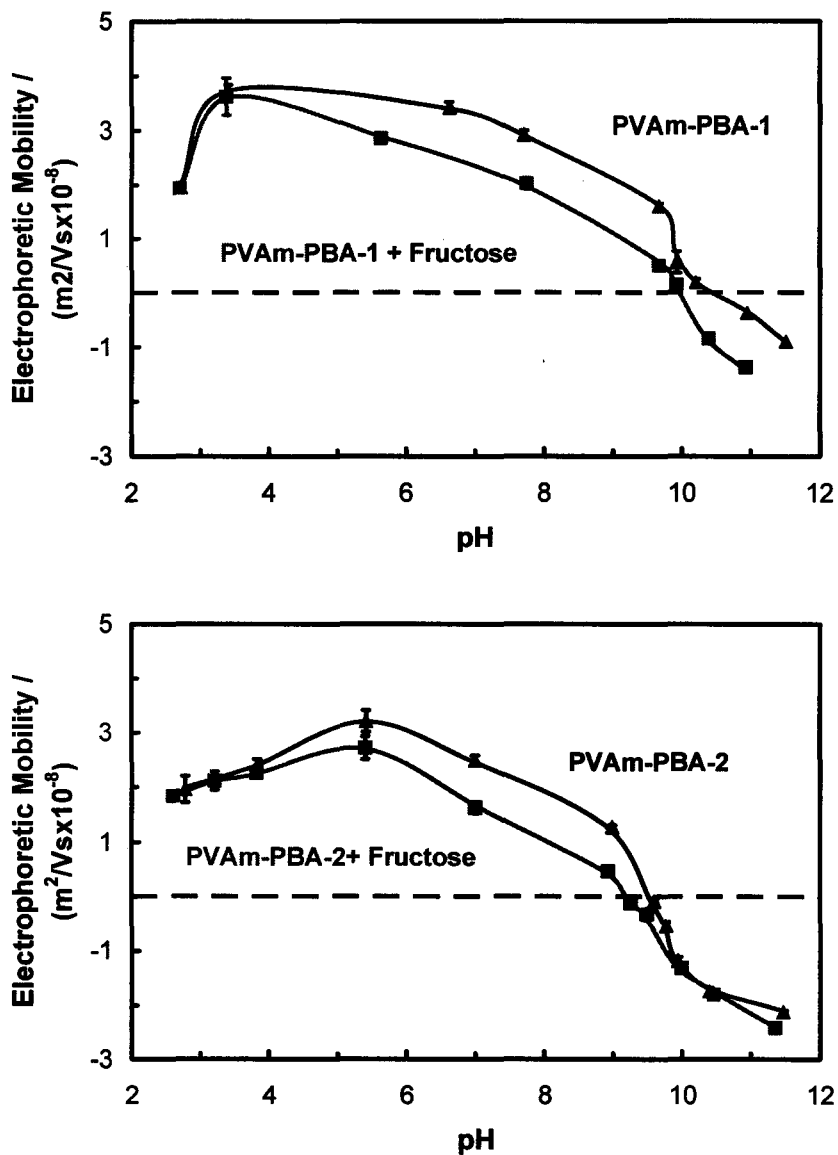


Figure 2.6 Electrophoretic mobility as functions of pH for 0.1 g/L PVAm-PBA adsorbed onto 0.01g/L 200nm diameter anionic polystyrene latex. All measurements were made in 5 mM NaCl aqueous solution at 25 °C. For the experiments with fructose the molar ratio of boronic acid to fructose was 1:10.

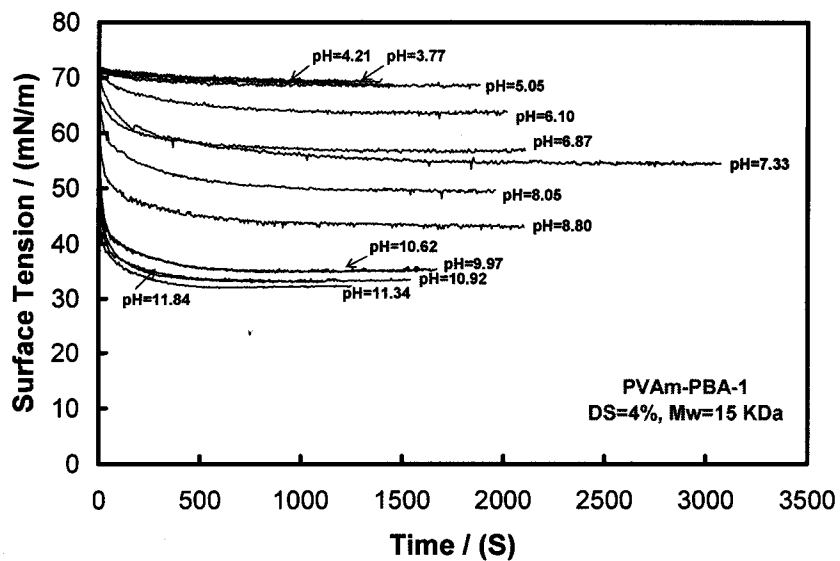


Figure 2.7 Surface tension versus drop age for 0.5 % (wt) PVAm-PBA-1 in 5 mM NaCl as functions of pendant drop age at 22 °C.

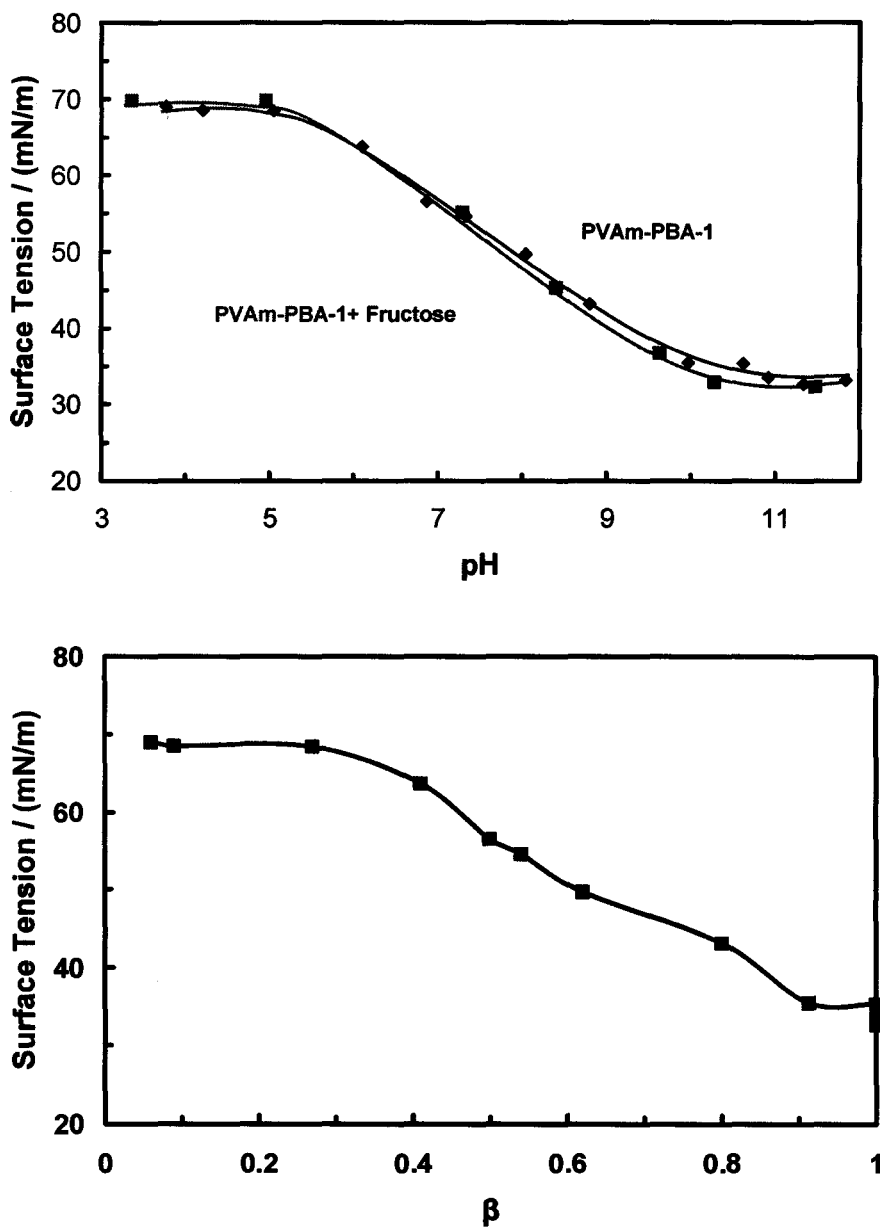


Figure 2.8 Equilibrium surface tension of PVAm-PBA-1 as functions of pH. Molar ratio of boronic acid to fructose was 1:10.

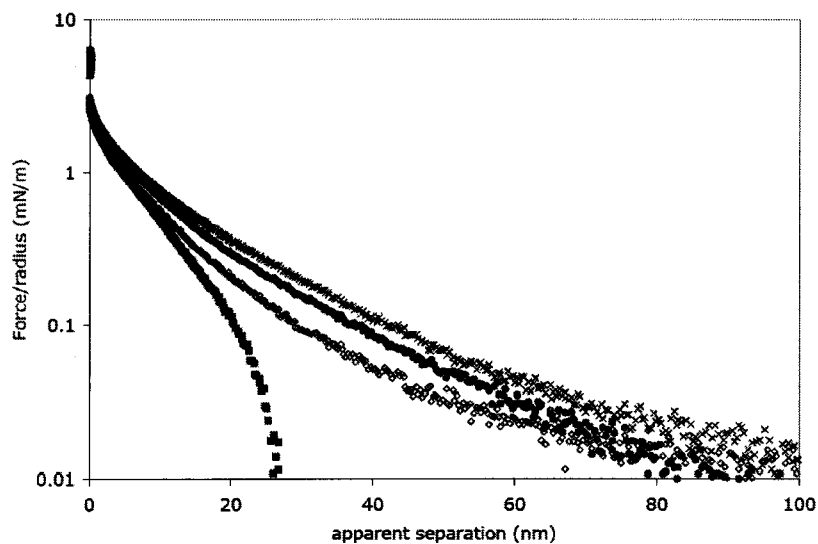


Figure 2.9 Force-distance curves between cellulose surfaces with adsorbed PVAm-PBA as a function of pH. Crosses are pH 3.8, filled circles are pH 5, open diamonds are pH 7 and closed squares are pH 10. The data for pH 3.8, 5 and 7 may be fit to DLVO theory within the limits of constant charge and potential with ψ_0 of + 39 mV, +32 mV and +30 mV respectively. (Adapted from Notley's work, 2008)

References

1. Deul, H.; Neukom, H.; Weber, F., Reaction of boric acid with polysaccharides. *Nature* **1948**, 161, 96-7.
2. Springsteen, G.; Wang, B. H., A detailed examination of boronic acid-diol complexation. *Tetrahedron* **2002**, 58, (26), 5291-5300.
3. Bergold, A.; Scouten, W. H., Borate chromatography. In *Solid phase biochemistry: Analytical and synthetic methods*, Scouten, W. H., Ed. Wiley: **1983**.
4. Soundararajan, S.; Badawi, M.; Kohlrust, C. M.; Hageman, J. H., Boronic acids for affinity-chromatography - spectral methods for determinations of ionization and diol-binding constants. *Analytical Biochemistry* **1989**, 178, (1), 125-134.
5. Kanekiyo, Y.; Sato, H.; Tao, H., Saccharide sensing based on saccharide-induced conformational changes in fluorescent boronic acid polymers. *Macromolecular Rapid Communications* **2005**, 26, (19), 1542-1546.
6. Cordes, D. B.; Gamsey, S.; Sharrett, Z.; Miller, A.; Thoniyot, P.; Wessling, R. A.; Singaram, B., The interaction of boronic acid-substituted viologens with pyranine: The effects of quencher charge on fluorescence quenching and glucose response. *Langmuir* **2005**, 21, (14), 6540-6547.
7. James, T. D.; Sandanayake, K. R. A. S.; Shinkai, S., Chiral discrimination of monosaccharides using a fluorescent molecular sensor. *Nature (London)* **1995**, 374, (6520), 345-7.
8. Hoare, T.; Pelton, R., Engineering glucose swelling responses in poly(*n*-isopropylacrylamide)-based microgels. *Macromolecules* **2007**, 40, (3), 670-678.
9. Lapeyre, V.; Gosse, I.; Chevreux, S.; Ravaine, V., Monodispersed glucose-responsive microgels operating at physiological salinity. *Biomacromolecules* **2006**, 7, (12), 3356-3363.
10. Nolan, C. M.; Serpe, M. J.; Lyon, L. A., Thermally modulated insulin release from microgel thin films. *Biomacromolecules* **2004**, 5, (5), 1940-1946.
11. Zhang, Y. J.; Guan, Y.; Zhou, S. Q., Synthesis and volume phase transitions of glucose-sensitive microgels. *Biomacromolecules* **2006**, 7, (11), 3196-3201.
12. Alexeev, V. L.; Sharma, A. C.; Goponenko, A. V.; Das, S.; Lednev, I. K.; Wilcox, C. S.; Finegold, D. N.; Asher, S. A., High ionic strength glucose-sensing photonic crystal. *Anal. Chem.* **2003**, 75, (10), 2316-2323.
13. Ben-Moshe, M.; Alexeev, V. L.; Asher, S. A., Fast responsive crystalline colloidal array photonic crystal glucose sensors. *Anal. Chem.* **2006**, 78, (14), 5149-5157.
14. Smoum, R.; Rubinstein, A.; Srebnik, M., Chitosan-pentaglycine-phenylboronic acid conjugate: A potential colon-specific platform for calcitonin. *Bioconjugate Chemistry* **2006**, 17, (4), 1000-1007.
15. Winblade, N. D.; Nikolic, I. D.; Hoffman, A. S.; Hubbell, J. A., Blocking adhesion to cell and tissue surfaces by the chemisorption of a poly-l-lysine-graft-

- (poly(ethylene glycol); phenylboronic acid) copolymer. *Biomacromolecules* **2000**, 1, (4), 523-533.
16. Chen, W.; Lu, C.; Pelton, R., Polyvinylamine boronate adhesion to cellulose hydrogel. *Biomacromolecules* **2006**, 7, (3), 701-702.
 17. Katchalsky, A.; Mazur, J.; Spitnik, P., Polybase properties of poly(vinylamine). *Journal of Polymer Science* **1957**, 23, 513-30.
 18. Feng, X.; Pelton, R.; Leduc, M.; Champ, S., Colloidal complexes from poly(vinyl amine) and carboxymethyl cellulose mixtures. *Langmuir* **2007**, 23, (6), 2970-2976.
 19. Zhu, L.; Shabbir, S. H.; Gray, M.; Lynch, V. M.; Sorey, S.; Anslyn, E. V., A structural investigation of the n-b interaction in an o-(n,n-dialkylaminomethyl) arylboronate system. *Journal of the American Chemical Society* **2006**, 128, (4), 1222-1232.
 20. Hong, J.; Pelton, R., The surface tension of aqueous polyvinylamine and copolymers with n-vinylformamide. *Colloid and Polymer Science* **2002**, 280, (2), 203-205.
 21. Chen, X. N.; Wang, Y.; Pelton, R., Ph-dependence of the properties of hydrophobically modified polyvinylamine. *Langmuir* **2005**, 21, (25), 11673-11677.
 22. Wulff, G., Selective binding to polymers via covalent bonds - the construction of chiral cavities as specific receptor-sites. *Pure and Applied Chemistry* **1982**, 54, (11), 2093-2102.
 23. Borkovec, M.; Jonsson, B.; Koper, G. J. M., Ionization processes and proton binding in polyprotic systems: Small molecules, proteins, interfaces and polyelectrolytes. *Surface and Colloid Science Volume 16* **2001**.

2.7 Appendix

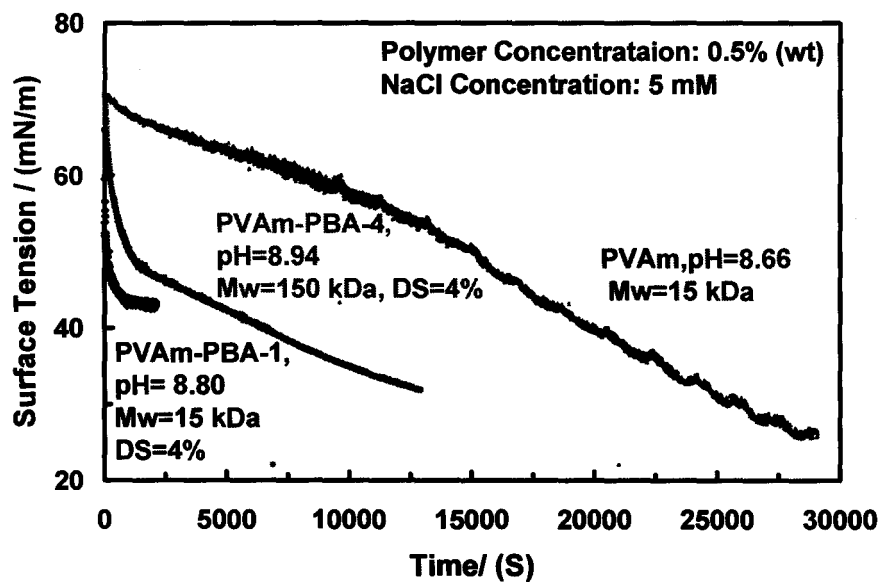


Figure 2.7.1 Comparison of the surface tension of PVAm-PBA-1, PVAm-PBA-4 and PVAm ($M_w = 15$ kDa) as functions of pendant drop age. Measurements were made with a polymer concentration 0.5 wt % in 0.005 M NaCl aqueous solution, 22 °C.

2.7.2 Modeling the ionization behavior of PVAm-PBA

Objective: This calculation is to demonstrate equations which predict PVAm-PBA titrated with NaOH.

Theory: Polyvinylamine and phenylboronic acid dissociate according to their individual ionization behaviors. There is no interaction between boronic acid and amine groups.

The dissociation of phenylboronic acid:

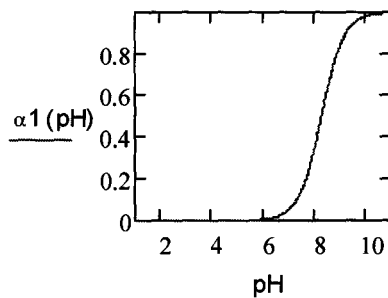
$$k_1 \equiv 10^{-8.3} = 5.0119 \times 10^{-9}$$

K_1 : the binding constant of PBA

$$\alpha_1(\text{pH}) := \frac{\frac{k_1}{10^{-\text{pH}}}}{1 + \frac{k_1}{10^{-\text{pH}}}}$$

$\alpha_1(\text{pH})$: Degree of ionization of PBA

Henderson-Hasselbalch equation



This graph is used to display the definition of $\alpha_1(\text{pH})$ in the formula above.

The dissociation of polyvinylamine: (Adapted from Xianhua Feng's Ph.D. thesis 2007)

$$\alpha \equiv 0.9$$

Degree of ionization of PVAm

$$pK_{pvam}(I) \equiv 8.4 + \frac{3.5 \cdot \frac{I}{\text{mol/L}}}{0.8 + 2 \cdot \frac{I}{\text{mol/L}}}$$

The intrinsic equilibrium constant as a function of ionic strength

$$A \equiv 87$$

Nearest neighbor interaction energy which is not sensitive to ionic strength

$$I \equiv 0.005 \frac{\text{mol}}{\text{L}}$$

Salt concentration

$$x(\alpha) \equiv \frac{A \cdot (2 \cdot \alpha - 1) - 2 \cdot \alpha + [A^2 \cdot (2 \cdot \alpha - 1)^2 + 4 \cdot A \cdot \alpha \cdot (1 - \alpha)]^{0.5}}{2 \cdot (A - 1)}$$

Fraction of doublets, modified Katchalsky's model

$$pH_{pvam}(\alpha, I) \equiv pK_{pvam}(I) + \log \left[\frac{\alpha}{1 - \alpha} \cdot \frac{(1 - 2 \cdot \alpha + x(\alpha))^2}{(\alpha - x(\alpha))^2} \right]$$

pH as function of α

$$\alpha_{pvam}(pH, I) \equiv \text{root}(pH_{pvam}(\alpha, I) - pH, \alpha)$$

α as a function of pH

Comprehensive dissociation results of PVAm-PBA polymers

$$0 \cdot (1 - \alpha_1(\text{pH})) + 1 \cdot (\alpha_{\text{pvam}}(\text{pH}, I))$$

Degree of ionization for PVAm

$$0.04 \cdot (1 - \alpha_1(\text{pH})) + 0.96 \cdot (\alpha_{\text{pvam}}(\text{pH}, I))$$

Degree of ionization for PVAm-PBA, 4%

$$0.19 \cdot (1 - \alpha_1(\text{pH})) + 0.81 \cdot (\alpha_{\text{pvam}}(\text{pH}, I))$$

Degree of ionization for PVAm-PBA, 19%

$$0.3 \cdot (1 - \alpha_1(\text{pH})) + 0.7 \cdot (\alpha_{\text{pvam}}(\text{pH}, I))$$

Degree of ionization for PVAm-PBA, 30%

Data from experiments:**PVAm**

| | | | |
|-------|---------|--------------------|------------|
| pH := | (3.7) | $\alpha_{PVAm} :=$ | (0.9593) |
| | 4 | | 0.9312 |
| | 4.6 | | 0.8165 |
| | 5.6 | | 0.6334 |
| | 6. | | 0.5834 |
| | 6.7 | | 0.5134 |
| | 7.2 | | 0.4758 |
| | 7.7 | | 0.412 |
| | 8.6 | | 0.2261 |
| | (9.4) | | (0.1111) |

PVAm-PBA, 4%

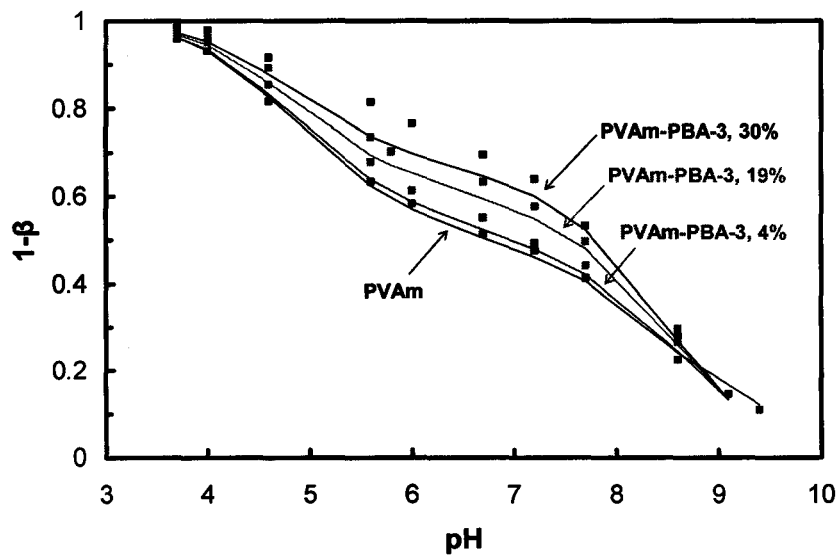
| | | | |
|--------|---------|---------------|------------|
| pH4 := | (3.7) | $\alpha_4 :=$ | (0.9734) |
| | 4 | | 0.9521 |
| | 4.6 | | 0.8545 |
| | 5.6 | | 0.6789 |
| | 6 | | 0.6131 |
| | 6.7 | | 0.5512 |
| | 7.2 | | 0.4934 |
| | 7.7 | | 0.4412 |
| | 8.6 | | 0.2667 |
| | (9.1) | | (0.1456) |

PVAm-PBA, 19%

| | | | |
|---------|-----|------------------|--------|
| pH19 := | 3.7 | α_{19} := | 0.9712 |
| | 4 | | 0.9648 |
| | 4.6 | | 0.8932 |
| | 5.6 | | 0.7349 |
| | 5.8 | | 0.7023 |
| | 6.7 | | 0.6324 |
| | 7.2 | | 0.5767 |
| | 7.7 | | 0.4965 |
| | 8.6 | | 0.2978 |
| | 9.1 | | 0.1456 |

PVAm-PBA, 30%

| | | | |
|---------|-----|------------------|--------|
| pH30 := | 3.7 | α_{30} := | 0.9853 |
| | 4 | | 0.9797 |
| | 4.6 | | 0.9165 |
| | 5.6 | | 0.8142 |
| | 6 | | 0.7652 |
| | 6.7 | | 0.6953 |
| | 7.2 | | 0.6395 |
| | 7.7 | | 0.5326 |
| | 8.6 | | 0.2808 |
| | 9.1 | | 0.1458 |

Comparison of mathematical model lines and experimental data of PVAm-PBA dissociations

2.7.3 Modeling the isoelectric points of PVAm-PBAs

The dissociation of polyvinylamine and phenylboronic acid followed the parameters in appendix 2.7.2.

Calculation of IEP of PVAm-PBA

IEP of PVAm-PBA, DS=30% $\text{pH} := 8.498$

Ionization degree of PVAm $0.7 \cdot (\alpha_{\text{pvam}}(\text{pH}, I)) = 0.1846$

Ionization degree of PBA $0.3 \cdot (\alpha_1(\text{pH})) = 0.1836$

IEP of PVAm-PBA, 19% $\text{pH} := 8.855$

$0.81 \cdot (\alpha_{\text{pvam}}(\text{pH}, I)) = 0.1488$

$0.19 \cdot (\alpha_1(\text{pH})) = 0.1486$

IEP of PVAm-PBA, 4% $\text{pH} := 9.76$

$0.96 \cdot (\alpha_{\text{pvam}}(\text{pH}, I)) = 0.0388$

$0.04 \cdot (\alpha_1(\text{pH})) = 0.0387$

Chapter 3

PVAm-Boronate: A New Wet Adhesive to Cellulose Hydrogel

3.1 Introduction

Polyvinylamine derivatized with 4-carboxyphenylboronic acid (PVAm-PBA) showed high adhesion strength at enhancing pH, which was attributed to the formation of covalent bonds between boronate and cellulose.¹ To the best of the authors' knowledge, no current polymer provides the same function. Herein, the influence of pH, salt concentration, Mw, the degree of substitution and the addition of sorbitol on the wet adhesion of PVAm-PBA to cellulose were systematically investigated.

The ability of a never-dried paper web to resist breakage on a paper machine is commonly referred to as paper wet web strength. Low wet-web strength, which is an issue to be addressed in papermaking technology, can lead to frequent breaks which interrupt production and lower paper machine efficiency.² The outer layer of cellulose in water is a layer of swollen hydrogel.³ Hydrogel has been studied and applied for several decades,⁴ however, the wet adhesion of swollen hydrogel is weak because water, which has a high surface energy, competes with adhesives and thus impairs the interaction of adhesives and hydrogel. Therefore, it is often difficult to acquire strong wet adhesion to cellulose in water.

The standard approaches to improving wet web strength in modern papermaking technology are to decrease the water content or increase the long fiber fraction.⁵ However, increased costs or lower production rates limit these options. Two polymeric additives, chitosan and cationic aldehyde starch, were proposed to enhance wet web tensile strength by cross-linking fibers.^{6,7} Unfortunately, both polymers are impeded in alkaline conditions, which are preferred in the modern papermaking process. Chitosan is water soluble only in an acidic condition, while the adhesion of cationic aldehyde starch to fiber is weakened significantly at above neutral pH.⁸ Therefore, it is necessary to invent new types of alkaline-favored wet web strengths which can form covalent bonds with cellulose.

The first report of the reaction of boronic acid with saccharides was published in 1954.⁹ This pioneer work has since attracted considerable attention. It is well accepted that only anionic boronates (the boron atom exists in a sp^3 form) can react with saccharides to get a stable complex, while the complex between

neutral boronates (the boron atom behaves in a sp^2 form) and saccharides is easily hydrolyzed and hardly exists.¹⁰ The pKa of boronic acid is 9.2. Therefore, the reaction between boronate and saccharides is advantageous at high pH values, which is preferable in modern papermaking industry. To date, boronic acid-based schemes have diverse applications related to polyol compounds, including saccharide detection,^{11,12} fluorescence,¹³ artificial tears,¹⁴ recognition of biological membranes,¹⁵ and chromatography.¹⁶

3.2 Experimental section

3.2.1 Materials

Commercial polyvinylamine (PVAm) with viscosity molecular weights of 15, 34,150 and 1500 kDa was obtained from BASF, Ludwigshafen. Since all PVAm polymers were synthesized from poly (N-vinyl formamide) by hydrolysis, they were further treated using 5% NaOH at 70°C for 48 h under nitrogen purge to remove residual formamide groups. Afterwards, they were exhaustively dialyzed against water for ten days and freeze-dried. Regenerated cellulose dialysis tubing (Spectra/Por[®] 4 product No: 132682 12kDa MWCO, Spectrum Laboratories, Inc.) was used as model cellulose surface. The tube was cut into 6×2 and 6×3 cm² strips, with the long axis paralleling to the long axis of the tube; the interior surface of the tube was used. 4-carboxyphenylboronic acid, N-(3-dimethylaminopropyl)-N'-ethylcarbodiimide hydrochloride (EDC), 4-carboxyphenyl boronic acid and sorbitol were purchased from Sigma-Aldrich and used as received. All experiments were performed with water from a Millipore Milli-Q system fitted with one Super C carbon cartridge, two ion-exchange cartridges, and one Organex Q cartridge.

3.2.2 Methods

The preparation of polyvinyl amine derivatives

Various PVAm pendant phenylboronic acid groups (PVAm-PBA) and PVAm pendant phenol groups (PVAm-Ph) were synthesized using the method described in Chapter 2.¹⁶ In a typical experiment, 0.2 g of PVAm were dissolved in 10 mL 0.1M MES buffer at pH 6.1 and 90 mL of 3 g/L 4-carboxyphenylboronic acid pH=6.1 in the buffer. Then, 8 g EDC were added and the mixture was stirred for 120 min at 25 °C. The product was dialyzed against water for two weeks. Proton NMR was used to characterize the degree of substitution. The structures and reaction routes of PVAm-PBA, PVAm-Ph and PVAm are shown in Scheme 3.1.

Electrophoretic mobility measurement

Electrophoretic mobility measurements were carried out at 25 °C using a ZetaPlus from Brookhaven Instruments Corporation. The mode adopted was PALS (phase analysis light scattering) version 2.5. The reported values were based on 5 measurements with 25 cycles for each value.

Wet adhesion measurement

a) Adsorption application

The water on the surface of the cellulose membranes was removed by dipping several times with tissues (Kimwipes). Afterwards, the cellulose membranes were soaked in PVAm-PBA solution for 10 minutes and then rinsed in a corresponding blank salt/sorbitol solution for 5 minutes. The bottom membrane was placed on a steel disk and a Teflon tape with a 1 cm width was put on one end of the cellulose membrane. Afterwards, the top cellulose membrane was carefully placed on the bottom membrane. Then, the resulting membrane pairs were put between two blotting papers and pressed using Hot Plate (Carver, Wabash, IN) at 18.5 MPa at room temperature for 3 min. Then, the membranes were peeled, using the above Instron 4411 universal testing system fitted with a 50 N load cell. The 90 degree peeling method was employed to get the delamination force. An illustration was demonstrated in Figure 3.7.1.

b) Direct application

Each top and bottom cellulose membrane ($6 \times 3 \text{ cm}^2$) was put onto a steel disk. The water on the surface of the cellulose membranes was carefully removed by dipping several times with tissues (Kimwipes). A Teflon tape with a 1 cm width was put on one end of the bottom cellulose membrane. Afterwards, PVAm-PBAs with certain concentrations were applied onto the central line of the bottom membranes, which were progressively covered by top membranes ($6 \times 2 \text{ cm}^2$). Then each cellulose membrane pair was sealed into a plastic zipper bag and pressed using Hot Plate (Carver, Wabash, IN) at 18.5 MPa at room temperature for 3 minutes. Then, the membranes were taken out from the bag and peeled using an Instron 4411 universal testing system (Instron Corp., Norwood, MA) fitted with a 50 N load cell. The 90 degree peeling method was employed to get the delamination force. An illustration was demonstrated in Figure 3.7.2.

Adhesion force by Colloid Probe Microscopy (CPM)

The CPM experiments were carried out by Dr. Shannon Notley at Department of Applied Mathematics, Research School of Physical Sciences and Engineering, Australian National University. Cellulose spheres in the size range of 10 – 14 μm in radius were used. The cellulose spheres were attached to triangular shaped atomic force microscopy cantilevers (Veeco Inc, USA) with a small amount of epoxy. The spring constant of the cantilevers was measured to be 0.35 N/m using the thermal noise method. A multi-mode scanning probe

microscope (Veeco Inc, USA) was used for the measurement of the apparent surface forces between the cellulose surfaces in the absence and presence of the polymeric additives. The forces on approach between cellulose surfaces in the absence and presence of the polymeric additives were measured under aqueous solution conditions with the pH varied and a constant ionic strength maintained. Furthermore, the adhesion was quantified by measuring the pull-off force as the cellulose surfaces were separated. A minimum 100 force curves were measured for each polymer and each pH. Force curves presented here are representative for each condition with the adhesion values reported an average for all force curves. Care was taken to maintain a constant maximum applied load in all experiments by using the trigger settings of the AFM equipment.

Quantification of polymers between cellulose membranes

The radiolabelled ^{125}I was grafted onto PVAm-PBA by using the iodogen method.¹⁷ The unbound ^{125}I were removed by dialysis against water for three days. The 0.5 mL of 0.5 g/L labeled PVAm-PBA was mixed with 125 mL of 0.1 g/L PVAm-PBA solution. The obtained PVAm-PBA solution was employed in the adsorption and rinsing process as described in the preceding adsorption method, except no pressing and peeling procedure was carried out. Following this, the cellulose membranes with labeled polymers were placed in measurement vials and the radioactivity was measured with a WizardTM 3" 1480 Automatic Gamma Counter (Perkin-Elmer life Sciences). The radioactivity of 500 μL aliquot of the above PVAm-PBA solution was counted and used as a control to quantify the adsorption amounts of PVAm-PBAs on the cellulose membranes.

3.3 Results

Handsheets made from pulp were the main approach to study the wet or wet web strength of paper. However, there are several disadvantages in handsheet based methods. Firstly, the retention of polymer additives is hard to control. Secondly, the locations of polymer in the handsheets and fracture mode can vary. Last, but not least, the flocculation of polymer influences the handsheet mechanical property. Pelton's group proposed a refined method to overcome all these problems.¹⁸ The regenerated cellulose membranes from dialysis tubing were employed as substrates and polymer adhesives were applied onto the membranes. The peeling force to delaminate cellulose membranes is plotted against the separation distance of the membranes. The bigger the peeling force, the higher the consumption of adhesion energy - that is, the higher is the wet strength of polymer. This method had advantages for good replication, easy process and good control of applied polymers.

A series of PVAm-PBA and PVAm-Ph were prepared and the molecular weight and degree of substitution (DS) are summarized in Table 3.1.

The peeling force of delaminating two cellulose membranes was used to characterize the strength of adhesives, which was first proposed by McLaren¹⁹ and developed by us.¹ The delamination force was normalized by dividing the peeling force by the width of cellulose membranes. The raw data sets of the delamination force for three polymers are shown in Figure 3.1. The average value of each curve was used as the delamination force and all experiments were repeated four times. As shown, PVAm showed the lowest delamination force (~2 N/m) while PVAm-PBA had a substantial increase (by a factor of ~30). Last, but not least, PVAm-Ph showed a slightly higher delamination result (by a factor of ~2) than did PVAm.

Due to the striking pH sensitive property of boronic acid, pH is the most important influencing factor worthy of study. Adsorption application was employed to study the influence of pH on PVAm-PBA wet strength. In the process of the adsorption method, there were two pHs to be controlled. One was the pH at which PVAm-PBA adsorbed onto the cellulose membranes (it was named adsorption pH), the other pH, (named the final pH in this publication), was the pH of blank water that was used to rinse cellulose membranes to remove excess PVAm-PBA and control the pH values of adsorbed PVAm-PBA. By contrast, there was only one pH (defined as the direct pH), which was employed in the direct application method.

The effect of DS on the wet strength of PVAm-PBA and PVAm-Ph was studied by using both direct and adsorption applications. The results are shown in Figure 3.2. Because of its good solubility, direct pH 10.5 was chosen in direct application to study the influence of DS on adhesion. For the same reason as above and a good adsorption effect, adsorption pH 7.5 was chosen in adsorption application. The reason for employing final pH 9.5 in the plot B was that high strength values were obtained at this pH (details are shown later in this paper). At final pH 9.5 and direct pH 11, the wet adhesion of both applications peaked at a maximum at DS 16%. However, for PVAm-Ph, there was no change of wet adhesion with the DS in both applications. Another noteworthy point was that PVAm-Ph showed intermedium wet strength in comparison with PVAm and PVAm-PBA over the whole range. Because of its high wet adhesion, PVAm-PBA-5 was selected to study the influence of other factors on adhesion.

Adsorption pH influenced the charge characterization of PVAm-PBA and, therefore, affected its adsorption and wet adhesion to cellulose membranes. The charge property could be measured by an electrophoretic mobility experiment. The mobility of PVAm-PBA-5 is shown as a function of pH in Figure 3.3. PVAm-PBA-5 showed positive mobility at low pH, whereas it had negative

values at high pH. The isoelectric point (IEP) of PVAm-PBA-5 is around 9.7. The relationship between adsorption amount of PVAm-PBA and wet strength was plotted against adsorption pH in the plot A of Figure 3.4. Similar trends were observed for both curves; *i.e.*, both curves increased first at low and intermediate pH ranges and decreased abruptly after obtaining a maximum value at pH 9.5. However, from pH 3.9 to 9.5, the delamination force increased by a factor of ~ 8 , while the adsorption amount increased by only a factor of ~ 2.8 . To elucidate this further, the delamination force was re-plotted against the adsorption amount of PVAm-PBA as shown in the plot B. Two regions were labeled. In region 1, the delamination force was weak (lower than 20 N/m), while the delamination force was much higher (higher than 70 N/m) than the above in the region 2. The difference of adsorption amount between region 1 and region 2 was around 5.5 mg/m^2 .

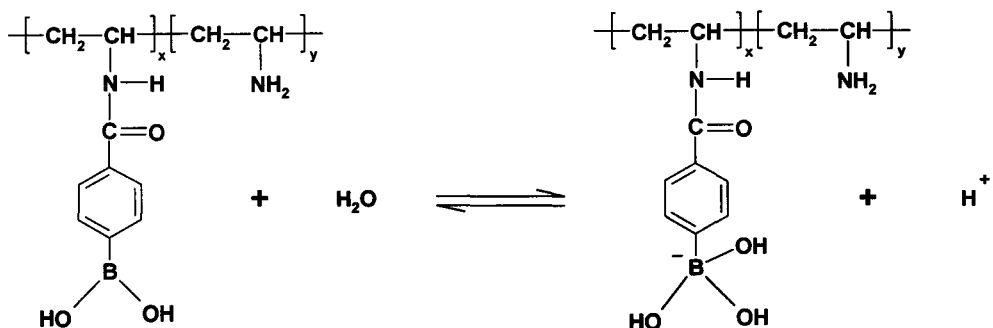
The wet strength of PVAm-PBA-5 adsorbed at different pH is shown as a function of final pH in the plot A of Figure 3.5. A contour curve was plotted against final and adsorption pH in the plot B based on the raw data in the plot A. The contour numbers represented the delamination force at the corresponding adsorption and final pH. By and large, the adhesion strength increased with adsorption or final pH. The region with the lowest adhesion corresponded to the low adsorption pH ($\text{pH} < 7$) and final pH ($\text{pH} < 8$), while the highest wet adhesion could be obtained in the region of adsorption pH from 9 to 10 and final pH from 5 to 9. The wet strength increased with final pH when adsorption pH was less than 5.5. When higher than 5.5, however, the wet strength passed the maximum regions at the middle final pH region (from 5 to 9.5) and then decreased. Note that an unexpected intermediate wet adhesion could be acquired in the region of high adsorption pH (> 9.5) and low final pH (3.8).

Sorbitol is a sugar which reacts with boronic acid. As shown in Figure 3.6, in the presence of sorbitol, adhesion strength decreased substantially over the entire pH range. In addition, the delamination force curve above was flat over the entire pH, whereas in the absence of sorbitol, the curve had a maximum region between pH 5 and 9.5.

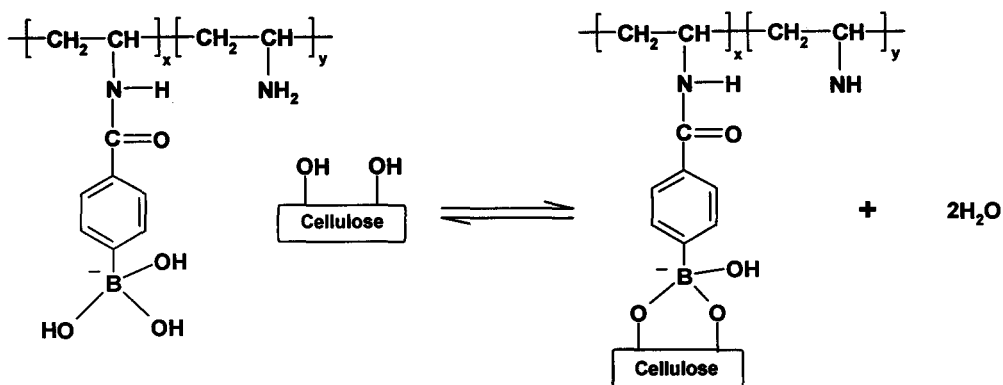
The wet strength is shown as a function of sorbitol concentration in Figure 3.7. The presence of sorbitol competed with cellulose by reacting with boronate groups of PVAm-PBA. The delamination curve decreased steeply at first and lessened gradually with the increase of sorbitol concentration.

In an effort to predict the influence of sorbitol, a model was derived from the chemical and mass balances of PVAm-PBA, cellulose and sorbitol. The three chemical reactions involved are shown as follows:

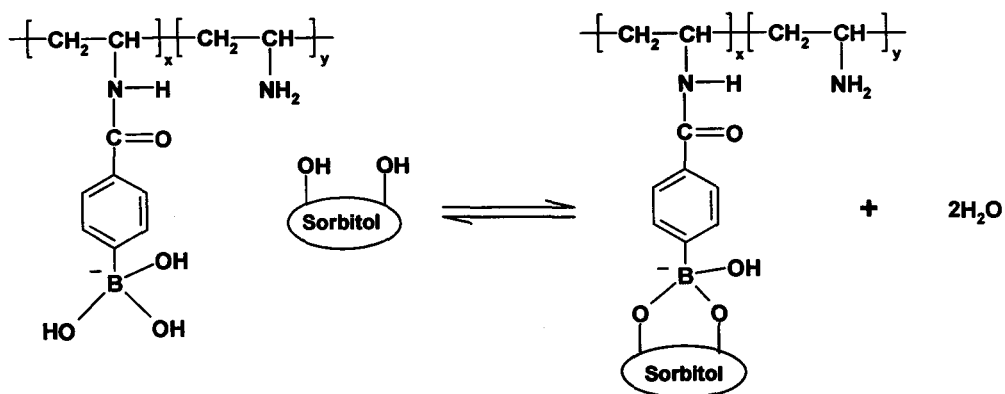
(1) The ionization of phenylboronic acid



(2) The reaction of boronate and cellulose



(3) The reaction of boronate and sorbitol



Equations (1) to (3) below are based on the chemical equilibrium:

$$K_1 = \frac{b_n}{b \cdot OH} \quad \text{the equilibrium of boronate dissociation} \quad (1)$$

$$K_2 = \frac{b_c}{b_n \cdot c_1} \quad \text{the reaction equilibrium of boronate and cellulose} \quad (2)$$

$$K_3 \cdot b_n \cdot s = b_s \quad \text{the reaction equilibrium of boronate and sorbitol} \quad (3)$$

Wherein, K_1 , K_2 and K_3 are the dissociation constant of boronate on PVAm-PBA, reaction constant of boronate with cellulose, and reaction constant of boronate with sorbitol, respectively. b , b_n , b_s are the concentration of undissociated boronic acid, the concentration of unreacted boronate anion, the concentration of boronate reacted with sorbitol. OH is the concentration of hydroxyl groups. c_1 and s are the concentration of cellulose and sorbitol reacted with boronate.

Equations (4) to (6) below are based on the concentration equilibrium:

$$c_0 = c_1 + b_c \quad \text{the concentration balance of cellulose} \quad (4)$$

$$s_0 = s + b_s \quad \text{the concentration balance of sorbitol} \quad (5)$$

$$b_0 = b_n + b + b_c + b_s \quad \text{the concentration balance of boronate} \quad (6)$$

Wherein, c_0 , s_0 , b_0 are the concentration of undissociated boronic acid, the concentration of unreacted boronate anionic, the concentration of boronate reacted with sorbitol. c_1 and s are the concentration of cellulose and sorbitol reacted with boronate.

The values of seven known parameters are: k_1 , k_2 , k_3 are 3.162×10^9 L/mol, 50 L/mol, 2000 L/mol, respectively. c_0 , b_0 , s_0 are 9×10^{-1} mol/L, 2.5×10^{-2} mol/L, 5.56×10^{-3} mol/L and OH is 3.16×10^{-4} mol/L. b_c is proportional to the wet strength. Therefore, the ratio of delamination force in the presence of sugar to delamination force in the absence of sugar can be predicted by the ratio of b_c (in the presence of sugars) to b_c (in the absence of sugars). MathCAD (Version 14.0) was employed to get predicted results. Experimental data was compared with the model predictions in Figure 3.7 and shows that the model fitted data over the sugar concentration from 0 to 10 g/L.

Molecular weight is an important parameter for polymers. The wet adhesion of PVAm-PBA at pH 9.5 was studied as a function of Mw in Figure 3.8. The concentration employed was 5g/L, which corresponded to a 150 mg/m² polymer coverage between cellulose membranes. The wet adhesion increased by a factor of 3 over the range of 15 to 150 kDa, whereas it increased by 30% from 150 to 1500 kDa.

PVAm-PBA is a polyelectrolyte. The ionic concentration influences the conformation of PVAm-PBA in solution and might affect its wet adhesion to cellulose. The wet strength of PVAm-PBA-5 was studied as a function of sodium chloride concentration in Figure 3.9. The adhesion strength does not vary over the range of 0 to 0.6 M NaCl at direct pH of 9.5.

The comparison of adhesion force from peeling tests and CPM methods is shown in Figure 3.10. Both graphs showed the exactly same trends of pH and polymer dependence. That is to say, the adhesion of PVAm and PVAm-Ph to cellulose membranes was not pH sensitive, whereas PVAm-PBA was strongly pH sensitive. PVAm-PBA showed a strikingly high wet adhesion at high pH, whereas, low or intermediate adhesion at low or moderate pH condition.

3.4 Discussion

The presence of boronate groups substantially increased wet adhesion with final pH, indicating the effect of covalent bonds produced between boronic acid and cellulose on wet strength. It seemed reasonable that the higher boronate content, the higher the wet strength. However, the solubility and probably the adsorption amount of PVAm-PBA also decreased with DS and resulted in smaller wet adhesion strength. Therefore, an intermediate DS was employed to obtain the highest adhesion.

PVAm-Ph gave a slightly higher wet adhesion than did PVAm, being consistent with the interaction of cellulose binding domain (CBD) to cellulose crystals. Lehtio *et al.* found the aromatic rings of CBD could coincide with the spacing of glucose rings on cellulose and, consequently, van der Waals and aromatic ring polarization interactions were contributed to the binding of CBD to cellulose. In addition, the hydrophobic interaction also played a role due to the hydrophobic character of cellulose.^{20,21} Takashima *et al.* found the moiety of OH group to help CBD bind to cellulose, indicating the importance of hydrogen bonding between cellulose and phenol groups of CBD.²²

The adsorption of PVAm or PVAm-PBA onto cellulose is a complicated process affected by many factors. Geffroy *et al.* studied the adsorption of PVAm onto cellulose and found that the adsorption amount of PVAm surpassed a

maximum at pH 10.6.²³ The driving force of the adsorption was the electrostatic attraction between cationic PVAm and anionic cellulose. When pH was less than 10.6, the repulsion from the adsorbed cationic PVAm blocked further adsorption of PVAm and resulted in a small adsorption amount. In contrast, the paucity of cationic amount limited the PVAm adsorption when pH was larger than 10.6. By comparison, for PVAm-PBA-5, the pH at which a maximum adsorption amount was acquired was 9.5. The difference was attributed to the polyampholyte property of PVAm-PBA, whose IEP was 9.7. Downward to the left side of pH 9.5, PVAm-PBA had a similar adsorption behavior as PVAm. On the other side, however, the anionic charge decreased the adsorption of PVAm-PBA on cellulose. Therefore, PVAm-PBA-5 obtained a maximum adsorption amount at pH 9.5 instead of 10.5.

One function of adhesive is that adhesives work as “gaskets” to provide bigger contact areas of adherends and, therefore, higher adherent strength. The adhesion strength is proportional to the content of adhesive before the saturation coverage is reached. Thus, the adsorption pH influenced PVAm-PBA peeling strength by affecting the adsorption amount. That is, it was seen that the more PVAm-PBA located between the joint region of two celluloses, the higher delamination force. In general, the saturation adsorption amount of monolayer polymer on a flat surface is $\sim 1 \text{ mg/m}^2$. However, the surface of the dialysis cellulose tube was very rough and full of small pores, indicating much more polymers were needed to get a full coverage of the surface. The remarkable difference between the two regions in Figure 3.4 (b) indicated that there was a critical adsorbed amount ($\sim 5.5 \text{ mg/m}^2$), at which PVAm-PBA-5 arrived at the saturated adsorption.

Interestingly, for adsorption pH 9.5 and 10, PVAm-PBA-5 had high adhesion strength when the final pH was 3.9. It is well accepted that the reaction of boronic acid and diols is alkaline favored, suggesting a high pH requirement for forming the covalent bonds. That is, boronic acid can react with diols only when the boron atom is in the sp^3 hybridized form. However, a number of publications reported that the introduction of electro-donating groups surrounding boronic acid could effectively lower the pKa via a coordination bond. For example, Otsuka reported that phenylboronic acid (PBA) could react with N-acetylneuraminic acid at pH 4,²² albeit the pKa of PBA is 8.6 which was explained by the occurrence of an amide group, which provided a pair of isolated electrons and stabilized the sp^3 hybridized form of boronic acid. Niwa also found that PBA reacted with fructose even at pH 5.8. He explained this by the presence of tertiary amino groups, which stabilized the sp^3 form of boron atom,²⁴ as shown in Scheme 3.2. PVAm is a polyelectrolyte with a broad disassociation region from pH 3 to 10.5. That is, there existed unprotonated amine groups at low pH and, therefore, donated excess electron pairs to boron atoms to decrease the apparent pKa of boronic acid and, therefore, make boronate react with diols. Wet adhesion

results indicated that the interaction of boronic acid and cellulose can function as low as 3.9. However, as proposed in Chapter 2, Anslyn *et al.* hold a different opinion on the structure of N-B interactions. They believed that there was only a small abundance of N-B dative bonds, the existence of anionic boronate groups at low pH were stabilized by neighboring tertiary ammonium groups. That is, zwitterionic species were formed in this case.²⁵ In summary, both opinions agreed with that neighboring amine groups resulted in the ionization of boronic acid at low pH.

Additionally, the results in chapter 2 showed PVAm-PBA-5 precipitated at between pH 9-10, that is, PVAm-PBA-5 demonstrated a hydrogel form in this case. A high adhesion was acquired indicated the function of hydrogel form in the wet adhesion of PVAm-PBA to cellulose. In hydrogel form, a bigger contact area with cellulose is proposed to explain this adhesion result.

In Figure 3.5 (b), the peeling force decreased when final pH increased from 9.5 to 10.5, suggesting the saturation of boronic acid groups in the joint region and nearest neighboring effect reduced the dissociation of boronate and, therefore, lowered the covalent bonding density between two cellulose membranes.

It is proposed that the failure mechanism in Figure 3.8 mainly involved the cohesion of PVAm-PBA rather than adhesion between PVAm-PBA and cellulose based on the fact of 150 mg/m² polymer coverage on cellulose membranes. The increase of wet strength from 15 kDa to 1500 kDa reflected the known Mw dependent rheological property of polymer. That is, the higher Mw of polymer, the more entanglement between polymer chains and, thus, the higher cohesion strength.

3.5 Conclusions

1. Adsorption pH determined adsorption amount and wet adhesion to cellulose. There existed an adsorbed amount corresponding to a transformation from maximum adhesion at 9.5, which corresponded to a maximum content of adsorbed polymer in the joint.
2. The weak but measurable wet adhesion was achieved at pH 3.9 which was much lower than the pKa of PBA (8.86), suggesting the reaction between PBA and cellulose can happen in this condition in the existence of neighboring amine groups.
3. In the presence of sorbitols in a rinsing solution, the wet adhesion decreased substantially, showing that the competitive reaction of sorbitols and PVAm-PBA reduced the content of boronate esters between cellulose

and PVAm-PBA. Moreover, the wet adhesion as a function of sorbitol concentration was well predicted by a mathematical model.

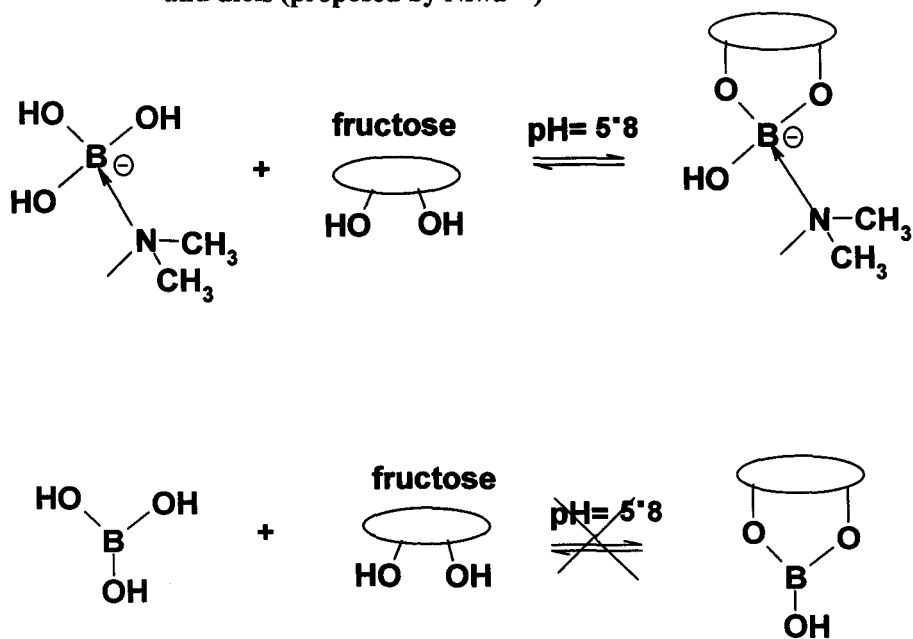
4. Phenol substituted PVAm gave slightly high wet adhesion of cellulose compared with PVAm.
5. Wet adhesion increased with the degree of substitution of PBA up to 16%, higher than which, the adhesion strength decreased. This was proposed by the low solubility or less adsorbed amount of PVAm-PBA with high degree of substitution.
6. Wet adhesion of PVAm-PBA to cellulose increased with M_w over the range of 15 to 1500 kDa. The wet adhesion increased by a factor of 3 over the range of 15 to 150 kDa, whereas it increased by 30% from 150 to 1500 kDa.
7. Salt concentration has no influence on the wet adhesion of PVAm-PBA to cellulose.
8. The wet adhesion of PVAm, PVAm-Ph and PVAm-PBA were measured by using colloidal probe microscopy. The adhesion behaviors of three polymers showed exactly the same pH- and polymer-dependent trends as those of peeling test.

3.6 Tables and Figures

Table 3.1 Polymer compositions and molecular weight. The degree of substitution is the number of substituted function group per nitrogen and the maximum possible value is 2 corresponding to tertiary amines.

| Sample Name | Degree of Substitution | Molecular Weight(kDa) |
|-------------|------------------------|-----------------------|
| PVAm-PBA-1 | 4% | 15 |
| PVAm-PBA-4 | 4% | 150 |
| PVAm-PBA-5 | 16% | 150 |
| PVAm-PBA-6 | 29% | 150 |
| PVAm-PBA-7 | 51% | 150 |
| PVAm-PBA-8 | 4% | 34 |
| PVAm-PBA-9 | 4% | 1500 |
| PVAm-Ph-1 | 4% | 150 |
| PVAm-Ph-2 | 17% | 150 |
| PVAm-Ph-3 | 24% | 150 |
| PVAm-Ph-4 | 47% | 150 |

Scheme 3.2 The influence of amino group on the complex of boronic acids and diols (proposed by Niwa²⁴)



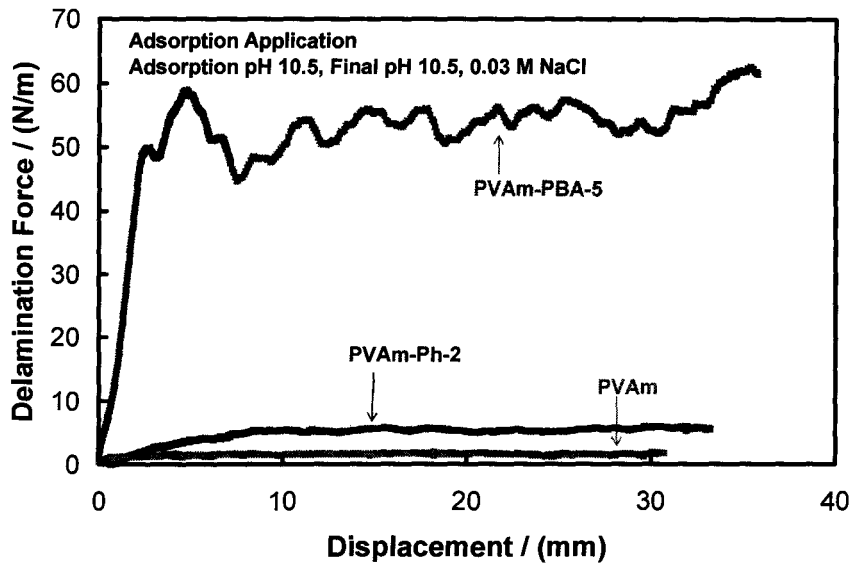


Figure 3.1 Comparison of delamination force versus displacement curves for PVAm-PBA-5, PVAm-Ph-2 and PVAm ($M_w=150$ kDa). The adsorption application was employed.

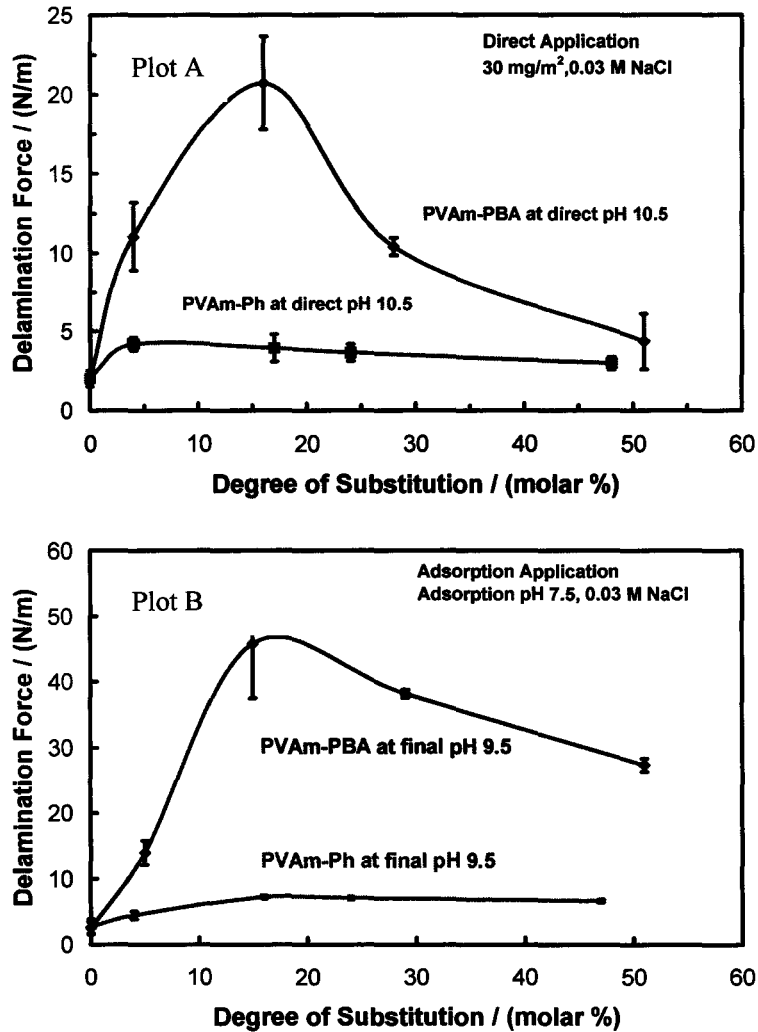


Figure 3.2 The influence of degree of substitution on the delaminating peel force of two cellulose films. Plot A: Direct Application, the applied PVAm-PBA and PVAm-Ph were 0.1 wt%, 0.03 M NaCl aqueous solution, 25 °C. Plot B: Adsorption Application, the applied PVAm-PBA and PVAm-Ph were 0.01 wt%, 0.03 M NaCl aqueous solution, 25 °C. The error bars are the standard derivations of the mean based on four measurements.

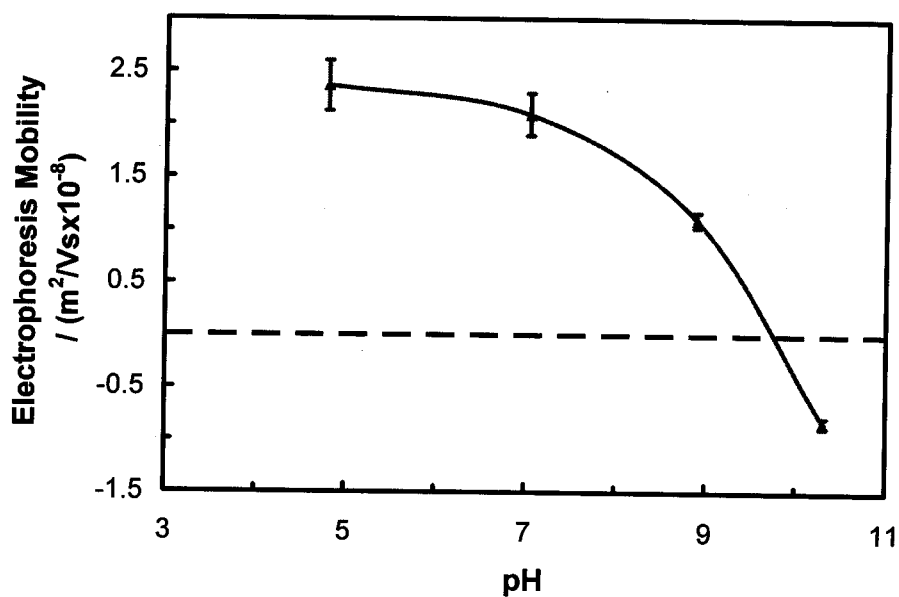


Figure 3.3 Electrophoresis mobility of PVAm-PBA-5 as a function of pH, 1000 ppm polymer in 0.03 M NaCl aqueous solution, 25 °C. The error bars are the standard deviations of the mean based on five measurements.

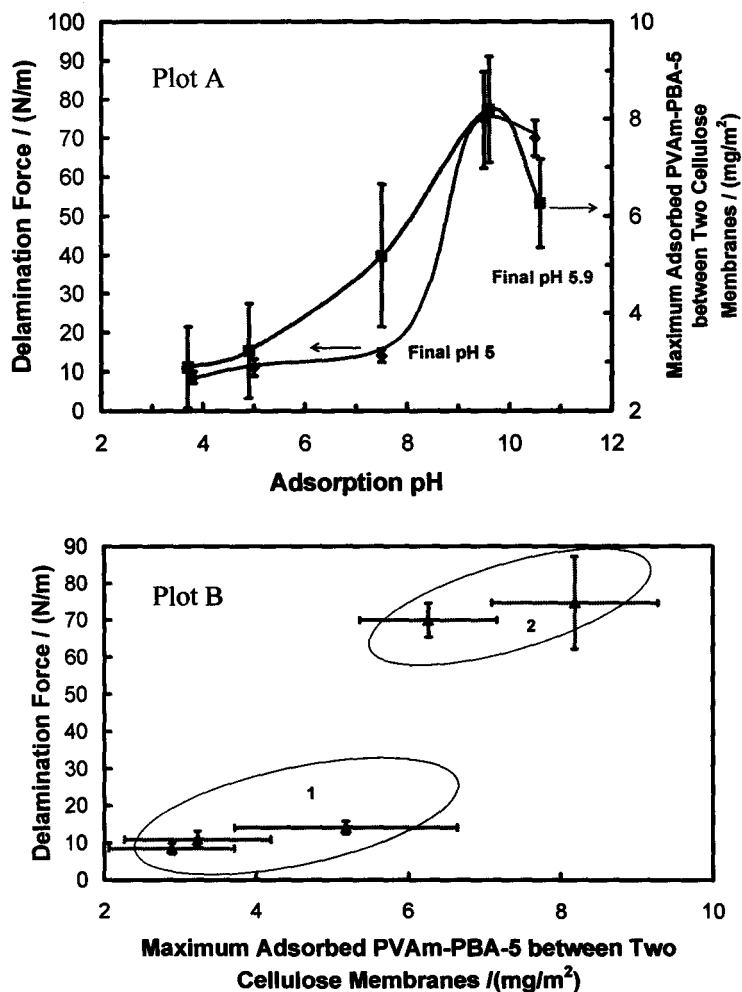


Figure 3.4 The delaminating peeling strength and maximum adsorbed amount of PVAm-PBA-5 onto cellulose membranes as functions of adsorption pH. The applied PVAm-PBA-5 was 0.01 wt%, 0.03 M NaCl aqueous solution, 25 °C. The error bars are the standard derivations of the mean based on four measurements. Plot A shows both curves of peeling strength and adsorption content against adsorption pH, wherein a final pH 5 for the former and a final pH 5.9 for the latter. Plot B replotted A to a curve of peeling strength as a function of corresponding adsorption content.

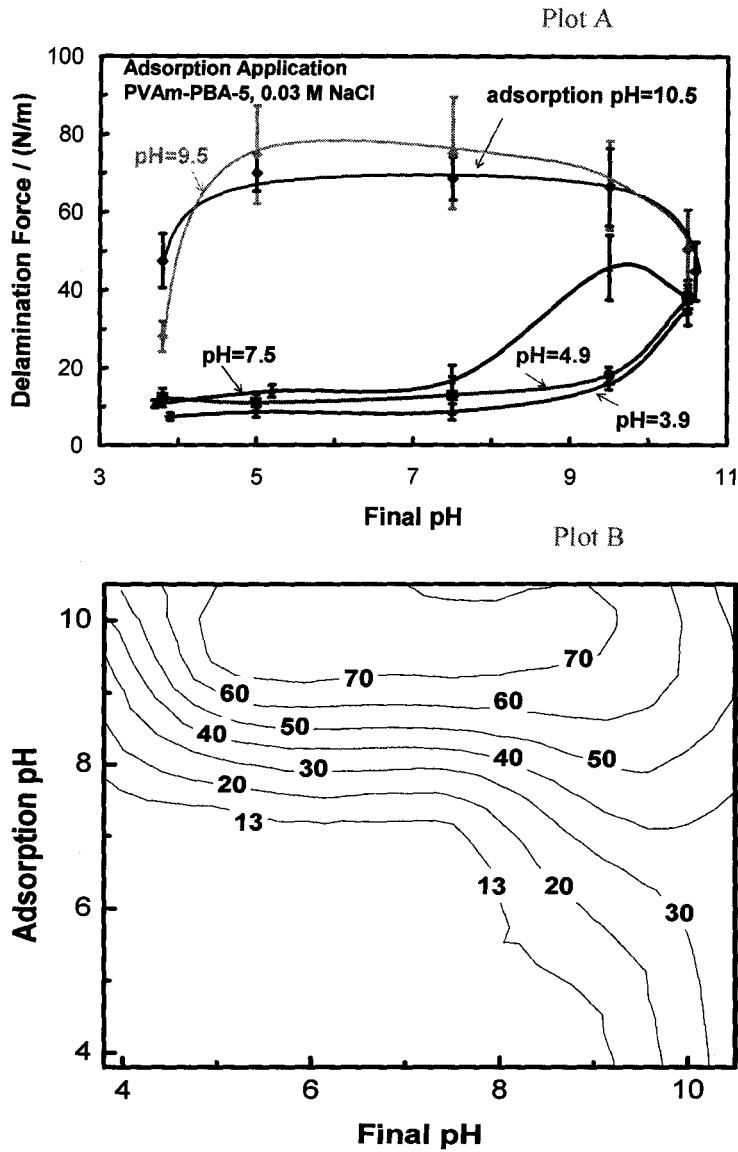


Figure 3.5 The delaminating peeling strength as a function of final pH. PVAm-PBA-5 applied was 0.01 wt%, 0.03 M NaCl aqueous solution, 25 °C. Plot A is the wet adhesion curves at different adsorption pH as functions of final pH. The error bars are the standard derivations of the mean based on four measurements.

Plot B is the contour plot of delamination force against adsorption and final pH.

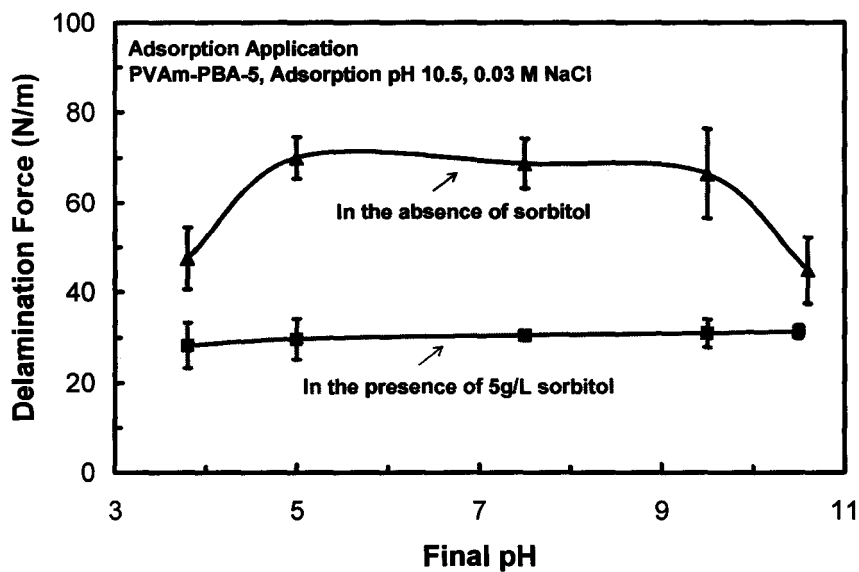


Figure 3.6 The influence of the addition of 5g/L sorbitol on the wet adhesion strength of PVAm-PBA-5 to cellulose. The applied PVAm-PBA-5 was 0.01 wt%, 0.03 M NaCl aqueous solution, 25 °C. The error bars are the standard derivations of the mean based on four measurements.

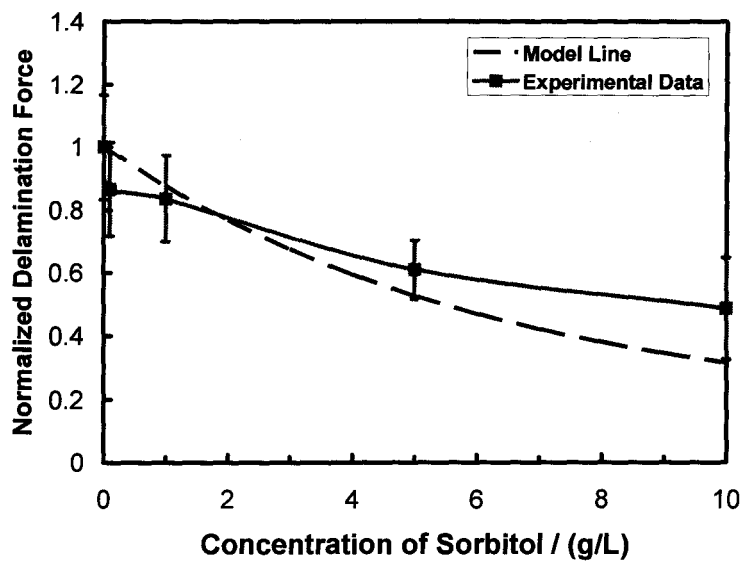


Figure 3.7 The influence of the addition of sorbitol on the wet adhesion strength of PVAm-PBA-5 to cellulose. The red line is experimental data and the blue line is the simulation curve. The applied PVAm-PBA-5 was 0.01 wt%, 0.03 M NaCl aqueous solution, 25 °C.

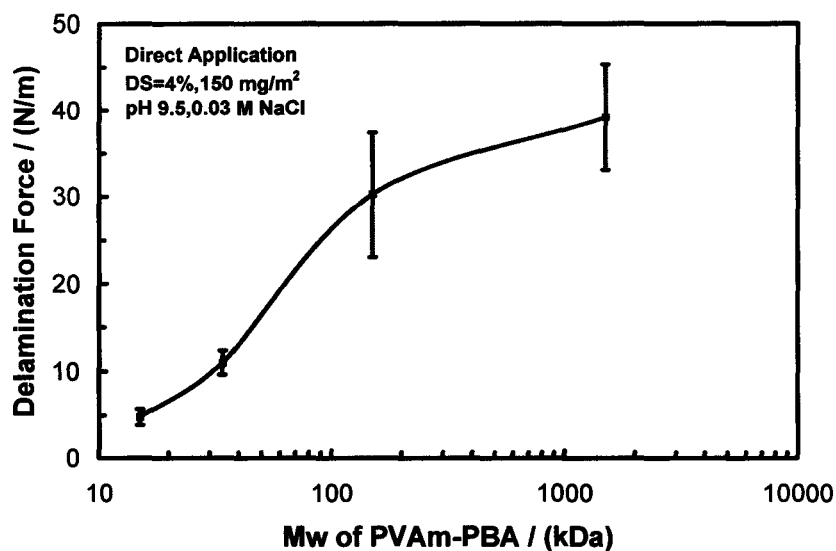


Figure 3.8 The effect of molecular weight of PVAm-PBA on the adhesion strength. PVAm-PBA applied was 0.5 wt%, 0.03 M NaCl aqueous solution, 25 °C. The error bars are the standard derivations of the mean based on four measurements.

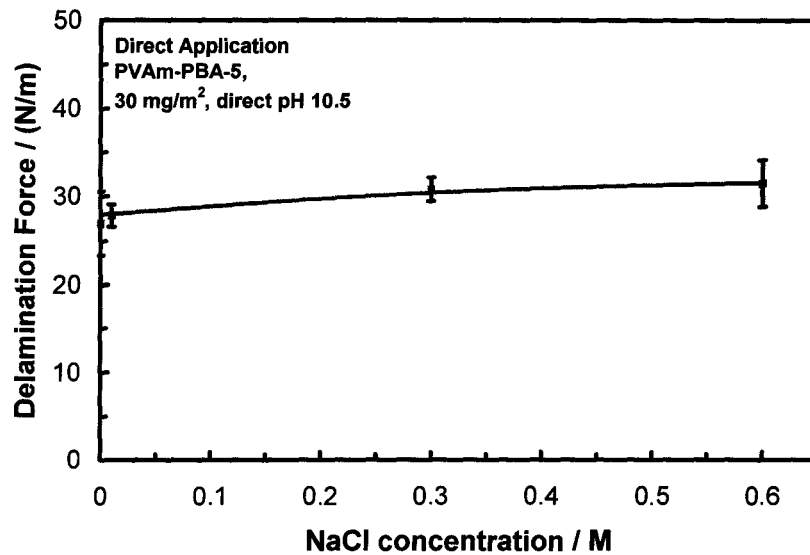


Figure 3.9 The change of delaminating peel force of cellulose films against ionic concentration for PVAm-PBA-5 that was applied in 0.1 wt% aqueous solution, 25 °C. The error bars are the standard derivations of the mean based on four measurements.

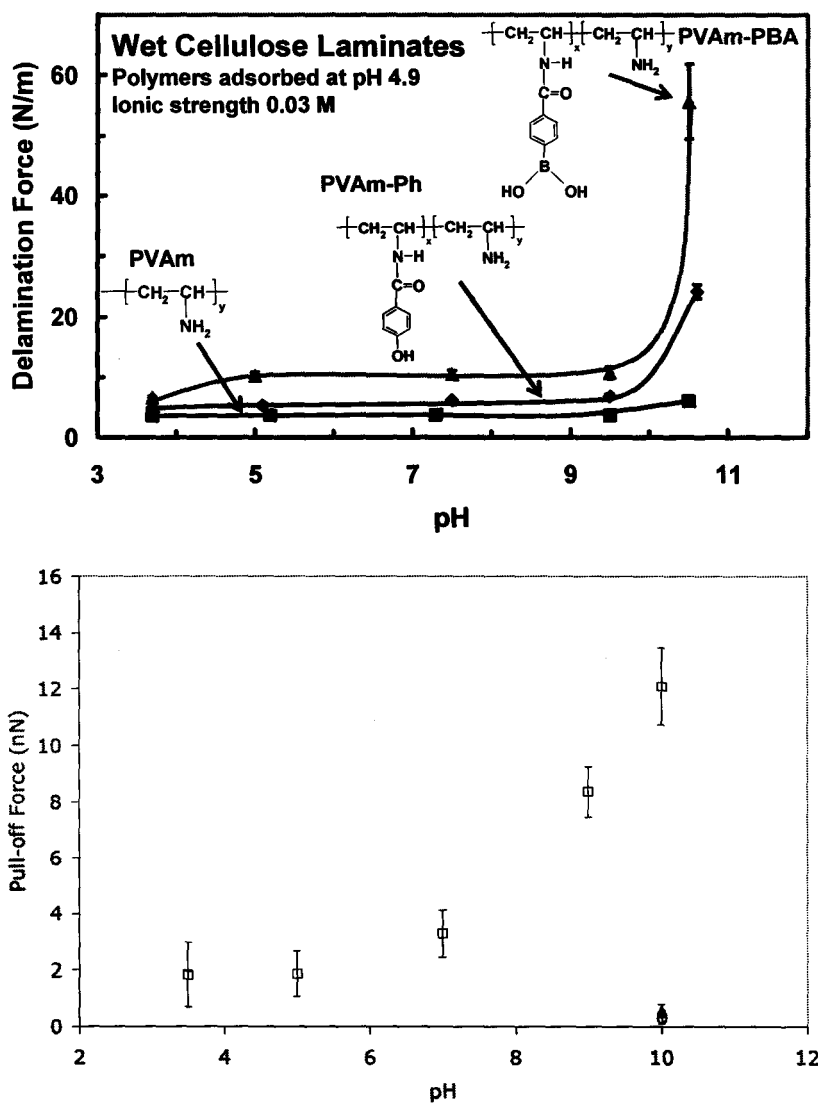
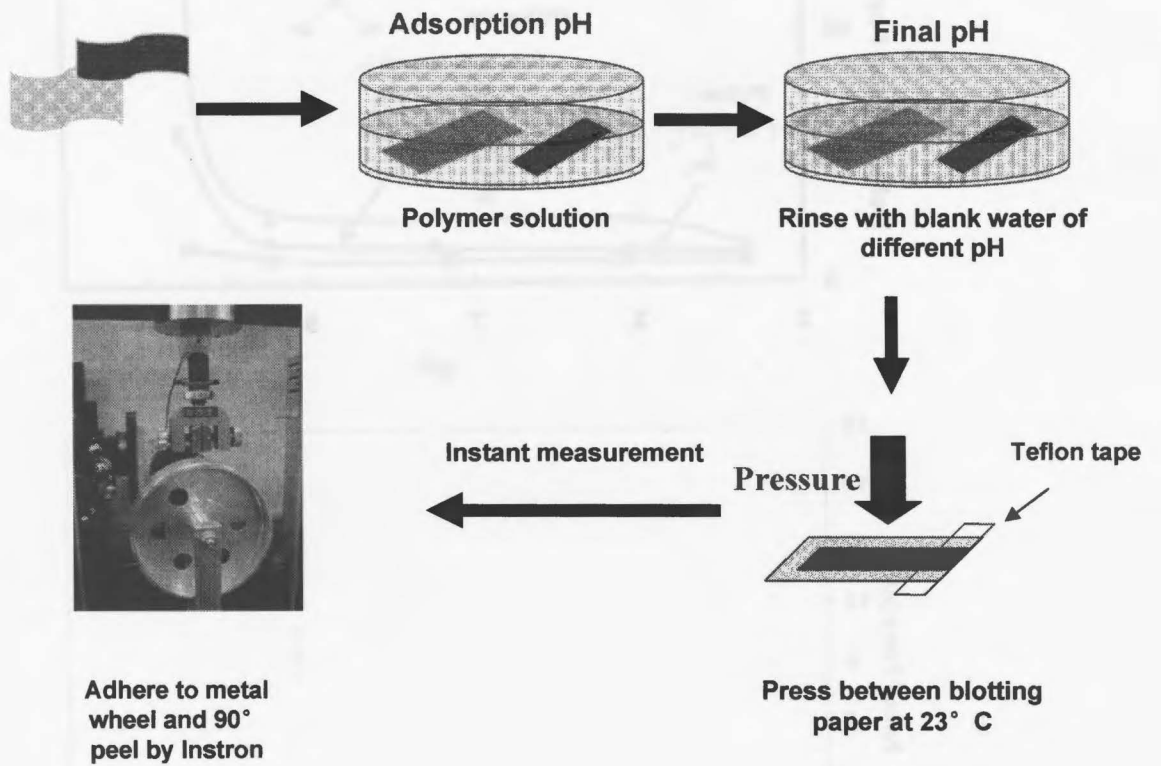


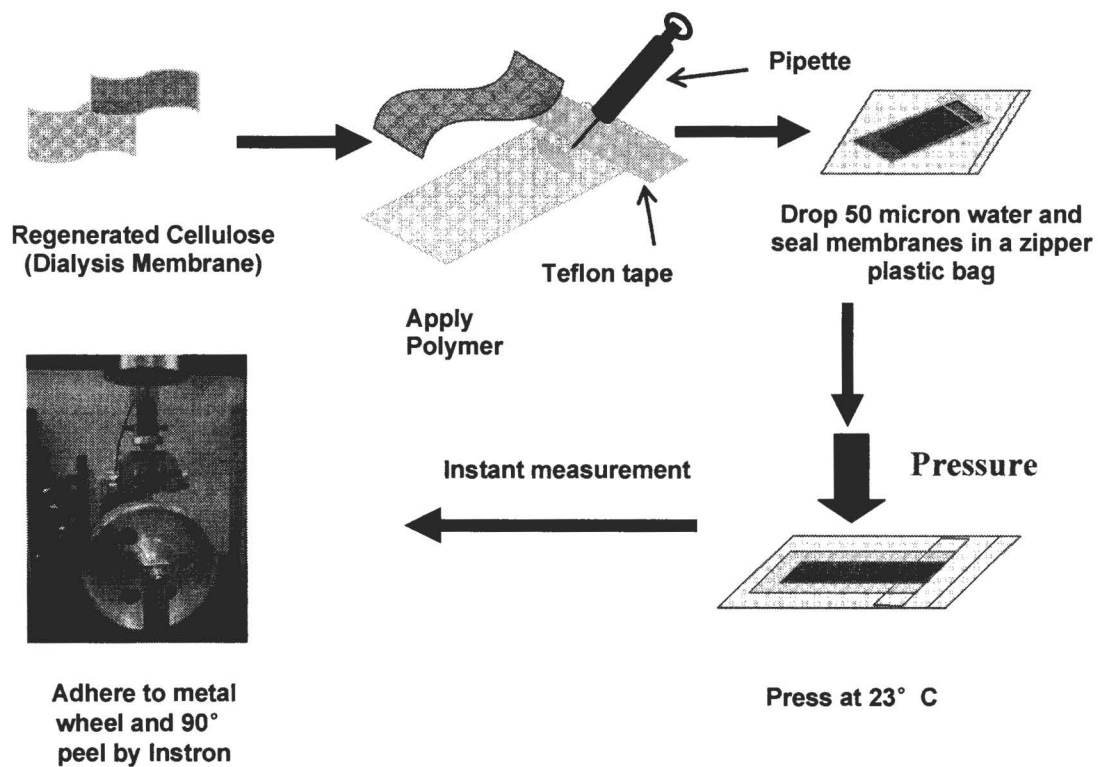
Figure 3.10 Comparison of pH- and polymer- dependent adhesion. The top graph was from peeling test whereas the bottom one was from CPM measurement. In the bottom graph, open circles, filled triangles and open squares represented PVAm, PVAm-Ph and PVAm-PBA, respectively.

3.7 Appendices

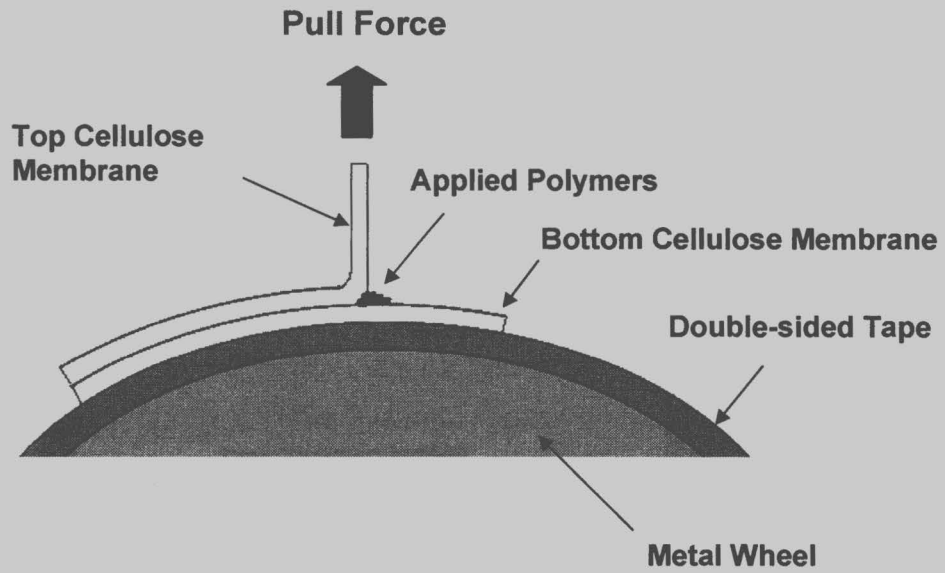
3.7.1 Adsorption Application



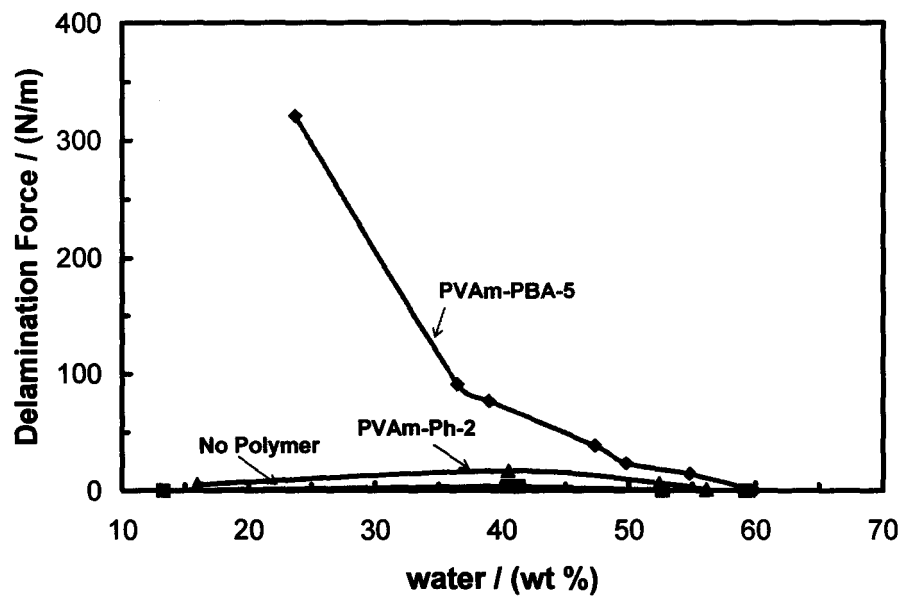
3.7.2 Direct Application



3.7.3 An illustration of ninety degree peeling test



3.7.4 The influence of water content on wet adhesion of applied polymers



3.7.5 Modeling wet adhesion of PVAm-PBA in the presence of sugars

Objective: Predicts the influence of added sugar concentration on the delamination force of two cellulose membranes laminated by PVAm-PBA-5.

Theory: There exist competition between sugars and cellulose to react with boronic acid. The delamination force of two cellulose membranes is proportional to the amount of covalent bonds of cellulose and boronate.

Three equations from chemical equilibrium:

$$K_1 = \frac{b_n}{b \cdot \text{OH}} \quad \text{the equilibrium of boronate dissociation}$$

$$K_2 = \frac{b_c}{b_n \cdot c_1} \quad \text{the reaction equilibrium of boronate and cellulose}$$

$$K_3 \cdot b_n \cdot s = b_s \quad \text{the reaction equilibrium of boronate and sorbitol}$$

Three equations from concentration balance:

$$c_0 = c_1 + b_c \quad \text{the concentration equilibrium of cellulose}$$

$$s_0 = s + b_s \quad \text{the concentration equilibrium of sorbitol}$$

$$b_0 = b_n + b + b_c + b_s \quad \text{the concentration equilibrium of boronate}$$

b_n : the concentration of $B(OH)_4^-$

b : the concentration of $B(OH)_3$

c_1 : the concentration of unreacted cellulose

s : the concentration of unreacted sorbitol

b_c : the concentration of cellulose reacted with boronate

b_s : the concentration of sorbitol reacted with boronate

Sample calculation:

Constants

$$K_1 := 10^{14-8} \frac{L}{mol} = 1 \times 10^3 \frac{m^3}{mol} \quad \text{the dissociation constant of 4-carboxyphenylboronic acid}$$

$$K_2 := 50 \frac{L}{mol} \quad \text{the reaction constant of 4-carboxyphenylboronic acid with cellulose (result from cellobiose)}$$

$$K_3 := 2000 \frac{L}{mol} \quad \text{the reaction constant of 4-carboxyphenylboronic acid with sorbitol}$$

$$b_o := 0.025 \frac{mol}{L} \quad \text{the concentration of total boronate of PVAm-PBA}$$

$$c_o := 0.7 \frac{mol}{L} \quad \text{the concentration of cellulose on the cellulose surface}$$

$$s_o := \frac{1}{180} \frac{\text{mol}}{\text{L}} = 5.556 \times 10^{-3} \frac{\text{mol}}{\text{L}} \quad \text{the concentration of total sugars}$$

$$\text{OH} := 10^{-3.5} \frac{\text{mol}}{\text{L}} = 3.162 \times 10^{-4} \frac{\text{mol}}{\text{L}} \quad \text{the concentration of OH}^- \text{ (because of pH=10.5)}$$

Initial guess

$$b := 3 \cdot 10^{-22} \frac{\text{mol}}{\text{L}}$$

$$c_1 := 0.00089 \frac{\text{mol}}{\text{L}}$$

$$s_n := 0.0078 \frac{\text{mol}}{\text{L}}$$

$$b_n := 0.005 \frac{\text{mol}}{\text{L}}$$

$$b_c := 0.0124 \frac{\text{mol}}{\text{L}}$$

$$b_s := 0.025 \frac{\text{mol}}{\text{L}}$$

Given

$$K_3 \cdot b_n \cdot s = b_s$$

$$c_o = c_1 + b_c$$

$$s_o = s + b_s$$

$$b_o = b_n + b + b_c + b_s$$

$$f(K_1, K_2, K_3, \text{OH}, s_o) := \text{Find}(b, c_1, s, b_n, b_c, b_s)$$

$$s_1 := 0 \frac{\text{mol}}{\text{L}}, 1 \frac{\text{mol}}{\text{L}} .. 10 \frac{\text{mol}}{\text{L}}$$

$$f(K_1, K_2, K_3, OH, s_0) = \begin{pmatrix} 1.983 \times 10^{-6} \\ 0.679 \\ 2.465 \times 10^{-3} \\ 6.271 \times 10^{-4} \\ 0.021 \\ 3.091 \times 10^{-3} \end{pmatrix} \frac{\text{mol}}{\text{L}}$$

Data from wet adhesion experiments:

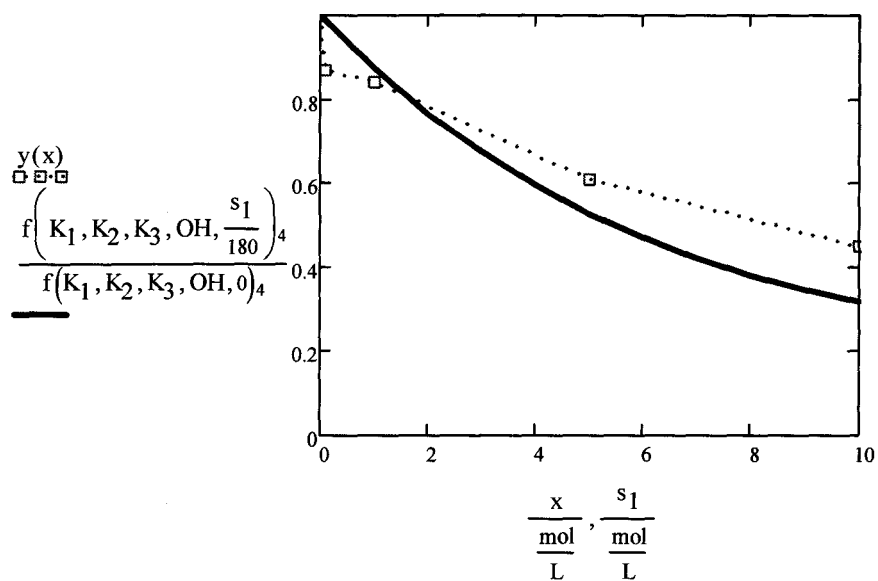
$$x := \begin{pmatrix} 0 \\ 0.1 \\ 1 \\ 5 \\ 10 \end{pmatrix} \frac{\text{mol}}{\text{L}}$$

the concentration of sorbitol

$$y(x) := \begin{pmatrix} 1 \\ 0.87 \\ 0.84 \\ 0.61 \\ 0.45 \end{pmatrix}$$

the ratio of the delamination force in the presence of sorbitol to the delamination force in the absence of sorbitol

Comparison of theoretical model and experimental data:



Conclusion: The mathematical model agrees with the wet adhesion result and can be employed to predict the influence of adding sugars on the reduction of PVAm-PBA wet adhesion to cellulose.

References

1. Chen, W.; Lu, C.; Pelton, R., Polyvinylamine boronate adhesion to cellulose hydrogel. *Biomacromolecules* **2006**, *7*, (3), 701-702.
2. Gurnagul, N.; Seth, R. S., Wet-web strength of hardwood kraft pulps. *Pulp & Paper Canada* **1997**, *98*, (9), 44-48.
3. Pelton, R., On the design of polymers for increased paper dry strength - A review. *Appita Journal* **2004**, *57*, (3), 181-190.
4. Kopecek, J., Hydrogel biomaterials: A smart future? *Biomaterials FIELD Full Journal Title: Biomaterials* **2007**, *28*, (34), 5185-5192.
5. Page, D. H., A quantitative theory of the strength of wet webs. *Journal of Pulp and Paper Science* **1993**, *19*, (4), 175-6.
6. Laleg, M.; Pikulik, I. I., Wet-web strength increase by chitosan. *Nordic Pulp & Paper Research Journal* **1991**, *6*, (3), 99-103, 109.
7. Laleg, M.; Pikulik, I. I., Unconventional strength additives. *Nordic Pulp & Paper Research Journal* **1993**, *8*, (1), 41-7.
8. Chen, N.; Hu, S. W.; Pelton, R., Mechanisms of aldehyde-containing paper wet-strength resins. *Industrial & Engineering Chemistry Research* **2002**, *41*, (22), 5366-5371.
9. Kuivila, H. G.; Keough, A. H.; Soboczenski, E. J., Areneboronates from diols and polyols. *Journal of Organic Chemistry* **1954**, *19*, 780-3.
10. Keita, G.; Ricard, A.; Audebert, R.; Pezron, E.; Leibler, L., The Poly(Vinyl Alcohol) Borate System - Influence of Polyelectrolyte Effects on Phase-Diagrams. *Polymer* **1995**, *36*, (1), 49-54.
11. Shoji, E.; Freund, M. S., Potentiometric saccharide detection based on the pKa changes of poly(aniline boronic acid). *Journal of the American Chemical Society* **2002**, *124*, (42), 12486-12493.
12. James, T. D.; Sandanayake, K. R. A. S.; Shinkai, S., Chiral discrimination of monosaccharides using a fluorescent molecular sensor. *Nature (London)* **1995**, *374*, (6520), 345-7.
13. Cordes, D. B.; Gamsey, S.; Sharrett, Z.; Miller, A.; Thoniyot, P.; Wessling, R. A.; Singaram, B., The interaction of boronic acid-substituted viologens with pyranine: The effects of quencher charge on fluorescence quenching and glucose response. *Langmuir* **2005**, *21*, (14), 6540-6547.
14. Lu, C.; Kostanski, L.; Ketelson, H.; Meadows, D.; Pelton, R., Hydroxypropyl guar-borate interactions with tear film mucin and lysozyme. *Langmuir* **2005**, *21*, (22), 10032-10037.
15. Otsuka, H.; Uchimura, E.; Koshino, H.; Okano, T.; Kataoka, K., Anomalous binding profile of phenylboronic acid with N-acetylneuraminic acid (Neu5Ac) in aqueous solution with varying pH. *J Am Chem Soc FIELD Full Journal Title:Journal of the American Chemical Society* **2003**, *125*, (12), 3493-502.

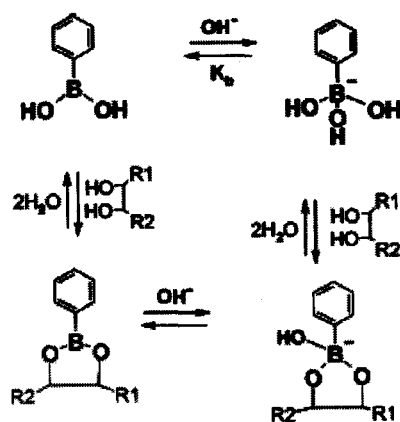
16. Gildengorn, V. D., Reversed-phase affinity chromatography of ecdysteroids with boronic acid-containing eluents. *Journal of Chromatography, A* **1996**, 730, (1 + 2), 147-152.
17. Korde, A.; Venkatesh, M.; Sarma, H. D.; Pillai, M. R. A., Preparation and pharmacokinetic evaluation of iodine-125 labeled alphamethyl-L-tyrosine. *J. Radioanal. Nucl. Chem. FIELD Full Journal Title:Journal of Radioanalytical and Nuclear Chemistry* **2000**, 246, (1), 173-178.
18. Kurosu, K.; Pelton, R., Simple lysine-containing polypeptide and polyvinylamine adhesives for wet cellulose. *Journal of Pulp and Paper Science* **2004**, 30, (8), 228-232.
19. McLaren, A. D., Adhesion of High Polymers to Cellulose . Influence of Structure, Polarity, and Tack Temperature. *Journal of Polymer Science* **1948**, 3, (5), 652-663.
20. Lehtio, J.; Sugiyama, J.; Gustavsson, M.; Fransson, L.; Linder, M.; Teeri, T. T., The binding specificity and affinity determinants of family 1 and family 3 cellulose binding modules. *Proceedings of the National Academy of Sciences of the United States of America* **2003**, 100, (2), 484-489.
21. Mattinen, M.-L.; Linder, M.; Teleman, A.; Annala, A., Interaction between cellohexaose and cellulose binding domains from *Trichoderma reesei* cellulases. *FEBS Letters* **1997**, 407, (3), 291-296.
22. Takashima, S.; Ohno, M.; Hidaka, M.; Nakamura, A.; Masaki, H.; Uozumi, T., Correlation between cellulose binding and activity of cellulose-binding domain mutants of *Hemicola grisea* cellobiohydrolase 1. *FEBS Letters* **2007**, 581, (30), 5891-5896.
23. Geffroy, C.; Labeau, M. P.; Wong, K.; Cabane, B.; Cohen Stuart, M. A., Kinetics of adsorption of poly(vinylamine) onto cellulose. *Colloids and Surfaces, A: Physicochemical and Engineering Aspects* **2000**, 172, (1-3), 47-56.
24. Niwa, M.; Sawada, T.; Higashi, N., Surface Monolayers of Polymeric Amphiphiles Carrying a Copolymer Segment Composed of Phenylboronic Acid and Amine. Interaction with Saccharides at the Air-Water Interface. *Langmuir* **1998**, 14, (14), 3916-3920.
25. Zhu, L.; Shabbir, S. H.; Gray, M.; Lynch, V. M.; Sorey, S.; Anslyn, E. V., A Structural Investigation of the N-B Interaction in an o-(N,N-Dialkylaminomethyl)arylboronate System. In **2006**; Vol. 128, pp 1222-1232.

Chapter 4

A Detailed Investigation of the Interaction between Cellulose and Boronate

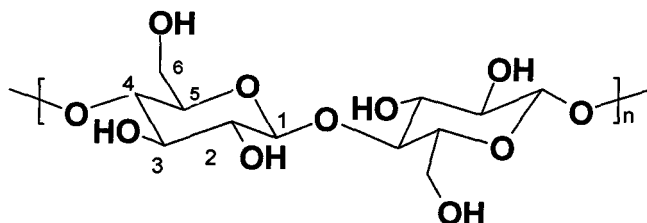
4.1 Introduction

Boric acid is known to react with many types of saccharides in basic conditions. This property has been widely applied in many fields, including saccharide detection,^{1,2} fluorescence,³ artificial tears,⁴ recognition of biological membranes,⁵ and chromatography.⁶



Scheme 4.1 The interaction of phenylboronic acid and diols-containing substances (Adapted from Keita *et al.* 1995)⁷

Polyvinylamine with pendant boronic acid groups (PVAm-PBA) showed good wet adhesion in chapter 3 of this thesis.⁸ Boronic acid was believed to react with carbon 2, 3-diols of cellulose⁹ and the covalent bonding was proposed to be the main reason for the high adhesion in alkaline conditions. However, 2, 3-diols are trans-diols. Spatial structure plays important role in the interaction of boronic acid and diols. Only cis-diols can react with boronic acid, trans-diols can not.¹⁰ According to this theoretical analysis, the spatial position of 2, 3-diols limits their formation of covalent bonds with boronic acid. Other diols, which might react with boronic acid on cellulose, include 1, 2-diols, 3, 4-diols and 4, 6-diols. The high adhesion of PVAm-PBA to cellulose inspired our interest in the reaction mechanism of cellulose and boronic acid.



Scheme 4.2 The structure and carbon sequence of cellulose

There are many publications focused on the interaction of monosaccharide and boric acid. There have been some work on the interactions of polysaccharides with boronic acid recently.⁴ However, there is no report on the reaction mechanism of the boronic acid and cellulose. Apparently, the poor solubility of cellulose limits the studies of its interactions with boronic acid. The main focus of this work is to investigate the interaction between cellulose and boronic acid. However, the experimental methods and conclusions can be expanded to investigate the interaction of boronic acid with other polysaccharides. To the best of our knowledge, this is the first study that investigates the interaction mechanism of boronic acid and cellulose.

4.2 Experiment section

4.2.1 Materials

Commercial polyvinylamine with viscosity molecular weights of 15 kDa and 150 kDa was obtained from BASF. Since both PVAm polymers were synthesized by hydrolysis from poly (N-vinyl formamide), they were treated further under a nitrogen purge using 5% NaOH at 70°C for 48 hours to remove residual formamide groups. The polymers were then dialyzed against water for ten days using regenerated cellulose dialysis tubing and were subsequently freeze-dried. Regenerated cellulose dialysis tubing (Spectra/Por[®] 4 product No: 132684 12kDa MWCO, Spectrum Laboratories, Inc.) and cellulose ester dialysis tubing (Spectra/Por[®] product No: 131273 10kDa MWCO, Spectrum Laboratories, Inc.) were used. 4-carboxyphenylboronic acid, N-(3-dimethylaminopropyl)-N'-ethylcarbodiimide hydrochloride (EDC), 2-morpholinoethanesulfonic acid (MES), 4-carboxyphenyl boronic acid, Alizarin Red S (ARS), fructose, cellobiose, dextran, hydroxyethyl cellulose and hydrogen chloride 1.25 M in methanol and boronic acid were purchased from Sigma-Aldrich and used as received. All experiments were performed with water from a Millipore Milli-Q system fitted with one Super C carbon cartridge, two ion-exchange cartridges, and one Organex Q cartridge.

4.2.2 Methods

The preparation of polyvinylamine boronate

PVAm pendant phenylboronic acid groups (PVAm-PBA) and PVAm pendant phenol groups (PVAm-Ph) were synthesized using the method described in chapter 3. In a typical experiment, 0.2 g of PVAm was dissolved in 10 mL 0.1M MES buffer at pH 6.1 and 90 mL of 3 g/L 4-carboxyphenylboronic acid in the same buffer; 8 g EDC were added and the mixture was stirred for 120 min at 25 °C. The product was dialyzed against water for two weeks. ¹H NMR was used to characterize the degree of substitution (DS) and the result is shown in Table 4.1.

Wet adhesion measurement

The direct application used previously was employed to measure the adhesion strength of PVAm-PBA/PBA-Ph to cellulose/cellulose ester membranes.¹ Surface water on cellulose membranes was carefully removed by dipping several times with Kimwipes tissue. PVAm-PBA or PVAm-Ph with certain concentrations was applied onto the central line of bottom membranes, which were carefully covered by top membranes and then pressed for 10 minutes using a pressure of 0.25 MPa. Then, 50µl water was dropped onto membranes and conditioned for 5 minutes. The membranes were sealed into zipper plastic bags and pressed using a pressure of 1.73 MPa. Afterward, the membranes were delaminated as long as they were taken out from the bags by using an Instron 4411 universal testing system (Instron Corp., Norwood, MA) fitted with a 50 N load cell. The 90 degree peeling method was employed to get the delamination force.

Etherization of 1, 2-diols end groups of cellulose membrane

Following Phillips's method,¹¹ cellulose membranes were dewatered with tissue paper and then put in the jar filled with anhydrous methanolic hydrogen chloride. The reaction was performed 12 h at room temperature and the jar was shaken every two hours.

Proton NMR measurement

¹H NMR experiments were performed in an AVANCE200 NMR instrument (Bruker) with 200 MHz at room temperature. A small amount of DCl in D₂O was used to dissolve the PVAm-PBA samples.

¹¹B NMR measurement

Calculated amounts of saccharides, polysaccharides and PVAm-PBA-3 were dissolved in 5 mM salt solution and pH was adjusted to 11 using 1 M NaOH solution. The boron NMR spectra of the solutions above were recorded by AV-600 NMR facility with an observed frequency of 600.0 MHz. The $\text{Et}_2\text{O}\cdot\text{BF}_3$ was chosen as the reference sample.

Fluorescence measurement

Firstly, a thick boric acid and ARS solution was prepared in 1mM salt solution. Then, calculated saccharides or polysaccharides were mixed with the solution and diluted to required concentrations for measurement. Steady-state fluorescence spectra were monitored by a Cary Eclipse fluorescence spectrophotometer at 25 °C.

Tensile strength measurement

PVAm-PBA-3 and HEC were dissolved into 5 mM water and pH values were adjusted using 0.1 M HCl and NaOH solutions. The solutions made above were cast onto a Petri dish plate and dried for one week to acquire membranes. Afterward, those membranes were conditioned at 23 ± 1 °C and $50\pm 2\%$ relative humidity for 24 h and then cut into 5 cm \times 1.5 cm strips. The tensile experiments were performed on an Instron 4411 universal testing system (Instron Corp., Norwood, MA) fitted with a 50 N load cell. The films were immersed and extended in 5 mM NaCl solutions with different pH values. The crosshead rates were controlled at 25 mm/min. The stress at the break was recorded as the tensile strength. The value was the mean value of three measurements. More details can be retrieved from Feng's paper.¹²

Viscosity measurement

HEC and boric acid were dissolved into a 0.3 M salt solution and the pH was adjusted to required values using 1 M NaOH and HCl. An Ubbelohde capillary viscometer (size 75, Cannon Instrument Company) was used to measure the viscosity of mixed solutions at 25 °C against the concentration.

4.3 Results

Owing to the poor solubility of cellulose, the interaction of cellulose and boric acid in solution is difficult to study. Therefore, polymers which are soluble and structurally similar to cellulose have to be employed as the substitutes of cellulose in solution. Herein, two model polysaccharides (dextran and HEC), which are structurally similar to cellulose, were employed to simulate the behavior of cellulose in solution. In addition, the smallest structure unit-cellobiose and the smallest component unit-glucose were also used because they react with

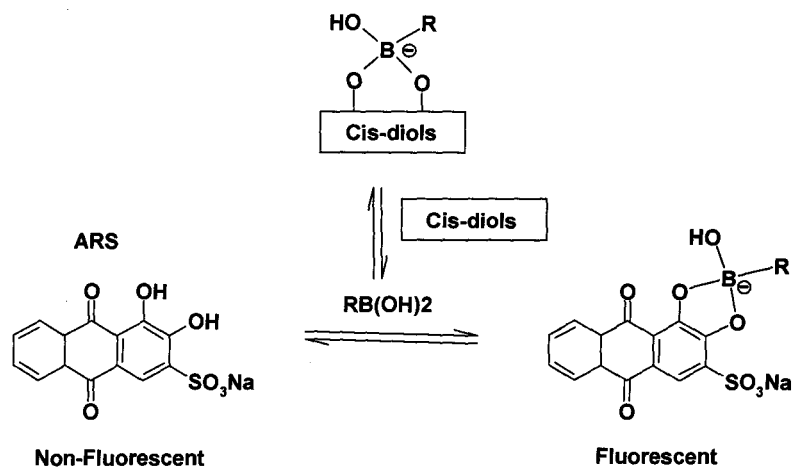
boronic acid. Therefore, the results of two polysaccharides can be compared with cellobiose and glucose. The molecular structures of the saccharides and polysaccharides are shown in later part.

The interaction between boronic acid and saccharides/polysaccharides was probed by several methods. For example, the complex of boronic acid and cis-diols can be observed in Boron NMR spectrum. The covalent bonding interaction between boronic acid and polysaccharides can result in an increased viscosity of mixture solution from polymer bearing boronic acid and polysaccharides or a higher tensile strength of film casted from this solution. Herein, ^{11}B NMR measurement, tensile experiment, fluorescence experiment and viscosity measurement are employed to investigate the interaction between boronic acid and two model polymers of cellulose.

Boron NMR was widely employed to probe the interaction between boronate and cis-diols containing compounds.^{13,14} The ^{11}B NMR spectra of PVAm-PBA with and without saccharides or polysaccharides are shown in Figure 4.1. As shown in the upper graph, there was one separate peak (at 2.5 ppm) which was attributed to the integrated signal of boronic acid and boronate.¹² Because the chemical exchange between boronate and boronic acid was too rapid to be recorded by NMR, no separate signal of boronate or boronic acid was observed. In the presence of dextran and HEC, no change was observed in the NMR spectra (the second and third graphs in Figure 4.1). By contrast, when cellobiose or glucose was added, there appeared two new peaks (at around 5 and 6 ppm) as shown in the bottom two graphs in Figure 4.1. These new signals represented the chemical shifts of the complex of boronate and sugars. The peak area of new peaks in cellobiose was smaller than glucose, which was consistent with the equilibrium constants of cellobiose (30.2 L/mol) and glucose (70.79 L/mol).¹⁰

In the presence of a strong interaction, the viscosity of polymer solutions should increase. The viscosity of mixed solutions of HEC and PVAm-PBA at pH of 3.5 and 9.5 is shown in Figure 4.2. There was almost no change of reduced viscosity in basic conditions compared with pH 3.9. The difference of elapsed time between pH 3.9 and 9.5 is only 3-4 seconds, whereas the difference of elapsed time of boric acid and HP-Guar (which is known to react with boric acid) at basic and acid conditions was 23 seconds (refer to Table 4.7.1).

The ARS fluorescent method was employed by other researchers to study the reaction constant of different cis-diols. The mechanism is as follows (shown in scheme 4.3): ARS is fluorescently active when mixed with boric acid. However, when cis-diols containing substances are added, they will compete with ARS to react with boric acid and therefore lower the fluorescence intensity of the ARS / boric acid system.¹⁵

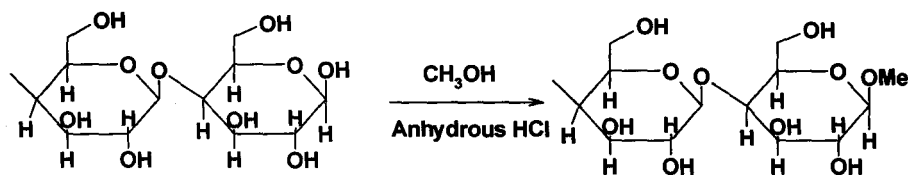


Scheme 4.3 The fluorescent mechanism of ARS and its competition with cis-diols to react with boric acid.

Herein, ARS/boric acid were used to investigate the interaction of polysaccharides and boric acid. The fluorescence spectra of ARS/boric acid with saccharides or polysaccharides are shown in Figure 4.3. The original emission intensity of boric acid/ARS at 600 nm is 74 a.u. The intensity decreased to 68 a.u. or 23 a.u. in the presence of cellobiose or glucose, whereas there was no change in intensity when dextran or HEC was added.

Uniform and transparent films were cast from the mixture solution of PVAm-PBA-3 and HEC. The tensile strength of the films will increase if there is an interaction of PVAm-PBA and HEC. Tensile experiments under 100% humidity were performed to study the strength of the films, that is, the interaction of PVAm-PBA and HEC at different pH. The experiments were performed in water; therefore, the pH, salt concentration and other factors of extension can be controlled. The results of tensile strength are shown in Table 4.2. There was no difference in tensile strength at different extending pH values. Additionally, the pH at which the films were prepared also had no influence on the tensile strength. The weak tensile strength of films was attributed to hydrogen bonding or the van der Waals interaction between PVAm and HEC rather than covalent bonds of boric acid and diols.

C-1 position is a hemiacetal structure (as shown in scheme 4.4). The hemiacetals can be reduced to acetal.²



Scheme 4.4 The conversion of carbon-1 end groups on the cellulose chain from hemiacetal to acetal.

Figure 4.4 shows the influence of the conversion of hemiacetal on the delamination force of regenerated cellulose. As shown, the delamination force eventually decreased with the reaction time. After 20 hours, the delamination force changed from 18.2 to 3.7 N/m, which was nearly the same as the values of PVAm-Ph-2 that showed a low wet adhesion and non-pH-sensitive behaviour.

Up to this point, the membranes used were regenerated cellulose. For comparison purposes, the delamination force of cellulose ester films made of cellulose acetates was measured. The degree of substitution of acetate is nearly 3, which means that there are not many end hydroxyl groups on the surface of cellulose ester membranes. As shown in Figure 4.5, the delamination force curve of cellulose ester remained flat over the whole pH range, whereas the curve of regenerated cellulose increased with pH. That is to say, the strength of cellulose ester membranes displayed non-pH sensitive properties and the value of adhesion strength was about 2 N/m, which is much lower than that of regenerated cellulose membranes.

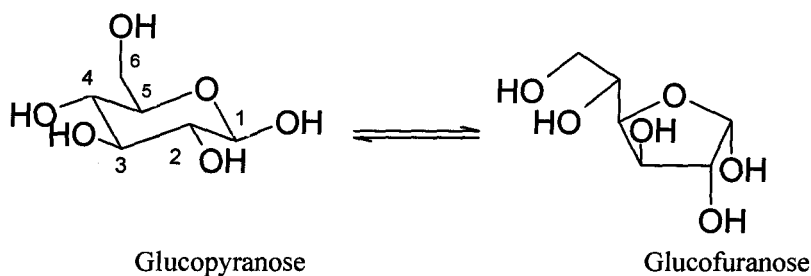
4.4 Discussion

The aim of this work is to understand the mechanisms of the interaction between boronate and cellulose. The discussion section is divided into three parts. The first part is the theoretical analysis and summary of interaction between boric acid and saccharides (glucose, methyl-glucopyranoside, and cellobiose). The second part is the experimental study of the interaction of boric acid, dextran, and HEC in comparison with glucose and cellobiose. Thirdly, the reason why PVAm-PBA showed a high lamination force to regenerated cellulose membranes is proposed.

Part A:

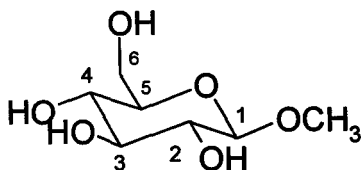
Cellulose consists of glucose units. Quite a few studies have been done on the interaction of glucose and boric acid.^{16, 17} However, there were debates concerning this point. Two different opinions were held. Some researchers believed that glucose interacted with boronic acid in furan forms.¹⁸ Carbon-1, 2 diols and 3, 5, 6-triols are believed to react with boronic acid. However, the other

researchers proposed that pyran forms (the main structures of glucose in water) also reacted with boric acid. The structures of both form are shown in scheme 4.5. Carbon-1, 2 diols and 4, 6-diols are considered as the reaction sites for boronic acid.¹⁹ Nicholls reviewed all existing works and used NMR to probe the complex structure of boronic acid and diol-containing substances. He arrived at a conclusion that if the pyranose glucose could react with boronic acid, it must adopt a boat conformation rather than a chair conformation - the normal conformation. Only in this situation, carbon-1, 2 diols could be cis-diols instead of trans-diols, whose special structure prevented the form of covalent bonding. The energy during the conformation transit from chair to boat form was compensated by the heat released from the covalent bonding between boric acid and sugars. The chair conformation of glucose was not reactive to boric acid.

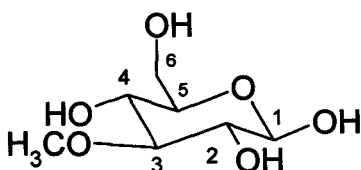


Scheme 4.5 The structure of glucose

Methyl-glucopyranoside is an ether of glucose; the carbon-1 or -3 hydroxyl group is replaced by methyl ether (as shown in scheme 4.6). As shown in Table 3, it is believed that 1-O-methyl-glucopyranoside does not react with boronic acid or has a very low reaction constant, whereas 3-O-methyl-glucopyranoside can react with boronic acid. The reason for this phenomenon is that the carbon-1 hydroxyl is displaced and there are no carbon-1, 2 diols. In addition, the 1-O-methyl group makes it impossible that 1-O-methyl-glucopyranoside change form from furanose to pyranose. By contrast, 3-O-methyl-glucopyranoside can transfer its conformation to furanose and its carbon-1, 2 diols can react with boronic acid. The striking difference between these two pyranosides clearly shows the importance of carbon-1, 2 diols for glucose to react with boric acid.



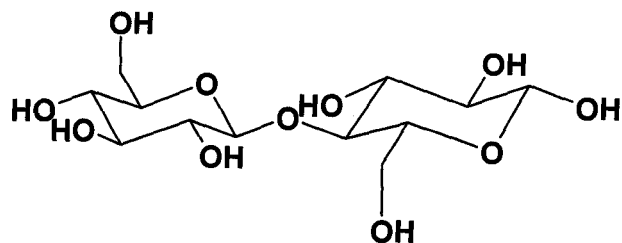
1-O-methyl-glucopyranoside



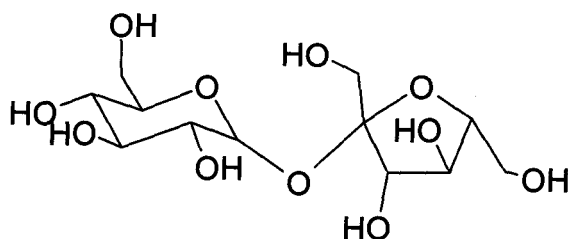
3-O-methyl-glucopyranoside

Scheme 4.6 The structure of methyl-glucopyranosides

Cellobiose and sucrose are disaccharides and the equilibrium constants are summarized in Table 4.3. Cellobiose is made up of two glucose units in a β -linkage. Sucrose constitutes a single glucose unit and one fructose unit. The structures of both disaccharides are shown in scheme 4.7. The ^{11}B NMR and other experiment results showed that one type of five-member ester was observed in cellobiose, indicating that the reaction sites of cellobiose are carbon-1, 2 diols rather than carbon-4, 6 diols.¹³ This is important considering cellobiose is the smallest unit of cellulose. In comparison, the reaction of sucrose and boronic acid is under debate. Some people believe that sucrose can not react with boronic acid, while others think that sucrose can react with a low stabilized reaction constant (as shown in Table 4.3). In summary, cellobiose reacts with boronic acid by its carbon-1, 2 diols, while no reaction occurred in its carbon-4, 6 diols. Regarding sucrose, there exist debates concerning its interaction with boronic acid through its carbon-4, 6 diols.



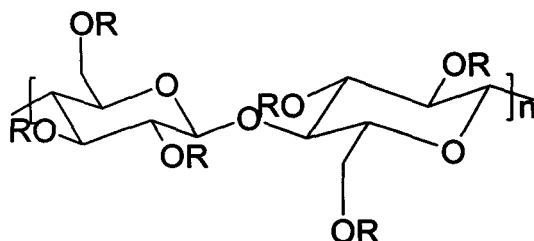
Cellobiose



Sucrose

Scheme 4.7 The structure of cellobiose and sucrose**Part B:**

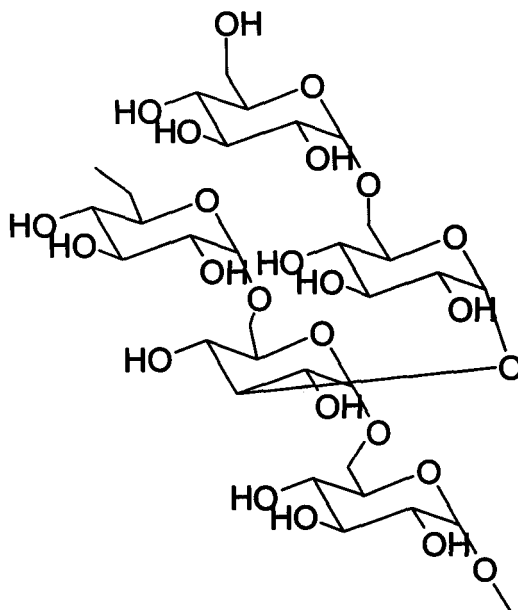
HEC is a cellulose derivative whose hydroxyl groups are substituted by hydroxyethyl groups (as shown in Scheme 4.8). From the chemical structure and degree of substitution (DS=1), the only possible reaction sites for HEC to boric acid are 2, 3-trans diols. The high molecular weight of HEC ($M_w=120,000$ Da) results in a small mass fraction of end groups. As shown in the ^{11}B NMR spectra of mixed solutions of PVAm-PBA-3 and HEC, no signal peak belonging to the complex of PVAm-PBA-3/HEC was observed, indicating that no complex was produced between HEC and PVAm-PBA-3. Additionally, the viscosity of the HEC/PVAm-PBA solution and the tensile strength of HEC/PVAm-PBA film showed non-pH sensitivity, further supporting the conclusion. Last but not least, the fluorescence spectra provided further support.



R: H or CH₂CH₂OH

Scheme 4.8 The structure of HEC

Dextran is a polymer that consists of a α -1, 6 linking main chain and α -1, 3 linking branch chains (as shown in scheme 4.9). The smallest component unit of dextran is also glucose. There are three pairs of possible reaction sites. The first two are carbon-2, 3 and carbon-3, 4-trans diols on the main chain and the other is carbon-4, 6 trans-diols on the branch chains. As with HEC, all experiments of ^{11}B NMR and fluorescence showed that there was no interaction between boronic acid and dextran, indicating that carbon-2, 3; carbon-3, 4 or carbon-4, 6 diols could not react with boronic acid.



Scheme 4.9 The structure of dextran

Part C:

There are three pairs of hydroxyl groups on the cellulose structure: one is on the main chain and two are at both ends of the chain. Based on the discussions above, we believe that the only reaction sites of cellulose with boric acid are carbon-1, 2 diols, which are located on one end of the chains. The diols on the other end can not react with boronic acid. However, in our previous papers, the cellulose membranes laminated with PVAm-PBA showed a substantial adhesion.¹ It seems that the two conclusions contradict each other.

But when we consider the extrusion producing process of cellulose dialysis tubes, it is not surprising that there are many end chains on the surface of membranes during the extrusion process. This means there exist many carbon-1, 2 diols on the surface of cellulose membranes to react with boronic acid groups. To prove this, the hydroxyl groups on carbon-1 positions were removed by etherisation and the delamination force of thus obtained cellulose membranes was measured. The final adhesion force was the same as PVAm-Ph, which was believed not to form covalent bonds with cellulose. This shows that the high wet adhesion strength brought on by boronic acid can be completely diminished by the modification of 1-hydroxyl groups.

Interestingly, the adhesion strength of cellulose triacetate membranes laminated with PVAm-PBA showed no pH sensitivity, indicating that the hydroxyl groups of end chains played a very important role in obtaining a high adhesion. By contrast, the delamination force had a dramatic enhancement with the increase of pH, which was consistent with the alkaline-favourable property of boronate. The adhesion behaviour of cellulose ester membranes further suggested that the existence of covalent bonding between hydroxyl groups of regenerated cellulose membranes and boronate and high wet adhesion in basic conditions was provided by the covalent bonding.

4.5 Conclusions

1. The reaction sites of cellulose with boronate are hydroxyl groups at carbon-1, 2. The hydroxyl groups at carbon-2, 3; carbon-3, 4 and carbon-4, 6 can not react with boronate.
2. The abundance of end groups on regenerated cellulose membranes contributed to the high wet adhesion strength. Peel adhesion comparison of modified regenerated cellulose and cellulose ester membranes clearly show the evidence.

4.6 Tables and Figures

Table 4.1 Polymer compositions and molecular weight. The degree of substitution is the number of substituted function groups per nitrogen atom, and the maximum possible value is 200% corresponding to tertiary amines.

| Sample Name | Degree of Substitution | Molecular Weight (kDa) |
|-------------|------------------------|------------------------|
| PVAm-PBA-3 | 30% | 15 |
| PVAm-PBA-5 | 15% | 150 |
| PVAm-Ph-2 | 16% | 150 |

Table 4.2 Tensile strength of film made of HEC and PVAm-PBA-3. The concentration of HEC and PVAm-PBA-3 are 2.5 g/L, respectively.

| Film casting pH | pH of doing the tensile test | Tensile Strength (lg Pa) |
|-----------------|------------------------------|--------------------------|
| 5 | 5 | 5.21±0.13 |
| 5 | 11 | 5.03±0.16 |
| 11 | 5 | 4.97±0.043 |
| 11 | 11 | 4.8±0.094 |

Table 4.3 Literature summary of association constants between boronate and saccharides (log K). R5, R6 represent five and six member ring of the complex of boronate and diols, respectively.

| Saccharide | Ref ¹⁷ | Ref ²⁰ | Ref ¹¹ | Ref ¹³ | Ref ²¹ | Ref ¹² | Ref ^{12,a} |
|--------------------------------|---------------------|-------------------|---------------------|-------------------|-------------------|-------------------|---------------------|
| glucose | 1.8(R6) 3.6 (R6) | 1.81(R5) | 1.8(R5) 1.23(R5) | 1.04 | 2.8 | 1.85 | 55% |
| cellobiose | | | 1.8(R5) | | | 1.48 | 6.5%(R5) |
| sucrose | | 0.6 | 1.8 | -0.17 | | 0 | 0% |
| 3-o-methyl- glucopyranoside | | | | | | | 59% |
| 1-o-methyl- glucopyranoside | | 0.48 | | | 0 | | 0% |

^a: Degree of Complex

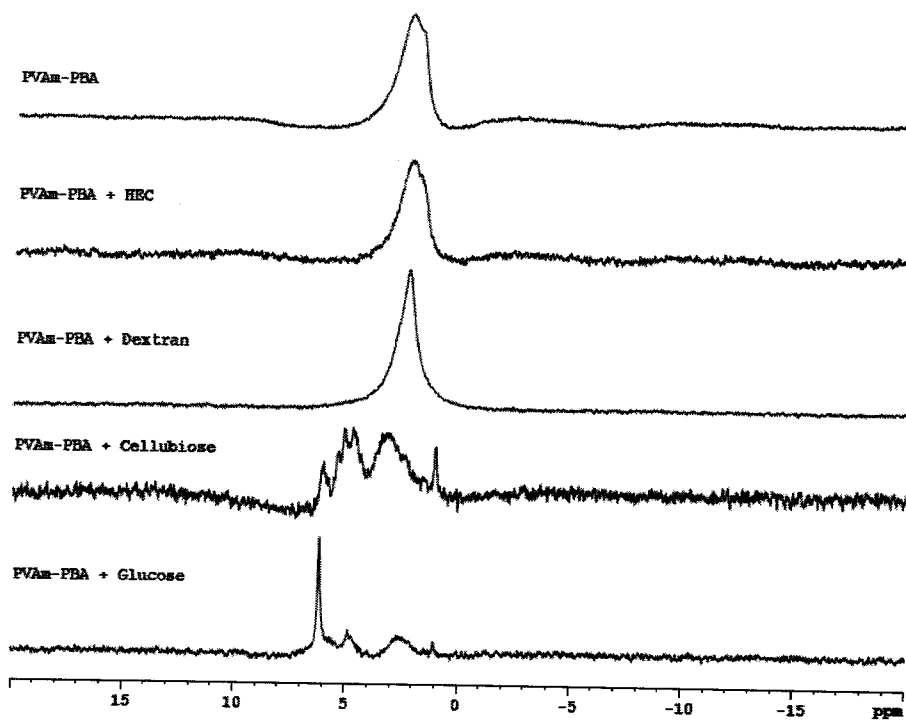


Figure 4.1 ^{11}B NMR of PVAm-PBA-3 (polymer concentration 10g/L) and saccharides. The molar ratio of boronate to saccharides or polysaccharides was 1:1.

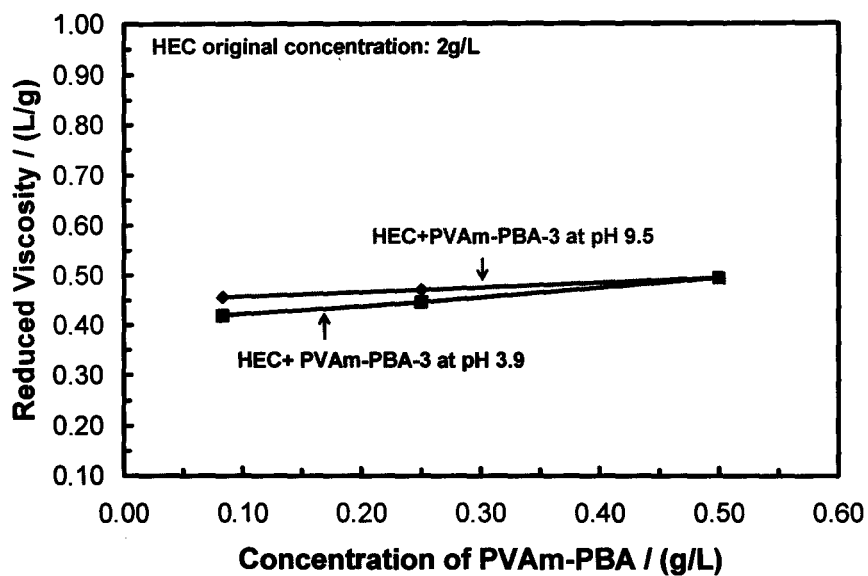


Figure 4.2 The reduced viscosity of mixed solution of HEC and PVAm-PBA-3 at pH 3.9 and 9.5. Each viscosity value in the figure represents the average of three measurements.

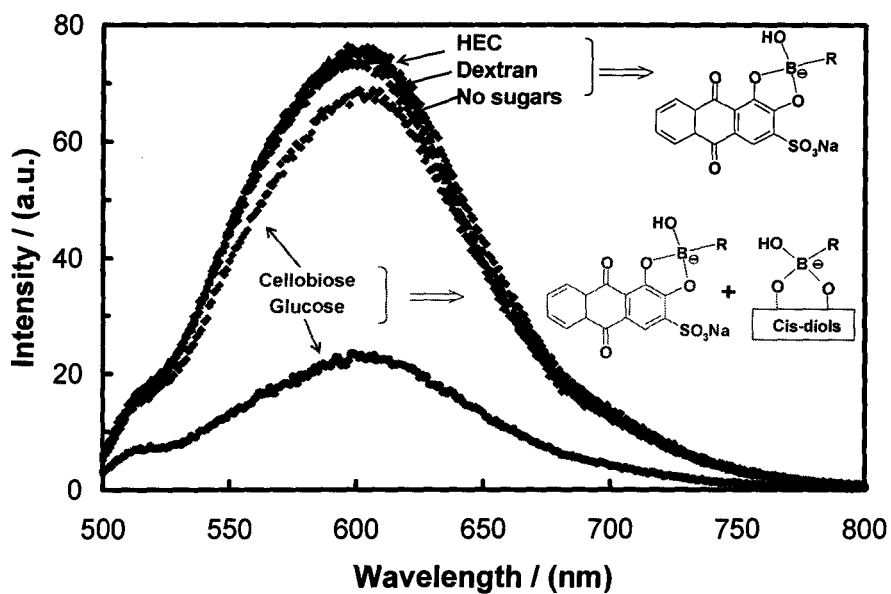


Figure 4.3 Fluorescence emission intensity for different saccharides with ARS and boric acid. The molar ratio of ARS, boric acid and saccharides/polysaccharides was 1:50:500. Emission wavelength is 480 nm. ARS concentration and pH were set to 0.2 mM and 9.0, respectively.

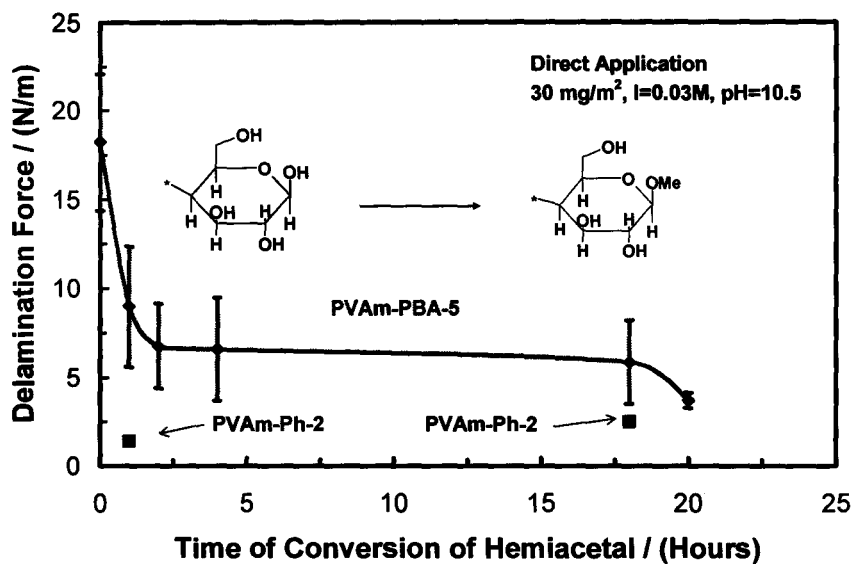


Figure 4.4 The influence of the conversion from hemiacetal to acetal on the delamination force of regenerated cellulose membranes. PVAm-PBA-5 applied was 0.1 wt%, 0.03 M NaCl aqueous solution, 25 °C. The error bars are the standard derivations of the mean based on four measurements.

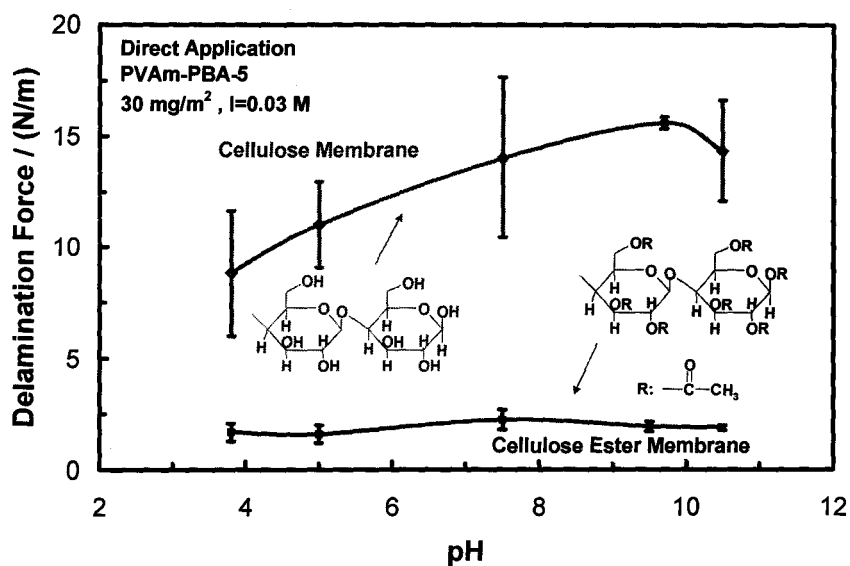


Figure 4.5 The delamination force of cellulose ester. PVAm-PBA-5 applied was 0.1 wt%, 0.03 M NaCl aqueous solution, 25 °C. The error bars are the standard derivations of the mean based on four measurements.

4.7 Appendix

Table 4.7.1 Viscosity of mixed solution of boric acid + HP-Guar or boric acid + HEC. The concentration of HEC, HP-Guar and boric acid are 2g/L, 1g/L and 0.62 g/L, respectively.

| pH of solution | Elapsed time of Boric acid + HP-Guar (seconds) | Elapsed time of Boric acid + HEC (seconds) |
|----------------|--|--|
| pH=3.6 | 295 | 155 |
| pH=10.5 | 317 | 155 |

References

1. Shoji, E.; Freund, M. S., Potentiometric saccharide detection based on the pKa changes of poly(aniline boronic acid). *Journal of the American Chemical Society* **2002**, 124, (42), 12486-12493.
2. James, T. D.; Sandanayake, K. R. A. S.; Shinkai, S., Chiral discrimination of monosaccharides using a fluorescent molecular sensor. *Nature (London)* **1995**, 374, (6520), 345-7.
3. Cordes, D. B.; Gamsey, S.; Sharrett, Z.; Miller, A.; Thoniyot, P.; Wessling, R. A.; Singaram, B., The interaction of boronic acid-substituted viologens with pyranine: The effects of quencher charge on fluorescence quenching and glucose response. *Langmuir* **2005**, 21, (14), 6540-6547.
4. Lu, C.; Kostanski, L.; Ketelson, H.; Meadows, D.; Pelton, R., Hydroxypropyl guar-borate interactions with tear film mucin and lysozyme. *Langmuir* **2005**, 21, (22), 10032-10037.
5. Otsuka, H.; Uchimura, E.; Koshino, H.; Okano, T.; Kataoka, K., Anomalous binding profile of phenylboronic acid with N-acetylneuraminic acid (Neu5Ac) in aqueous solution with varying pH. *J Am Chem Soc FIELD Full Journal Title:Journal of the American Chemical Society* **2003**, 125, (12), 3493-502.
6. Gildengorn, V. D., Reversed-phase affinity chromatography of ecdysteroids with boronic acid-containing eluents. *Journal of Chromatography, A* **1996**, 730, (1 + 2), 147-152.
7. Keita, G.; Ricard, A.; Audebert, R.; Pezron, E.; Leibler, L., The Poly(Vinyl Alcohol) Borate System - Influence of Polyelectrolyte Effects on Phase-Diagrams. *Polymer* **1995**, 36, (1), 49-54.
8. Chen, W.; Lu, C.; Pelton, R., Polyvinylamine boronate adhesion to cellulose hydrogel. *Biomacromolecules* **2006**, 7, (3), 701-702.
9. Shao, C.; Miyazaki, Y.; Matsuoka, S.; Yoshimura, K.; Sakashita, H., Complexation of Borate with Cross-Linked Polysaccharide Anion Exchanger: ¹¹B NMR and Adsorption Properties Studies. *Macromolecules* **2000**, 33, (1), 19-25.
10. Nicholls, M. P.; Paul, P. K. C., Structures of carbohydrate-boronic acid complexes determined by NMR and molecular modelling in aqueous alkaline media. *Organic & Biomolecular Chemistry* **2004**, 2, (10), 1434-1441.
11. Phillips, D. D., The synthesis of glucofuranosides. *Journal of the American Chemical Society* **1954**, 76, 3598-9.
12. Feng, X.; Pelton, R., Carboxymethyl Cellulose: Polyvinylamine Complex Hydrogel Swelling. *Macromolecules* **2007**, 40, (5), 1624-1630.
13. Bishop, M.; Shahid, N.; Yang, J.; Barron, A. R., Determination of the mode and efficacy of the crosslinking of guar by borate using MAS ¹¹B NMR of borate crosslinked guar in combination with solution ¹¹B NMR of model systems. *Dalton Transactions* **2004**, (17), 2621-2634.

14. Pezron, E.; Ricard, A.; Lafuma, F.; Audebert, R., Reversible Gel Formation Induced by Ion Complexation .1. Borax Galactomannan Interactions. *Macromolecules* **1988**, 21, (4), 1121-1125.
15. Springsteen, G.; Wang, B., A detailed examination of boronic acid-diol complexation. *Tetrahedron* **2002**, 58, (26), 5291-5300.
16. Norrild, J. C.; Eggert, H., Evidence for Mono- and Bidentate Boronate Complexes of Glucose in the Furanose Form. Application of 1JC-C Coupling Constants as a Structural Probe. *Journal of the American Chemical Society* **1995**, 117, (5), 1479-84.
17. Shiomi, Y.; Saisho, M.; Tsukagoshi, K.; Shinkai, S., Specific complexation of glucose with a diphenylmethane-3,3'-diboronic acid derivative: correlation between the absolute configuration of mono- and disaccharides and the circular dichroic-activity of the complex. *Journal of the Chemical Society, Perkin Transactions 1: Organic and Bio-Organic Chemistry (1972-1999)* **1993**, (17), 2111-17.
18. Bielecki, M.; Eggert, H.; Norrild, J. C., A fluorescent glucose sensor binding covalently to all five hydroxy groups of α -D-glucopyranose. A reinvestigation. *Journal of the Chemical Society, Perkin Transactions 2: Physical Organic Chemistry* **1999**, (3), 449-456.
19. James, T. D.; Sandanayake, K. R. A. S.; Iguchi, R.; Shinkai, S., Novel saccharide-photoinduced electron transfer sensors based on the interaction of boronic acid and amine. *Journal of the American Chemical Society* **1995**, 117, (35), 8982-7.
20. van den Berg, R.; Peters, J. A.; van Bekkum, H., The structure and (local) stability constants of borate esters of mono- and disaccharides as studied by ^{11}B and ^{13}C NMR spectroscopy. *Carbohydrate Research* **1994**, 253, 1-12.
21. Shiino, D.; Murata, Y.; Kataoka, K.; Koyama, Y.; Yokoyama, M.; Okano, T.; Sakurai, Y., Preparation and characterization of a glucose-responsive insulin-releasing polymer device. *Biomaterials* **1994**, 15, (2), 121-8.

Chapter 5

Preparation and characterization of polyvinylamine microgels

5.1 Introduction

Microgels are small hydrogels, normally less than 5 μm and microgels have many special properties and advantages over larger hydrogels. Microgels have been applied in the manufacture of coatings,¹ biomaterials,² catalysts³ *etc.* Depending on the function groups used, microgels can be pH,⁴ temperature⁵ and/or glucose sensitive.⁶

There are two methods for preparing microgels. The most common one is polymerization from monomers. The other one is crosslinking from linear polymers,⁷ (including polymer complexation). Coacervation, gelation and emulsion approaches are the three basic ways to prepare microgels or nanoparticles from linear polymers.

Polyvinylamine (PVAm) is a cationic polyelectrolyte which was invented in the 1940s.¹ However, due to its difficulty in acquiring a high molecular weight, PVAm was not obtained on an industrial scale until the 1990s. Due to its abundance in amine groups, PVAm has a number of special properties, including pH-sensitivity, high reactivity and strong adhesion. PVAm and its derivatives have been widely used in papermaking,⁸ chelation of metal ions,⁹ adhesives,¹⁰ biomaterials¹¹ and dyes¹².

PVAm hydrogels have been studied by some researchers. For example, bis-epoxide was employed to crosslink linear PVAm to make hydrogels for a viscosity study.¹² Hydrogels are polymers crosslinked by chemical or physical methods so that they swell but do not dissolve in solvents.

Until now, not much work has been done on the preparation of PVAm microgels,^{13,14} and, to our knowledge, none on the preparation of narrowly distributed PVAm microgels. The difficulty in finding a suitable crosslinker makes it difficult to obtain fully hydrolyzed and narrowly distributed PVAm microgels from N-vinylformamide, which is the monomer from which PVAm is made. In this chapter, an easy but effective approach is presented for preparing uniform-sized PVAm microgels. The method was inspired by the preparation of Chitosan microgels.

Chitosan, which is a plentiful natural polymer, is a basic polysaccharide with many pendant amine groups on its side chains.¹⁵⁻¹⁷ Chitosan and PVAm have

the same molecular characterization of abundance in pendant amine groups, but the former has a much more rigid main chain and poorer solubility. Calvo *et al.* first used TPP, a polyanion, to make chitosan nanoparticles.¹⁸⁻¹⁹ They found that by carefully controlling the ratio of TPP to chitosan, nanoparticles of chitosan could be obtained. This mechanism of producing nanoparticles is gelation arising from electrostatic interactions between carboxyl and amine groups. Recently, Wang *et al.* used a two-step crosslink method to make chitosan microgels. First, they made micron size microgels by a membrane emulsification technology, and then TPP and glutaraldehyde were added as the crosslinkers for each of the two steps. The reason for using TPP as the first crosslinker was to increase the release of protein from the chitosan microgels.²⁰

5.2 Experiments

5.2.1 Materials

Commercial PVAm ZD1989/104 (M=34 kDa), ZD1989/105 (M=150 kDa), and PolyminRPR 8182 (M=1.5 MDa), all with a hydrolysis degree 95%, were obtained from BASF. Tripolyphosphate (TPP) and glutaraldehyde solutions were purchased from Sigma Corp. All experiments used pure water from a Millipore Milli-Q system filled with one Super C carbon cartridge, two ion-exchange cartridges and one Organex Q cartridge.

5.2.2 Preparation of completely hydrolyzed PVAm

Following Feng's method,¹⁷ the PVAm solutions were hydrolyzed in 5 wt% sodium hydroxide solutions at 75 °C for five days to obtain 100% hydrolysis degree. Following this, the solutions were dialyzed in water for two weeks.

5.2.3 Preparation of PVAm microgels

Linear PVAm and TPP solutions were made, and their pH was adjusted to 7. In a typical experiment, 1 mL of TPP solution at pH 3 was dropped into 5mL of PVAm solution at pH 10 while the PVAm solution was stirred quickly. After the drop process (20 minutes) was finished, the solution was stirred for another ten minutes. After this, a calculated amount of glutaraldehyde solution was dropped into the solution and allowed to react for eight hours at room temperature. The prepared microgels were alternately centrifuged and rinsed with pure water to remove the TPP and other impurities. This two-step process of making PVAm microgels is shown in Figure 5.1.

5.2.4 Characterization of PVAm microgels

Dynamic light scattering was applied to measure the sizes of the PVAm microgels. The values were obtained at a 90° angle, using a He/Ne laser generator (Brookhaven Instruments Corp.) with a wavelength of 633 nm. Correlation data were processed using a BI-9000 AT digital autocorrelator, and the CONTIN algorithm was applied to obtain the sizes of microgels.

The distribution of microgels was determined by Mastersizer 2000 (Malvern Instrument Ltd., Version 5.1). Particle RI and dispersant RI were 1.39 and 1.33 respectively. Hydro 2000G (A) was used as the accessory. The top graphs in Figure 5.2-10 showed the results of distribution and the bottom graphs showed the average diameter and the smallest and largest diameter of microgels.

Proton NMR was recorded in D₂O solution by AVANCE200 and AVANCE600 instruments respectively. During the recording of the NMR spectrum, a 6.7 μs pulse width and 2.0 s delay time were applied and 128 scans were carried out for measurement at 298K.

Electrophoretic mobility measurements were made at 25 °C using a Zeta Plus (Brookhaven). The modes adopted were PALS (phase analysis light scattering) [version 2.5] and Zeta Potential Analyzer [version 3.27]. The reported values were based on 20 measurements with six cycles for each sample.

A transmission electron microscope (TEM) was employed to observe the size and morphology of the PVAm microgels. A drop of PVAm microgel solution was placed onto a copper grid and dried at room temperature and then observed by TEM (JEOL JEM-1200 EX).

5.3 Results

5.3.1 The influence factors of forming PVAm microgels

5.3.1.1 The salt concentration of PVAm

The increase of ionic concentration effectively shields the interaction between TPP and PVAm. As shown in Figure 5.2, the sizes of PVAm microgels increased with ionic concentration. In addition, the distribution of microgels produced at high salt concentration (>0.1 g/L) was also broader than that formed at a low salt concentration.

5.3.1.2 The pH of PVAm

The pH of PVAm is another influential factor in PVAm microgel preparation. As shown in Figure 5.3, at high pH (pH=10), bigger and broader PVAm microgels were obtained than those made at intermediate pH. At low pH

(pH=3), a much bigger and broader PVAm microgel was obtained than that formed at pH 10.

5.3.1.3 The pH of TPP

In addition to the pH of PVAm, the pH of TPP solution played an important role in the formation of PVAm microgels. As shown in Figure 5.4, at high pH (>7), no microgel was formed. At low pH (<5), small and narrowly distributed microgels were observed. And at intermediate pH, a bigger microgel was obtained.

5.3.1.4 The Mw of PVAm

The Mw influences size and distribution of PVAm microgels mainly by conformation. As shown in Figure 5.5, at high Mws ($M_w > 150$ kDa), a small and narrowly distributed microgel was obtained. For a low Mw (15 kDa), a relatively bigger microgel was formed. Surprisingly, at intermediate Mw (34 kDa), a very broad microgel was observed.

5.3.1.5 The volume of TPP

The addition of TPP increased the density of crosslinking and, consequently, formed a smaller and narrower distributed PVAm microgel. As shown in Figure 5.6, with the increase of TPP volume (from 20 to 95 ml), the PVAm microgels were a smaller size and of a more narrow distribution.

5.3.1.6 The concentration of TPP

Compared to increasing the volume of TPP, an increase of TPP concentration was a more effective way to enhance the crosslinking degree of PVAm microgel, as well as resulting in the formation of smaller and more narrowly distributed PVAm microgels (at concentrations of 1 g/L to 42.5 g/L). However, as shown in Figure 5.7 when TPP concentration was up to 50 g/L, a relatively bigger and broader microgel was obtained.

5.3.1.7 The storage time

The storage time is the time following the dropping of TPP. The crosslinking inside the PVAm microgels is physical crosslink. Therefore, with the increase of placing time, the microgels swell and, consequently, the size and distribution of microgels are bigger and broader. As shown in Figure 5.8, with the increase of storage time (from 7 to 120 minutes), PVAm microgels became bigger and broader, specifically, after 60 minutes, a new peak occurred.

5.3.1.8 The dropping speed

The dropping speed played an important role in the formation of PVAm microgels. As shown in Figure 5.9, at low dropping speed a messy and broad microgel with a large average size was observed. At high dropping speed, a large and broadly distributed microgel was formed. Only at intermediate dropping speed, a narrowly distributed microgel with a small average size was obtained.

5.3.1.9 The stirring speed

As shown in Figure 5.10, the stirring speed of PVAm solution was not as important as dropping speed. The change of stirring speed had little influence on size and distribution of PVAm microgels.

5.3.2 Electrophoretic mobility result

Figure 5.11 shows the effect of pH on the electrophoretic mobility of PVAm microgels. The electrophoretic mobility first increased with the decrease of pH, reflecting the higher degree of ionization of amine groups at lower pH environments. When the pH was lower than 5, however, the electrophoretic mobility of microgels began to drop (from 4 to 2 mobility units over a pH range from 5 to 2).

5.3.3 The size by dynamic light scattering

The effect of pH on the size of PVAm microgels is shown in Figure 5.12. The microgel size decreased almost one half when pH changed from 2.5 to 10.5.

5.3.4 The morphology and size by TEM

TEM images of PVAm microgels are shown in Figure 5.13. The sizes of dried microgels were smaller than those in aqueous solutions. This results from the shrinkage of microgels in dried conditions. The microgels clearly show round shapes. More interestingly, there is a thick penumbra outside each microgel, similar to core-shell structures, due to the liner PVAm polymers sticking to the outer layers of microgels. The white spots in the right image are attributed to the different shrinkage degrees of the microgels and linear PVAm in the drying process.

5.3.5 The size distribution by Mastersizer

The size distribution of PVAm microgels as measured by the Mastersizer is shown in Figure 5.14. The variation in the size of the microgels showed a

uniform-sized distribution. The average particle size is about 200 nm, close to the result obtained from dynamic light scattering.

5.4 Discussion

Part A: The preparation of PVAm microgel

Compared with chitosan, PVAm is more flexible and readily dissolved. The structures of PVAm and TPP are shown in Scheme 5.1. The more coiled chain structure of PVAm makes it easier than did chitosan for producing small and narrowly distributed microgels. In addition, the high solubility of PVAm enlarges the pH range of application; in contrast, chitosan can dissolve only at pH less than 6.

On the other hand, the high solubility of PVAm over whole pH makes its microgels to collapse when the pH are changed from acid to basic condition. In contrast, the poor solubility of chitosan at basic condition makes its microgels be stable, although there is not much electrostatic attraction inside the microgels in this case. Therefore, to acquire stable PVAm microgels, chemical crosslinkers were employed. Due to the high reactivity of amine groups, many kinds of crosslinkers can be exploited, for example, epichlorohydrin,²¹ resimene,²² N, N-disuccinimidyl suberate²³, *etc.* Recently, genipin, a kind of extract from Chinese traditional drugs was used because of its environmentally friendly character.²⁴ In the present study, glutaraldehyde was employed to crosslink the amine groups of PVAm. Glutaraldehyde reacts easily with amine groups to produce Schiff bases at room temperature. A disadvantage is that Schiff bases are not very stable in acid or heat conditions. However, it is easy to reduce Schiff bases to stable imine groups by adding a sodium cyanoborohydride solution.²⁵

The driving force of forming PVAm microgel is the electrostatic force between protonated amine groups and anionic phosphate groups. Therefore, pH and salt concentration are the two most important influencing factors. The addition of salt can shield the ionic bonds. Because both amine groups and phosphate groups are pH-sensitive, the change of pH influences the abundance of charge on PVAm and TPP and, therefore, results in PVAm microgels with different average size and distribution. From the experimental results, the lower salt concentration, the smaller and more narrowly distributed PVAm microgels. However, there was an optimum pH for the formation of the PVAm microgel; too high or too low pH resulted in an inferior microgel. The reason behind this was that, although the amount of cationic amine groups increased at low pH, the anionic phosphate groups decreased at that pH. Therefore, there were not enough amounts of electrostatic bonds between amine and phosphate groups in that condition. The same thing happened at high pH. Consequently, the smallest and most narrowly distributed PVAm microgels were obtained at intermediate pHs.

In addition to pH and salt concentration, there are other influencing factors. The Mw of PVAm influenced microgel structure by affecting the conformation of linear PVAm polymers.²⁶ The higher Mw of the PVAm, the more coiled structure of the polymer and, therefore, the denser the microgel. The increase of TPP resulted in more electrostatic bonds and, consequently, smaller and more narrowly distributed microgels. However, the salt concentration also increased with TPP concentration. In this condition, the shield effect played the main role and resulted in a broadly distributed microgel with a big average size. Compared with storage time and stirring speed, the dropping speed had an important impact on size and distribution of microgel. At low dropping speed, the obtained PVAm microgels were easily destroyed due to the small amount of electrostatic bonds and, therefore, a very broad microgel was observed. However, at high dropping speed, there was not enough time for TPP to penetrate and interact with PVAm and, thus, a relatively big and broad microgel was obtained.

Part B: The characterization of PVAm microgel

With the lowering of pH, the positive charges of microgels kept increasing, indicating there were more driving force for the movement of the microgels. However, the structure of the microgels became swollen due to electrostatic repulsion. These swollen structures produce a much higher drag force than that of the compact structures at high pH. The effect of dragging was bigger than that of the increase of driving force and therefore, the electrophoretic mobility values decreased at low pH. This hypothesis is supported by the apparent hydrodynamic diameter measurements (Figure 5.12). Chen *et al.* observed the same phenomenon in hydrophobically modified PVAm systems.²⁷

The microgel size decreased at high pH values. This is reasonable considering the pH-sensitive neutralization of amine groups. In the intermediate pH range, the microgel size increased slowly with decreasing pH. This phenomenon reflects the neighboring effect of PVAm, which limits the ionization of amine groups and consequently decreases the electrostatic repulsions. At pH 2, the microgels had the highest charge density and acquired the largest apparent diameter.

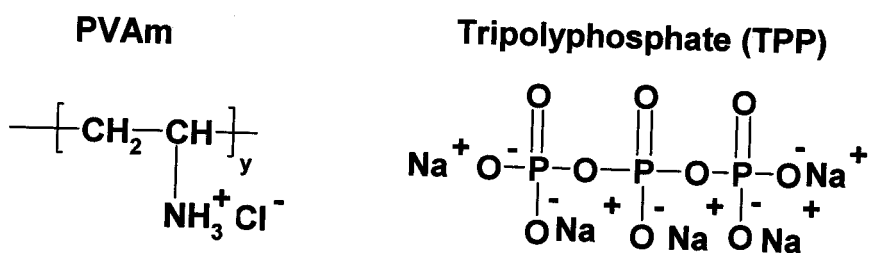
5.5 Summary

Narrowly distributed PVAm microgels were prepared for the first time and their properties were investigated. The preparation process is easy and quick. The sizes of microgels were found to range from 100nm to 1000 nm, depending on the conditions of preparation. The results indicate that TPP concentration plays a more important role in microgel size than PVAm concentration. Furthermore, this approach can also be used to make microgels or nanoparticles from other amines

containing polymers, for example, polyethylene imine. This novel system of microgel production is expected to have many promising applications.

5.6 Tables and Figures

Scheme 5.1 Structures of PVAm and TPP



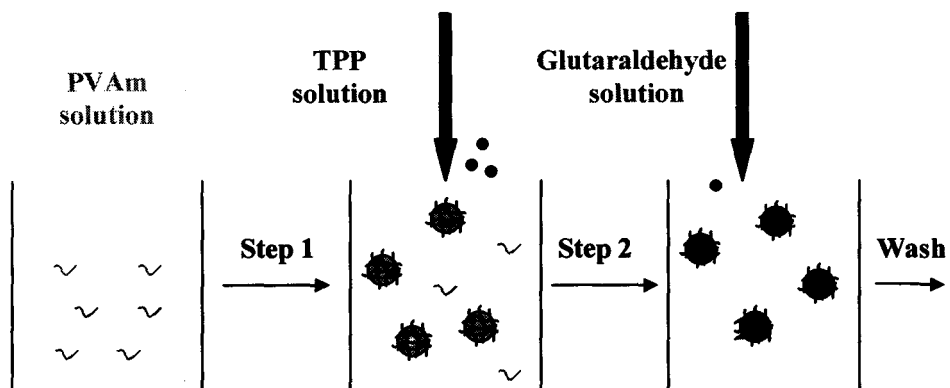


Figure 5.1 Two steps in the production of uniform-sized PVAm microgels. Step 1 is the production of uniform-sized microgels. Step 2 is the chemically crosslinked process to obtain stable microgels.

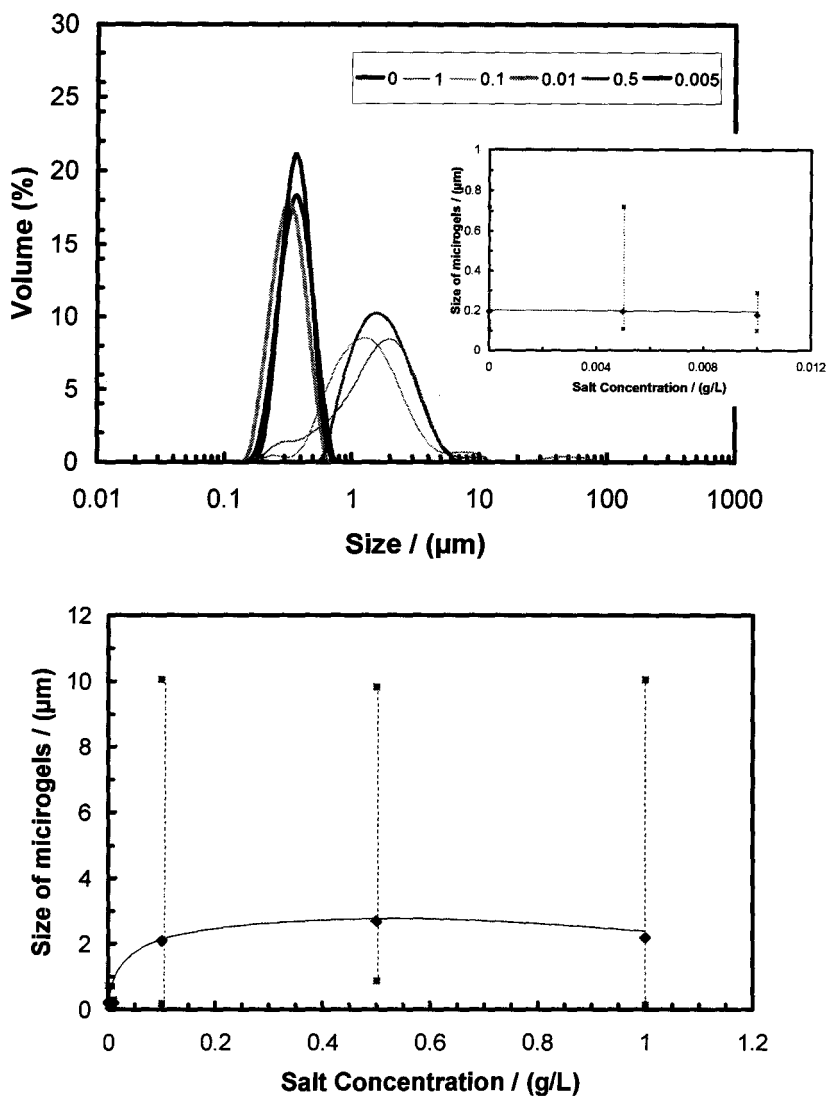


Figure 5.2 The influence of salt concentration on the size and distribution of PVAm microgels. The unit of salt concentration is mol/L. PVAm ($M_w=150$ kDa) 0.1 g/L (50mL) pH=10, TPP 1g/L (20 mL) pH=3, stirring speed level 8, dropping speed 0.333 mL/s, storage for 10 minutes.

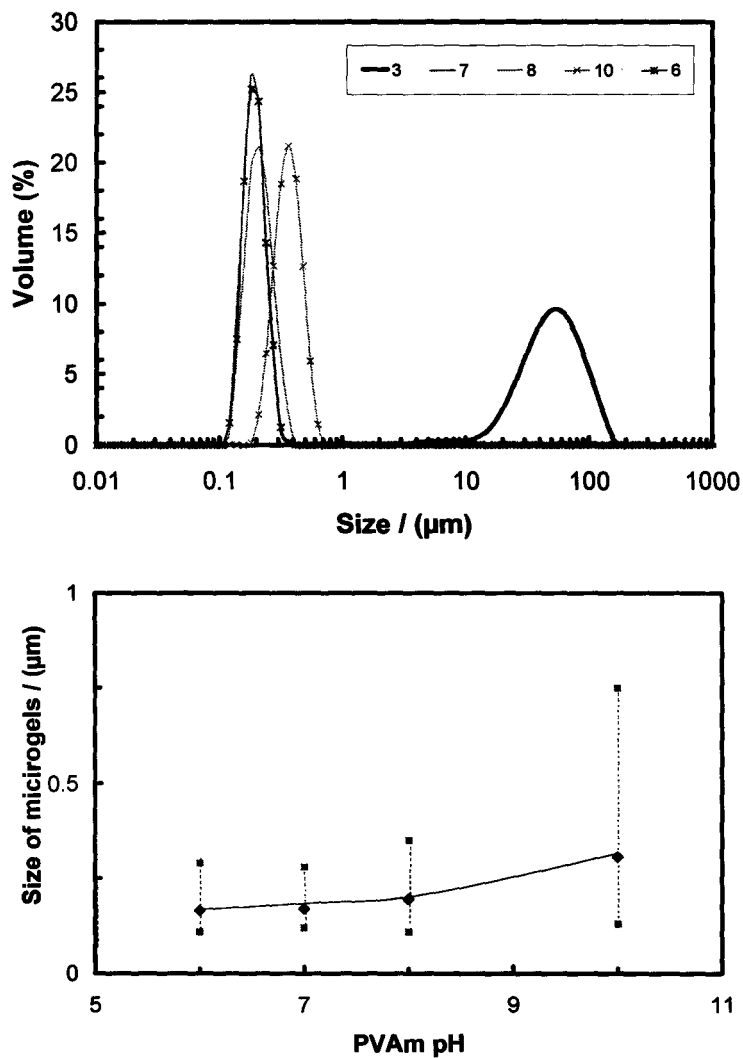


Figure 5.3 The influence of PVAm pH on the size and distribution of PVAm microgels. PVAm ($M_w=150$ kDa) 0.1 g/L (50 mL), [NaCl] =5 mM, TPP 1g/L (20 mL) pH=3, stirring speed level 8, dropping speed 0.333 mL/s, storage for 10 minutes.

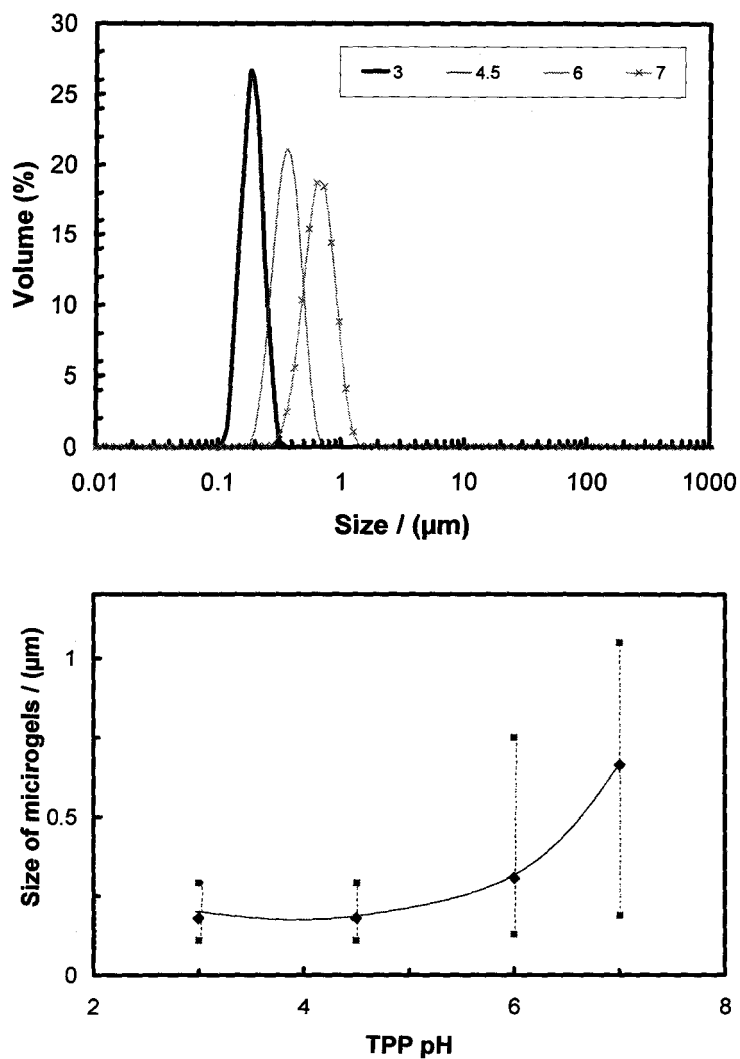


Figure 5.4 The influence of TPP pH on the size and distribution of PVAm microgels. PVAm ($M_w=150$ kDa) 0.1 g/L (50 mL) pH=10, [NaCl] =5 mM, TPP 1g/L (20 mL), stirring speed level 8, dropping speed 0.333 mL/s, storage for 10 minutes.

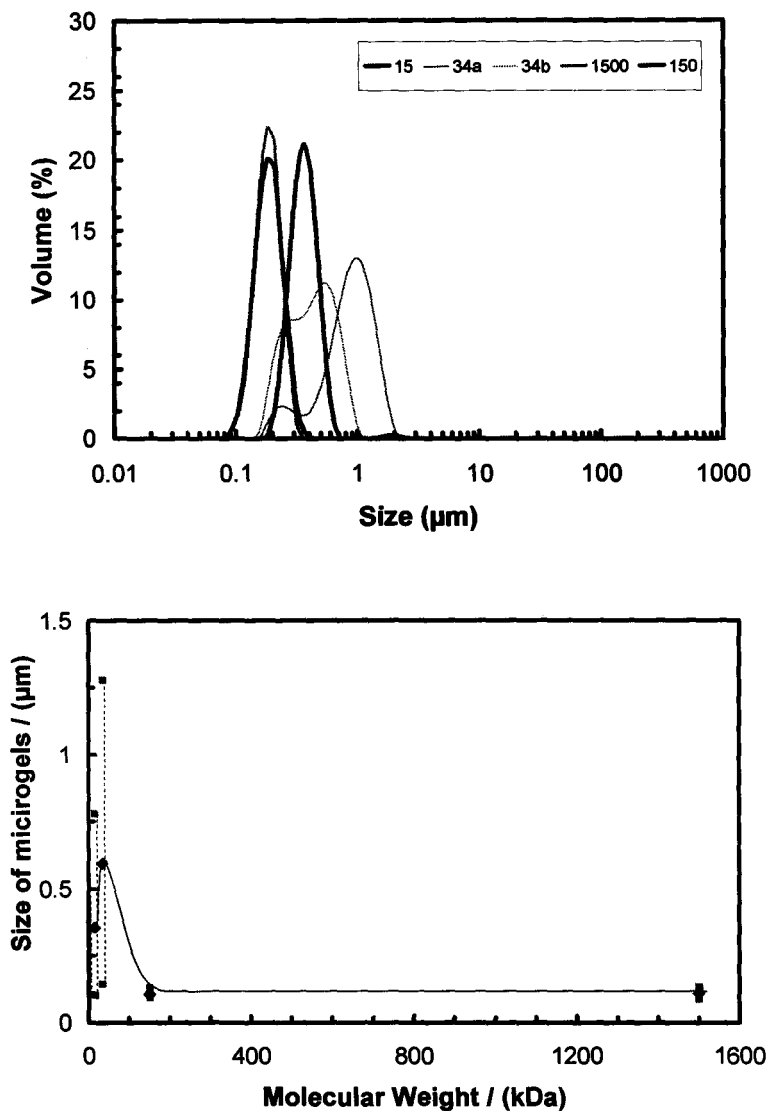


Figure 5.5 The influence of PVAM Mw on the size and distribution of PVAM microgels. PVAM (Mw as shown in figure and unit is kDa) 1 g/L (50 mL) pH=10, [NaCl] =5 mM, TPP 1g/L (20 mL) pH=3, stirring speed level 8, dropping speed 0.333 mL/s, storage for 10 minutes.

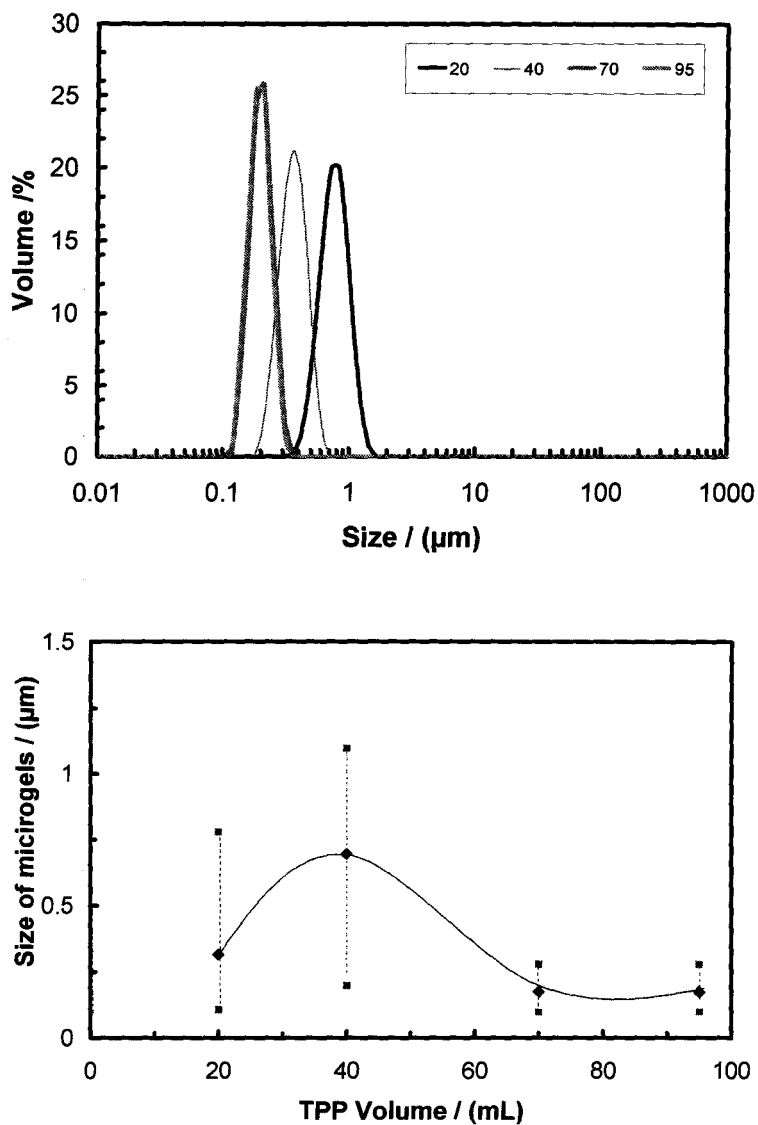


Figure 5.6 The influence of TPP volume on the size and distribution of PVAm microgels. PVAm ($M_w=150$ kDa) 0.1 g/L (50 mL) pH=10, [NaCl] =5 mM, TPP 1g/L, pH=3, stirring speed level 8, dropping speed 0.333 mL/s, storage for 10 minutes.

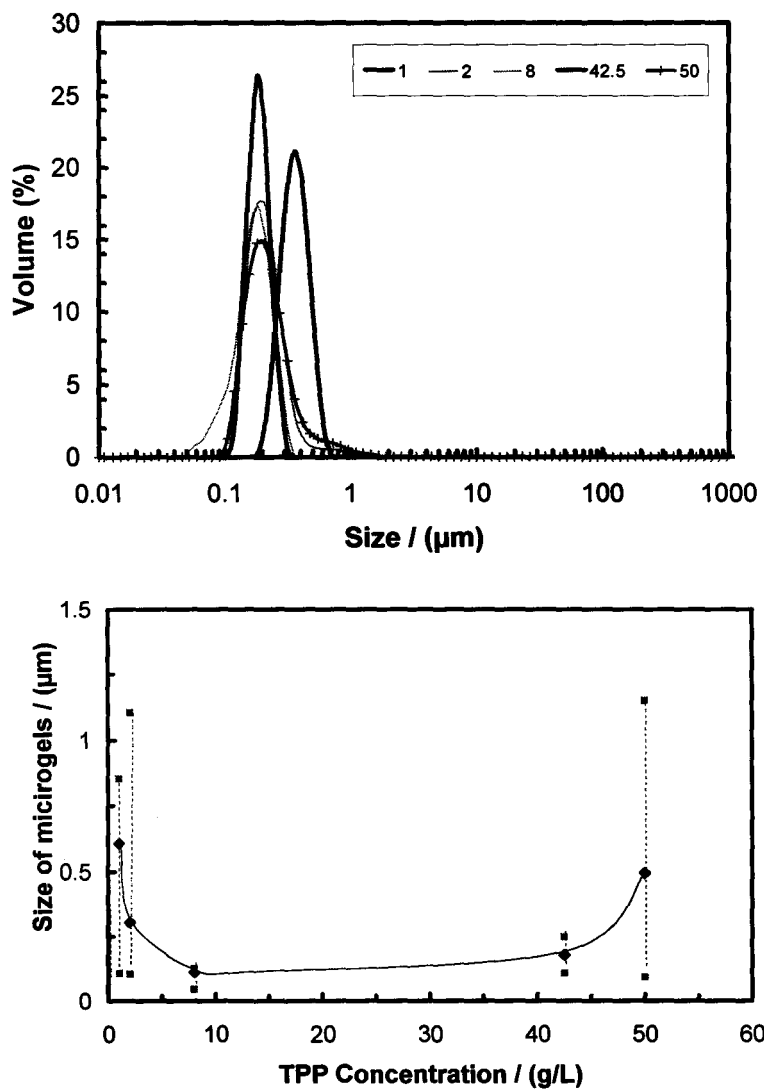


Figure 5.7 The influence of TPP concentration on the size and distribution of PVAm microgels. PVAm ($M_w=150$ kDa) 0.1 g/L (50 mL) pH=10, [NaCl] =5 mM, TPP (20 mL) pH=3, stirring speed level 8, dropping speed 0.333 mL/s, storage for 10 minutes.

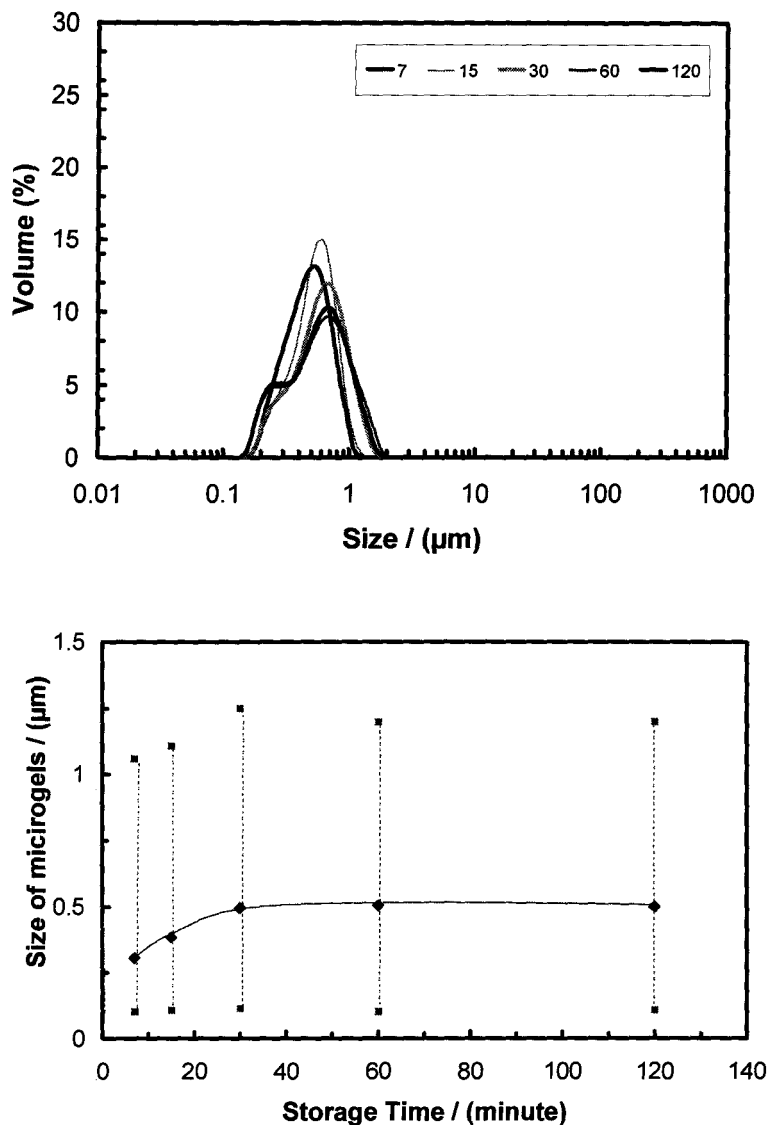


Figure 5.8 The influence of Storage time on the size and distribution of PVAm microgels. PVAm ($M_w=150$ kDa) 0.1 g/L (50 mL) pH=10, [NaCl] =5 mM, TPP 1g/L (20 mL) pH=3, stirring speed level 8, dropping speed 0.333 mL/s.

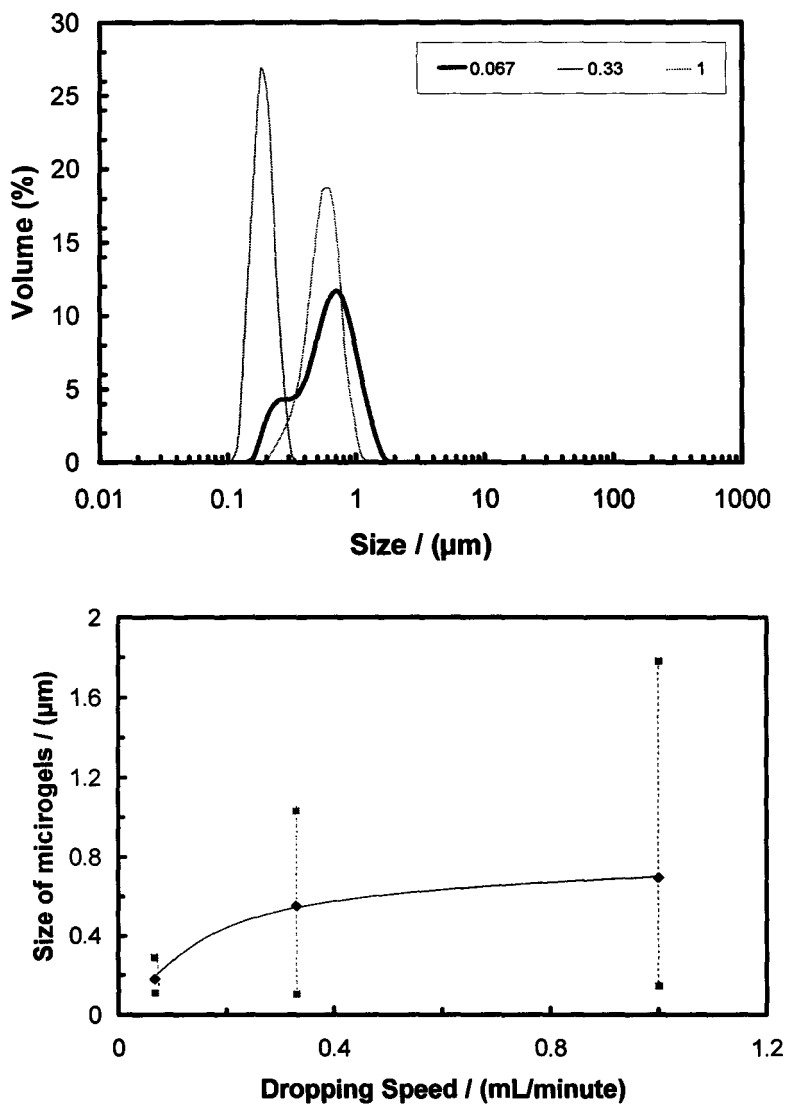


Figure 5.9 The influence of dropping speed on the size and distribution of PVAm microgels. PVAm ($M_w=150$ kDa) 0.1 g/L (50 mL) pH=10, [NaCl]=5 mM, TPP 1g/L (20 mL) pH=3, stirring speed level 8, storage for 10 minutes.

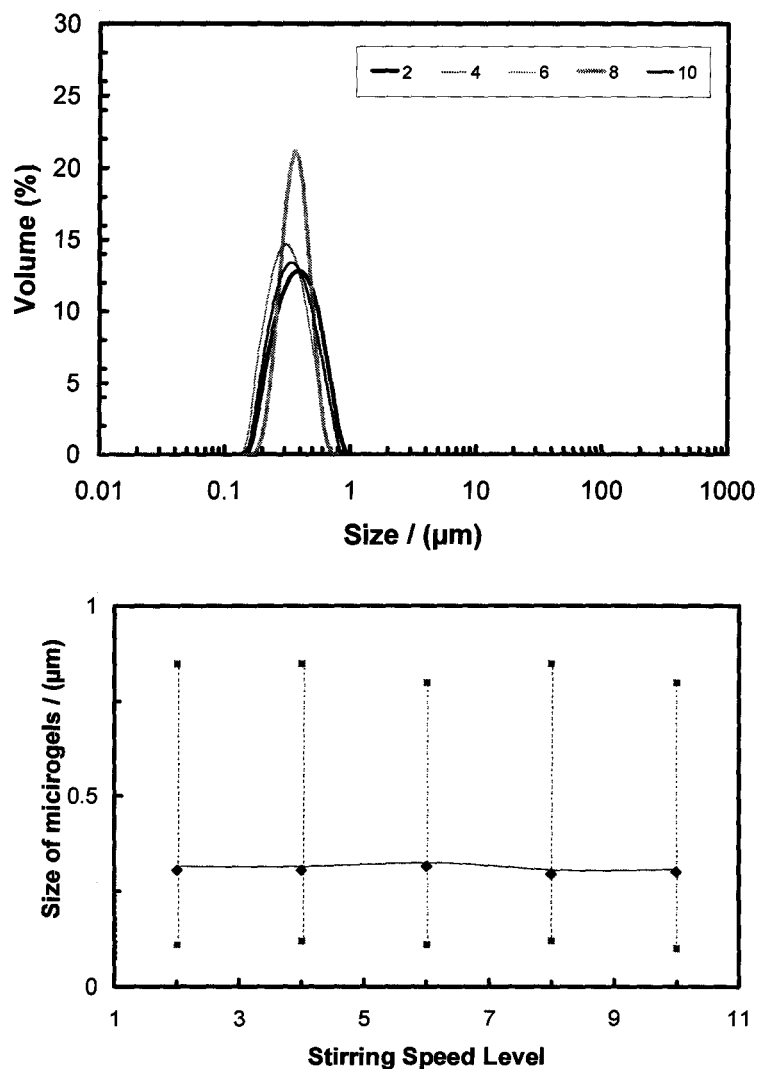


Figure 5.10 The influence of stirring speed on the size and distribution of PVAm microgels. PVAm ($M_w=150$ kDa) 0.1 g/L (50 mL) pH=10, [NaCl] =5 mM, TPP 1g/L (20 mL) pH=3, dropping speed 0.333 mL/s, storage for 10 minutes.

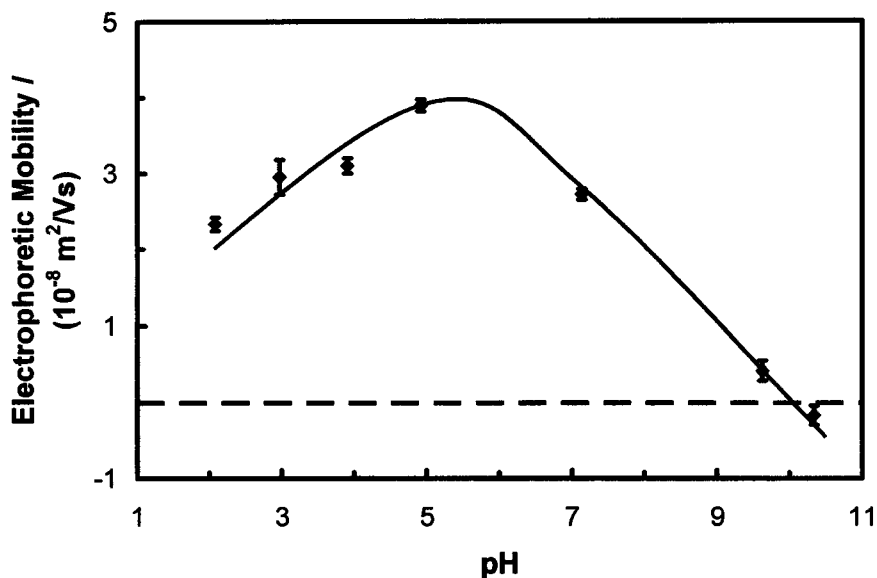


Figure 5.11 pH effect on the electrophoretic mobility of 500 ppm microgel in 5 mM NaCl aqueous solution, 25 °C. The preparation condition: PVAm ($M_w=150$ kDa) 1 g/L (50 mL) pH=10, [NaCl] =5 mM, TPP 1g/L (20 mL) pH=3, stirring speed level 8, dropping speed 0.333 mL/s, storage for 10 minutes. The error bars are the standard deviations from the mean based on five measurements. 0.1 M HCl and NaOH were used to adjust pH.

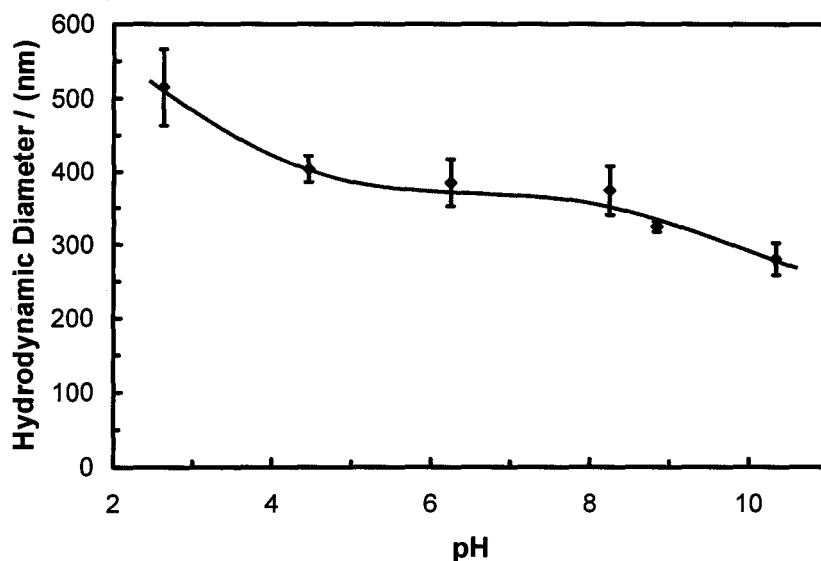


Figure 5.12 The hydrodynamic diameter of PVAm microgel-1 as a function of pH. The preparation condition: PVAm ($M_w=150$ kDa) 1 g/L (50 mL) pH=10, [NaCl] =5 mM, TPP 1g/L (20 mL) pH=3, stirring speed level 8, dropping speed 0.333 mL/s, storage for 10 minutes. The error bars are the standard deviations from the mean based on six measurements. 0.1 M HCl and NaOH were used to adjust pH. 50 ppm microgel in 5 mM NaCl aqueous solution, 25 °C.

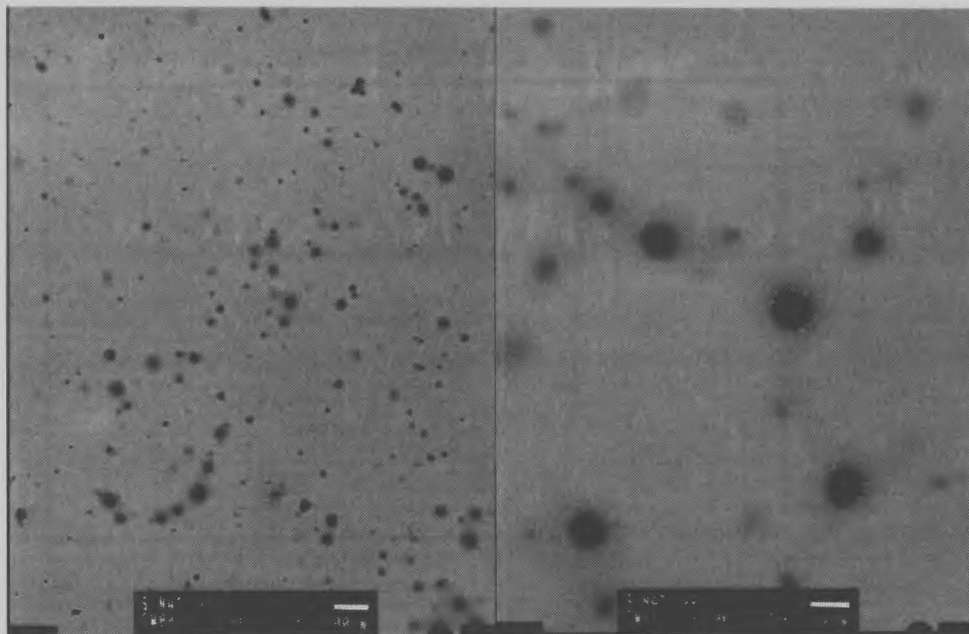


Figure 5.13 TEM images of PVAm microgel. The scale bars are 500 (left) and 200 (right) nm, respectively. The preparation condition: PVAm ($M_w=150$ kDa) 1 g/L (50 mL) pH=10, [NaCl] =5 mM, TPP 1g/L (20 mL) pH=3, stirring speed level 8, dropping speed 0.333 mL/s, storage for 10 minutes.

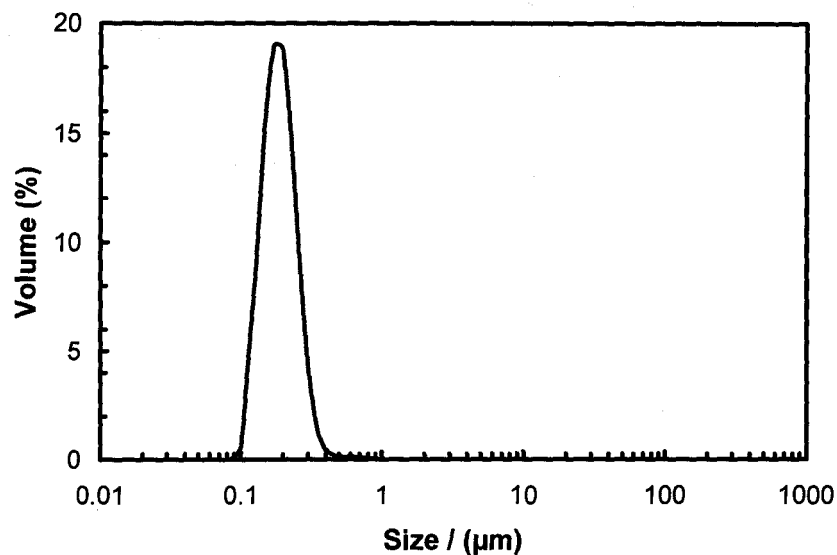


Figure 5.14 Size distribution of PVAm microgel. Experiments were measured at pH 10.2, $I=5$ mM. The preparation condition: PVAm ($M_w=150$ kDa) 1 g/L (50 mL) pH=10, $[NaCl]=5$ mM, TPP 1g/L (20 mL) pH=3, stirring speed level 8, dropping speed 0.333 mL/s, storage for 10 minutes.

Reference

1. Biffis, A.; Minati, L., Efficient aerobic oxidation of alcohols in water catalyzed by microgel-stabilized metal nanoclusters. *Journal of Catalysis* **2005**, *236*, (2), 405-409.
2. Hoare, T.; Pelton, R., Titrimetric Characterization of pH-Induced Phase Transitions in Functionalized Microgels. *Langmuir* **2006**, *22*, (17), 7342-7350.
3. Pelton, R., Temperature-sensitive aqueous microgels. *Advances in Colloid and Interface Science* **2000**, *85*, (1), 1-33.
4. Zhang, Y.; Guan, Y.; Zhou, S., Synthesis and volume phase transitions of glucose-sensitive microgels. *Biomacromolecules* **2006**, *7*, (11), 3196-3201.
5. Saunders, B. R.; Vincent, B., Microgel particles as model colloids: theory, properties and applications. *Advances in Colloid and Interface Science* **1999**, *80*, (1), 1-25.
6. Reynolds, D. D.; Kenyon, W. O., Preparation of polyvinylamine, polyvinylamine salts, and related nitrogenous resins. *Journal of the American Chemical Society* **1947**, *69*, 911-15.
7. Pinschmidt, R. K., Jr.; Smigo, J. G.; Nordquist, A. F. Alkyl glycidyl ether-modified poly(vinylamine) for use in papermaking. 93-4339193 4339193, 19931116., **1994**.
8. Kobayashi, S.; Suh, K. D.; Shirokura, Y., Chelating ability of poly(vinylamine): effects of polyamine structure on chelation. *Macromolecules* **1989**, *22*, (5), 2363-6.
9. Chen, W.; Lu, C.; Pelton, R., Polyvinylamine Boronate Adhesion to Cellulose Hydrogel. *Biomacromolecules* **2006**, *7*, (3), 701-702.
10. Sagnella, S.; Kligman, F.; Marchant Roger, E.; Kottke-Marchant, K., Biometric surfactant polymers designed for shear-stable endothelialization on biomaterials. *J Biomed Mater Res A FIELD Full Journal Title:Journal of biomedical materials research. Part A* **2003**, *67*, (3), 689-701.
11. Tang, Y.; Zhang, S.; Yang, J.; Tang, B., Synthesis of a new, yellow crosslinking polyvinylamine dye and its crosslinking/dyeing process through a crosslinker. *Journal of Applied Polymer Science* **2006**, *102*, (2), 1568-1573.
12. Kobayashi, S.; Suh, K. D.; Shirokura, Y.; Fujioka, T., Viscosity behavior of poly(vinylamine) and swelling-contraction phenomenon of its gel. *Polymer Journal (Tokyo, Japan)* **1989**, *21*, (12), 971-6.
13. Kim, Y.-B.; Kim, H.-K.; Hong, J.-W., Epoxy-acrylic microgels in electrodeposition coating films. *Surface and Coatings Technology* **2002**, *153*, (2-3), 284-289.
14. Zhang, H.; Oh, M.; Allen, C.; Kumacheva, E., Uniform-sized Chitosan Nanoparticles for Mucosal Drug Delivery. *Biomacromolecules* **2004**, *5*, (6), 2461-2468.
15. Miao, C.; Pelton, R.; Chen, X.; Leduc, M., Microgels Versus Linear Polymers For Paper Wet Strength – Size Does Matter *Appita (in press)* **2007**.

16. Xu, J.; Pelton, R., A new route to poly(N-isopropylacrylamide) microgels supporting a polyvinylamine corona. *Journal of Colloid and Interface Science* **2004**, 276, (1), 113-117.
17. Feng, X.; Pelton, R.; Leduc, M.; Champ, S., Colloidal Complexes from Poly(vinyl amine) and Carboxymethyl Cellulose Mixtures. *Langmuir* **2007**, 23, (6), 2970-2976.
18. Yi, H.; Wu, L.-Q.; Bentley, W. E.; Ghodssi, R.; Rubloff, G. W.; Culver, J. N.; Payne, G. F., Biofabrication with Chitosan. *Biomacromolecules* **2005**, 6, (6), 2881-2894.
19. Calvo, P.; Remunan-Lopez, C.; Vila-Jato, J. L.; Alonso, M. J., Novel hydrophilic chitosan-polyethylene oxide nanoparticles as protein carriers. *Journal of Applied Polymer Science* **1997**, 63, (1), 125-132.
20. Wang, L.; Gu, Y.; Zhou, Q.; Ma, G.; Wan, Y.; Su, Z., Preparation and characterization of uniform-sized chitosan microspheres containing insulin by membrane emulsification. *Colloids and Surfaces B: Biointerfaces* **2006**, 50, 10.
21. Wei, Y. C.; Hudson, S. M.; Mayer, J. M.; Kaplan, D. L., The crosslinking of chitosan fibers. *Journal of Polymer Science, Part A: Polymer Chemistry* **1992**, 30, (10), 2187-93.
22. Ligler, F. S.; Lingerfelt, B. M.; Price, R. P.; Schoen, P. E., Development of Uniform Chitosan Thin-Film Layers on Silicon Chips. *Langmuir* **2001**, 17, (16), 5082-5084.
23. Schauer, C. L.; Chen, M.-S.; Chatterley, M.; Eisemann, K.; Welsh, E. R.; Price, R. R.; Schoen, P. E.; Ligler, F. S., Color changes in chitosan and poly (allyl amine) films upon metal binding. *Thin Solid Films* **2003**, 434, (1-2), 250-257.
24. Jin, J.; Song, M.; Hourston, D. J., Novel Chitosan-Based Films Cross-Linked by Genipin with Improved Physical Properties. *Biomacromolecules* **2004**, 5, (1), 162-168.
25. Peng, L.; Calton, G. J.; Burnett, J. W., Effect of borohydride reduction on antibodies. *Applied Biochemistry and Biotechnology* **1987**, 14, (2), 91-9.
26. Chen, W., Unpublished data.
27. Chen, X.; Wang, Y.; Pelton, R., pH-Dependence of the Properties of Hydrophobically Modified Polyvinylamine. *Langmuir* **2005**, 21, (25), 11673-11677.

Chapter 6

Boronate Microgels Adhesion to Wet Cellulose

6.1 Introduction

Microgels are cross-linked three dimensional polymer networks with a size between 50 nm to 5 μ m. Microgels can disperse and swell, but cannot dissolve in solvents. Generally, there are three ways to prepare microgels.

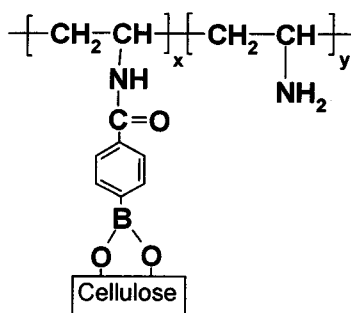
- (1) Microgels can be prepared from the polymerization of monomers and crosslinkers.
- (2) Microgels can be prepared by chemically or physically crosslinking linear polymers.
- (3) Microgels can be made from macrogels through grinding.

Because of their three dimensional and swelling properties, microgels can work as a much better filling adhesive than linear polymers of the same substance. The working mechanism of microgels in adhesion science is related to its spatial property. For example, Wågberg *et al.* found the polyelectrolyte complexes of methylcellulose and poly (amideamine) epichlorohydrin condensate (PAE) had a higher adsorption amount than PAE itself. Furthermore, the dry and wet strength of wood fibers modified by this complex had a higher value than that of fibers modified by PAE.^{1,2}

Miao *et al.* prepared a series of PVAm microgels with different average sizes and cross-linking degrees and studied their application in papermaking. The wet strength of linear PVAm and microgels was compared in three application conditions. (1) With impregnated filter paper, linear PVAm showed a higher wet strength. (2) In the handsheet experiments, microgels displayed a higher wet strength. (3) In the peeling test of cellulose membranes, both linear polymers and microgels had the same strength. The results indicated that microgels can adsorb more on fibers than on linear polymers, but their big dimension limited the penetration of microgels into fibers. By contrast, linear PVAm had a smaller adsorption amount on fibers, but was easier to impregnate into the gaps between fibers.^{3,4} In addition, the results from delaminating regenerated cellulose membranes showed that the highest wet strength was not observed for the large and highly cross-linked microgels.⁴

In our previous work, PVAm-boronate showed high wet adhesion, indicating the covalent bonding between regenerated cellulose membranes and boronic acid.⁵ Therefore, it is believed that substantially increased wet adhesion to cellulose membranes will be observed in the microgel-boronate system (as shown

in scheme 6.1). In this work, preliminary experiments were performed to probe the wet adhesion of boronate containing microgels to cellulose membranes.



Scheme 6.1 PVAm-boronate displays exceptional adhesion to cellulose due to ester formation. (Adapted from Chen *et al.* 2006)⁵

6.2 Experiments

6.2.1 Materials

Regenerated cellulose dialysis tubing (Spectra/Por® 4 product No: 132682 12kDa MWCO, Spectrum Laboratories, Inc.) was used. The tube was cut into 6×2 and 6×3 cm² strips, with the long axis paralleling to the long axis of the tube; the interior surface of the tube was used. Aminophenylboronic acid, 4-carboxyphenylboronic acid, and N-(3-dimethylaminopropyl)-N'-ethylcarbodiimide hydrochloride (EDC) were purchased from Sigma-Aldrich and used as received. All experiments were performed with water from a Millipore Milli-Q system fitted with one Super C carbon cartridge, two ion-exchange cartridges, and one Organex Q cartridge.

6.2.2 Preparation of Boronate-modified microgels

PolyNIPAM microgel: The original microgels were kindly provided by Dr. Hoare. The average size for the polyNIPAM microgel was 260 nm in 1mM NaCl at pH 9 at 25 °C. For boronate modification, 0.1 g of polyNIPAM microgel was dispersed in 10 mL 0.1M MES buffer at pH 6.1 and 90 mL of 3 g/L aminophenylboronic acid pH=6.1 in the buffer. Then, 8 g EDC were added and the mixture was stirred for 120 min at 25 °C. The product was dialyzed against water for two weeks to remove free boronic acid.

PVAm microgel: The original microgels were kindly provided by Dr. Miao. There was a broad distribution for the PVAm microgel and the average size was

1500 nm in 5mM NaCl at pH 7 at 25 °C. For boronate modification, 0.1 g of PVAm microgel was dispersed in 10 mL 0.1M MES buffer at pH 6.1 and 90 mL of 3 g/L 4-carboxy-phenylboronic acid pH=6.1 in the buffer. Then, 8 g EDC were added and the mixture was stirred for 120 min at 25 °C. The product was dialyzed against water for two weeks to remove free boronic acid.

6.2.3 Wet adhesion measurement

The water on the surface of the cellulose membranes was removed by dipping several times with tissues (Kimwipes). Afterwards, the cellulose membranes were soaked in microgel solutions with desired pH (adsorption pH) for 10 minutes and then rinsed in a salt solution with the desire pH (final pH) for 5 minutes. The bottom membrane was placed on a steel disk and a Teflon tape with a 1 cm width was put on one end of the cellulose membrane. Afterwards, the top cellulose membrane was carefully placed on the bottom membrane. Then, the resulting membrane pairs were put between two blotting papers and pressed using Hot Plate (Carver, Wabash, IN) at 88000 N at room temperature for 3 min. Then, the membranes were peeled, using the above Instron 4411 universal testing system fitted with a 50 N load cell. The 90 degree peeling method was employed to get the delamination force.

6.3 Results

Handsheets made from pulp were the main approach to study the wet or wet web strength of paper. However, there are several disadvantages in handsheet based methods. Firstly, the retention of microgels is hard to control. Secondly, the locations of microgels in the handsheets and fracture mode can vary. Last, but not least, the flocculation of microgels influences the handsheet mechanical property. Pelton's group proposed a refined method to overcome all these problems.⁶ The regenerated cellulose membranes from dialysis tubing were employed as substrates and microgels were applied onto the membranes. The peeling force to delaminate cellulose membranes is plotted against the separation distance of the membranes. The bigger the peeling force, the higher the consumption of adhesion energy - that is, the higher is the wet strength of microgels. This method had advantages for good replication, easy process and good control of applied microgels.

The adhesion force of PVAm microgel increased from 5.8 N/m to 22 N/m when the final pH changed from 9 to 11.03. After modification with boronate, microgels showed a substantially increased adhesion. At pH 11.15, the wet adhesion could reach 72.2 N/m, which is six times the value of the original PVAm microgels. The adhesion of both microgels increased with the final pH.

The adhesion of original polyNIPAM microgels was not sensitive to final pH, whereas boronate-modified polyNIPAM had a substantial adhesion at high pH's (from pH 9.4 to 11.2, the adhesion increased about 10 times). A similar phenomenon was observed in PVAm and boronate-modified PVAm systems, indicating the interaction of boronate and cellulose.

The influence of adsorption pH on the wet adhesion of modified microgels was shown in Figure 6.3. Boronate modified PVAm microgels passed a minimum at pH 7.5, whereas modified polyNIPAM microgels kept decreasing over the whole measurement pH range.

The comparison of wet adhesion of boronate PVAm microgels and linear PVAm-boronate to cellulose membranes is shown in Figure 6.4. The boronate microgels had a higher wet strength than linear PVAm-PBA over the whole final pH range.

6.4 Discussion

For boronate-modified PVAm microgels, a high wet adhesion was observed, indicating the function of boronate. In addition, a high adhesion was acquired at low pH, which was consistent with boronate modified PVAm polymers. It is believed by some researchers that the excess electron pair on amine groups effectively lowered the pKa of boronate and resulted in the occurrence of covalent bonding at low pH.^{7, 8} Another explanation is the formation of zwitterion structure between amine groups and boronic acid groups. This structure resulted into the ionization of boronic acid at low pH.⁹

For boronate-modified polyNIPAM microgels, the increase of adhesion happened only at high pH (around 11), indicating the pKa of boronate in the absence of amine groups. Furthermore, the weak adhesion strength of original polyNIPAM microgels and intermediate adhesion strength of original PVAm microgels showed that there existed some interaction between PVAm microgels and cellulose. Hydrogen bonds and/or electrostatic attraction are presumably the main interaction.¹⁰

The microgels might desorb from cellulose membranes at different final pH. Therefore, the low adhesion could be induced by the desorption of microgels rather than the strong interaction of boronate and cellulose at high final pHs. However, the data in Figure 6.3 showed that a lower adhesion was observed at high adsorption pH when the final pH remained the same, indicating that low pHs benefited the adsorption of microgels on cellulose membranes. Therefore, at high final pH, the high adhesion result unequivocally showed the influence of boronate on adhesion.

Because of the paucity of boronate content measurement on the microgels, it is difficult to compare the adhesion results in Figure 6.4. However, the result in chapter 3 showed that the highest adhesion was observed for the PVAm-PBA used herein. That is, a higher wet adhesion was observed in the boronate PVAm microgels systems than the highest wet adhesion acquired in the linear PVAm-PBA systems. There are two probable contributions to the high adhesion of boronate microgels. One is that microgels can improve the adsorption or retention amount onto fibers, and the other is that a bigger contact area can be acquired due to the three dimensional structure of microgels.

6.5 Conclusions

It is hard to compare two boronate-modified microgels because there is no quantitative data about boronate groups and different crosslinking degrees of two microgels. However, the adhesion results clearly showed that the incorporation of boronate groups substantially improved the wet adhesion strength of microgels.

Interestingly, a high wet adhesion, not observed previously in linear PVAm-boronate, was acquired in boronate PVAm microgels. This preliminary work indicates that the microgel-boronate system is a promising wet-web-strength enhancing agent.

In the future work, the size, cross-linking degree, surface groups, pH and other influence factors are to be controlled to study the wet adhesion of microgels to cellulose.

6.6 Tables and figures

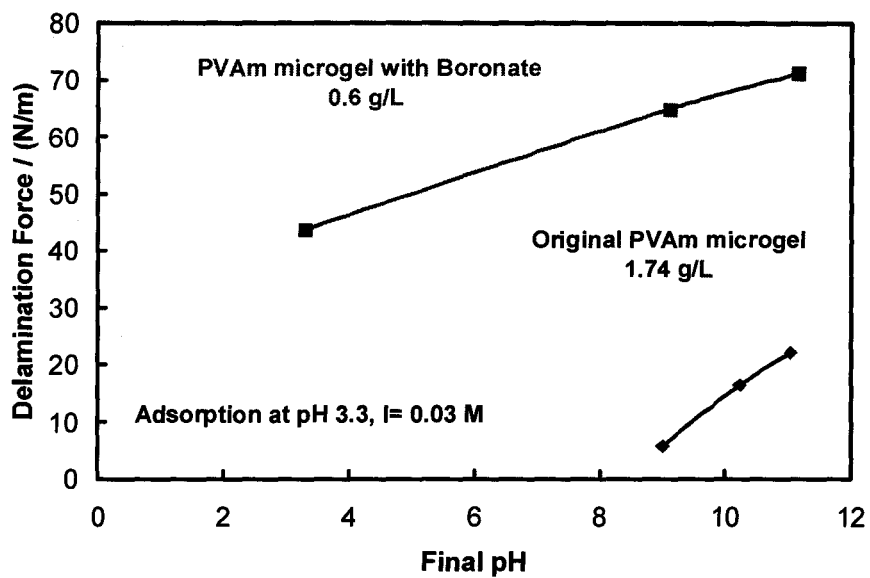


Figure 6.1 The delamination force of PVAm microgel and boronate modified PVAm microgel as functions of final pH. The adsorption pH was 3.3, 0.03 M NaCl aqueous solution, 25 °C.

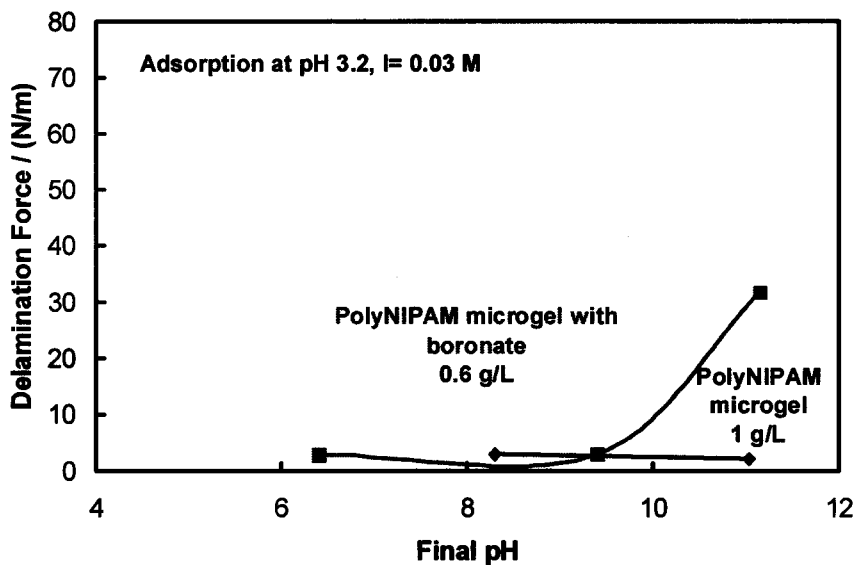


Figure 6.2 The delamination force of PolyNIPAM microgel and boronate modified PolyNIPAM microgel as functions of final pH. The adsorption pH was 3.2, 0.03 M NaCl aqueous solution, 25 °C.

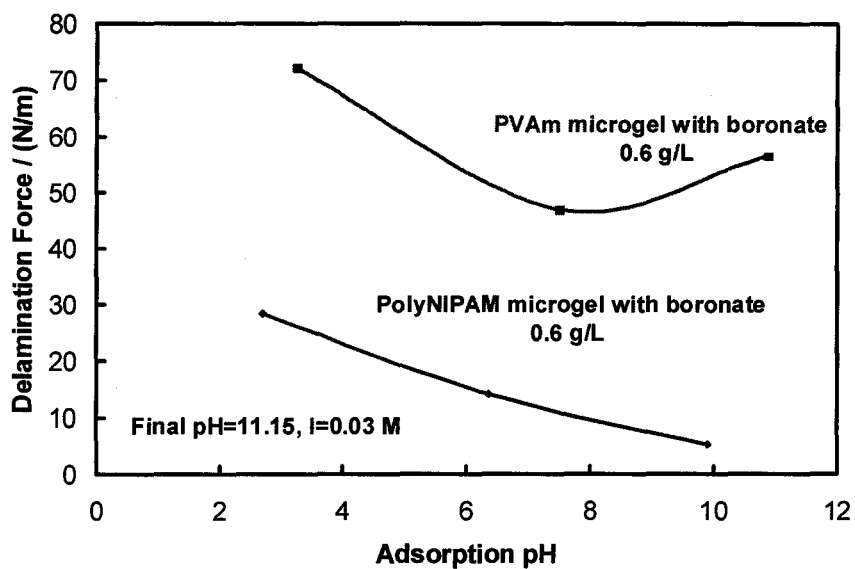


Figure 6.3 The delamination force of PVAm microgel and boronate modified PVAm microgel as functions of adsorption pH. The final pH was 11.15, 0.03 M NaCl aqueous solution, 25 °C.

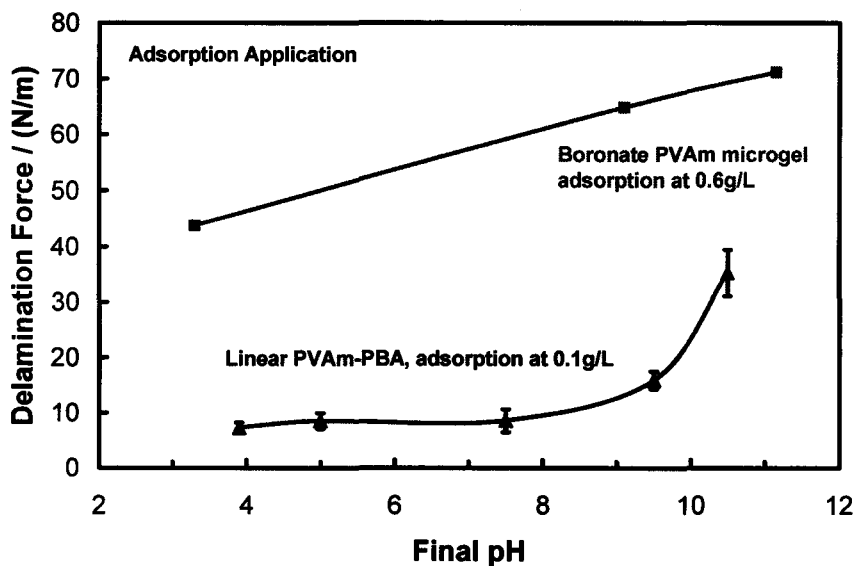


Figure 6.4 The delamination force of boronate PVAm microgel and linear PVAm-boronate (DS 15%, 150 kDa) as functions of final pH. The adsorption pH was 3.3 for microgel and 3.8 for linear PVAm-boronate, in 0.03 M NaCl aqueous solution at 25 °C.

Reference

1. Gardlund, L.; Wagberg, L.; Gernandt, R., Polyelectrolyte complexes for surface modification of wood fibres II. Influence of complexes on wet and dry strength of paper. *Colloids and Surfaces, A: Physicochemical and Engineering Aspects* **2003**, 218, (1-3), 137-149.
2. Gernandt, R.; Wagberg, L.; Gardlund, L.; Dautzenberg, H., Polyelectrolyte complexes for surface modification of wood fibres - I. Preparation and characterization of complexes for dry and wet strength improvement of paper. *Colloids and Surfaces, A: Physicochemical and Engineering Aspects* **2003**, 213, (1), 15-25.
3. Miao, C. W.; Pelton, R.; Chen, X. N.; Leduc, M., Microgels versus linear polymers for paper wet strength - size does matter. *Appita Journal* **2007**, 60, (6), 465-468.
4. Miao, C. W.; Chen, X. N.; Pelton, R., Adhesion of poly(vinylamine) microgels to wet cellulose. *Industrial & Engineering Chemistry Research* **2007**, 46, (20), 6486-6493.
5. Chen, W.; Lu, C.; Pelton, R., Polyvinylamine boronate adhesion to cellulose hydrogel. *Biomacromolecules* **2006**, 7, (3), 701-702.
6. Kurosu, K.; Pelton, R., Simple lysine-containing polypeptide and polyvinylamine adhesives for wet cellulose. *Journal of Pulp and Paper Science* **2004**, 30, (8), 228-232.
7. Niwa, M.; Sawada, T.; Higashi, N., Surface Monolayers of Polymeric Amphiphiles Carrying a Copolymer Segment Composed of Phenylboronic Acid and Amine. Interaction with Saccharides at the Air-Water Interface. *Langmuir* **1998**, 14, (14), 3916-3920.
8. Otsuka, H.; Uchimura, E.; Koshino, H.; Okano, T.; Kataoka, K., Anomalous Binding Profile of Phenylboronic Acid with N-Acetylneuraminic Acid (Neu5Ac) in Aqueous Solution with Varying pH. *Journal of the American Chemical Society* **2003**, 125, (12), 3493-3502.
9. Zhu, L.; Shabbir, S. H.; Gray, M.; Lynch, V. M.; Sorey, S.; Anslyn, E. V., A Structural Investigation of the N-B Interaction in an o-(N,N-Dialkylaminomethyl)arylboronate System. In **2006**; Vol. 128, pp 1222-1232.
10. DiFlavio, J. L.; Bertoia, R.; Pelton, R.; Leduc, M. In *The Mechanism of Polyvinylamine Wet-Strengthening*, 13th Fundamental Research Symposium, Cambridge, UK, 2005; FRC: Cambridge, UK, **2005**; pp 1293-1316.

Chapter 7

Concluding Remarks

The major contributions of this work are in the following:

1. The boronic acid groups are responsible for the instantaneous wet adhesion in cellulose/PVAm-PBA/cellulose laminates. A contour plot of PVAm-boronate adhesion to cellulose was developed based on adsorption pH and final pH. This plot is of practical significance: it gives the criteria for acquiring high adhesion.
2. PBA derivatization lowers the water solubility of PVAm. Phase diagrams of PVAm boronate with different degrees of substitution were developed. The diagrams were based on the solution pH and the polymer concentrations. Three phases, solution, colloid and precipitate were compared in the diagrams.
3. Polyvinylamine is slightly surface active at high pH (56 mN/m), whereas, surface activity is substantially increased at high pH by adding as little as 4% PBA.
4. The greatest wet adhesion measurements were acquired when the pH of the PVAm-PBA adsorption onto cellulose was 9 to 10. Under these conditions the net charge density and the solubility of PVAm-PBA was low, leading to high concentrations of adsorbed PVAm-PBA in the cellulose/PVAm-PBA/cellulose joints.
6. The wet adhesion was surprisingly insensitive to the pH under which the laminates tested. We propose that the high local concentration of ammonium ions on the PVAm backbone extend the ionization pH range of phenylboronic acid below pH 7 enabling borate to carbohydrate bonding under acid conditions.
7. The reaction mechanism of boronic acid and cellulose was studied. Based on the theoretical analysis and experimental evidences, only hydroxyl groups on one end of cellulose chain (hydroxyl groups on carbon-1, 2) could react with boronic acid. The hydroxyl groups on carbon-2, 3 or carbon-4, 6 could not react with cellulose.
8. A simple and effective methodology to synthesize PVAm microgel was developed. For the first time, PVAm microgels with narrow distribution were prepared. The influential factors of preparing the microgels were systematically studied.

9. The adhesion of boronate-microgels to wet cellulose was studied. Preliminary results showed that boronate-microgels provided higher wet adhesion than linear PVAm-boronate. Specifically, at pH 7-8, boronate-microgels showed a high wet adhesion, indicating the application value of microgel in modern papermaking process.